AN INVESTIGATION OF STRESSES PRODUCED, IN A STEEL-CONCRETE COMPOSITE BEAM SECTION, BY RAPID TEMPERATURE CHANGES

A THESIS

PRESENTED TO

THE FACULTY OF GRADUATE STUDIES AND RESEARCH

UNIVERSITY OF MANITOBA

IN PARTIAL FULFILLMENT

OF THE REQUIREMENTS FOR THE DEGREE

OF MASTER OF SCIENCE IN CIVIL ENGINEERING

BY

GLENN ALLEN MORRIS

APRIL, 1958

THE UNIVERSITY OF MANITOBA LIBRARY

ACKNOWLEDGMENT

The author wishes to express his sincere appreciation to Mr. J. C. Trueman of the Dominion Bridge Company, upon whose suggestion this thesis is based. His helpful advice and his efforts in obtaining the theoretical information used in this report were invaluable.

Grateful acknowledgment is also made to Professor W. F. Riddell for the aid, advice and encouragement which he so generously gave throughout the preparation of this thesis.

The author wishes to thank the Dominion Bridge Company who supplied the structural and reinforcing steel used.

The generosity of the University of Manitoba in supplying all additional material is gratefully acknowledged.

A sincere thank you is expressed to Messrs. R. Muir, J. Wiebe and H. Wiebe for their assistance in constructing the apparatus.

TABLE OF CONTENTS

CHAPTER VI. CONCLUSIONS AND RECOMMENDATIONS

LIST OF FIGURES

LIST OF TABLES

LIST OF SYMBOLS

Δ_s = steel contraction due to temperature change assuming no restraint.

Δ_c = concrete contraction due to temperature change assuming no restraint.

$\Delta = \Delta_s - \Delta_c$

e_s = steel strain due to composite action at the contact plane.

e_c = concrete strain due to composite action at the contact plane.

A_s, I_s, M_s = steel area, moment of inertia and moment.

A_c, I_c, M_c = concrete area, moment of inertia and moment.

N_c = longintudinal shear in the concrete at the contact surface.

N_s = longitudinal shear in the steel at the contact surface.

E_s = modulus of elasticity of steel.

E_c = modulus of elasticity of concrete.

$n = E_s/E_c$ = modular ratio.

d = depth of steel beam.

t = slab thickness.

z = distance between c.g. of slab and c.g. of steel beam, $= t/2 + c$.

c = distance between c.g. of steel beam and top flange of steel beam.

α_s = coefficient of linear expansion for steel.

α_c = coefficient of linear expansion for concrete.

S_s = section modulus of steel beam.

I = moment of inertia.

d_1 = distance from composite neutral axis to concrete neutral axis.

d_2 = distance from composite neutral axis to steel neutral axis.

f_s = steel stress

f_c = concrete stress

S_{ct} = section modulus for top of concrete.

S_{cb} = section modulus for bottom of concrete.

S_{st} = section modulus for top of steel.

S_{sb} = section modulus for bottom of steel.

M_{dl} = dead load moment.

M_{ll} = live load moment.

S.Comp. = composite section modulus

W = allowable uniform beam load in lb./ft.^{2}

L = beam span

R_t = total load beam reaction

R_l = live load beam reaction

Q = moment of transformed concrete area about composite neutral axis

I.comp. = composite moment of inertia

Quc = useful shear capacity of one shear connector

h = maximum thickness of channel flange

t' = thickness of channel web.

W' = width of channel connector.

$f'c$ = 28 day compressive strength in p.s.i. of 6 x 12 in. concrete cylinders.

Q_{des} = design load on shear connector.

S_{pl} = plastic section modulus of a composite beam.

S_c = section modulus of composite beam.

f_{yp} = yield point strength of steel.

f'_s = steel working stress.

A_r = steel reinforcing area.

M_{sl} = maximum moment in slab.

jd_s = distance between slab reinforcing center line and center of gravity, of concrete compression diagram.

δ = beam deflection.

ABSTRACT

The material herein presented is the result of an investigation of the thermal stresses produced, in a composite steel beam-concrete slab unit, by rapid heating and rapid cooling. The test procedure is described and the results are tabulated for three rapid heating and cooling tests. The theoretical method of determining these stresses is stated and an attempt made to determine the applicability of this theory. A comparison is made between the deflections and stresses actually measured, and those determined theoretically.

From the results obtained, the following conclusions are drawn:

(1) In general, the actual stresses and deflections are larger than those calculated theoretically.

(2) The derived theory does not apply to the determination of temperature stresses due to a temperature differential between the beam and the slab of a composite unit.

(3) The reason that this theory does not apply is because the temperature variation across a vertical section of a composite unit is gradual, rather than changing abruptly at the steel-concrete interface.

(4) The fact that temperature stresses are uniform over the entire span of the beam has been verified.

CHAPTER I

INTRODUCTION

Composite construction is a well established design in the field of highway bridges. This type of construction has several advantages over conventional beam and slab designs; because the steel girders and the concrete slab act as a unit in resisting flexure, smaller girders can be used. This results in shallower construction with greater economy and an increase in stiffness.

A great deal of investigation into composite beam stresses has been carried out notably by I.M.Viest, N.M.Newmark and C.P. Siess at the University of Illinois.[1] Most of this work has dealt with stress distribution in the slab, shear connectors, and steel girders using different types of shear connectors. Studies of relative efficiencies of different types of shear connectors have also been made.

However, little or no investigation has been performed to determine the effect, on composite beam bridges, of rapid heating and cooling such as occur in Canadian climates. Until recently it was assumed that structural concrete and structural steel had approximately the same coefficients of expansion. It was felt, therefore, that when a composite beam was subjected to a rapid temperature change, the concrete and steel would expand approximately equal amounts and negligible temperature stresses would result. No allowance for temperature stresses was made, therefore, in composite beam design.

The fact that concretes have widely varying coefficients of expansion, depending on their proportions and the nature of their aggregates was pointed out by R. David and G. C. Meyerhoff,[3] who listed expansion coefficients for concretes with different types of aggregates. It has also been recognized that the amount and arrangement of reinforcing in a concrete slab affects its thermal expansion coefficient. In addition, because of its relatively bulky cross-section, the concrete slab, in a composite beam-slab unit, heats and cools less rapidly than does the steel beam.

Because of these facts, it is felt that the temperature stresses set up in a composite beam, when it is subjected to a rapid temperature change, are due to two causes:

(1) A difference in the thermal expansion coefficients of the steel beam and the concrete slab.

(2) A slower rate of heating and cooling of the slab than of the beam.

A theoretical method of determining composite beam temperature stresses has been derived by Messrs. R. David and G. C. Meyerhoff.

This thesis is an attempt to check the applicability of this theory to the problem of the rapid heating and cooling of a composite beam-slab unit.

CHAPTER II

THEORETICAL CONSIDERATIONS

A portion of a composite beam is shown in elevation in Fig. 1. Consider a section of the beam a unitdistance from a datum line. If the beam has been kept at the temperature at which the concrete set, the strain diagram for the cross-section would be as shown in Fig. 1(a).

Assume that the steel and concrete portions have different coefficients of expansion.

Then, if the beam were cooled and the beam and slab were allowed to contract independently, the section would assume the shape shown in Fig. 1(b).

However, due to the shear capacity between the slab and the beam, provided by the shear connectors, the beam actually deforms as shown in Fig. 1(c).

To prevent relative movement at the steel-concrete interface, forces N_S and N_C must be applied to the steel and concrete respectively as shown in Fig. 2(a). The force system shown in this figure can then be replaced by that shown in Fig. 2(b).

Since the beam is in equilibrium at the section shown:

$$N_S = N_C = N \quad \ldots\ldots\ldots\ldots\ldots\ldots (1)$$

and $$M_S \neq M_C = N \times z \quad \ldots\ldots\ldots\ldots\ldots\ldots (2)$$

Since there is no slip on the contact surface:

$$e_S \neq e_C = \Delta \quad \ldots\ldots\ldots\ldots\ldots\ldots (3)$$

But for any material, $e = f/E$

Therefore: $$f_S/E_S \neq f_C/E_C = \Delta \quad \ldots\ldots\ldots\ldots\ldots\ldots (4)$$

Since the beam and slab are tied together by the shear connectors, they have the same radius of curvature: R.

Therefore: $$\frac{1}{R} = \frac{M}{EI} = \frac{M_s}{E_s I_s} = \frac{M_c}{E_c I_c} = \frac{Nz}{E_s I_s + E_c I_c} \quad \ldots (5)$$

From the stress system in Fig. 2(b), it can be seen that the stress at any point across the section will be the sum of the direct stress due to the loads N and the flexural stress due to the moments M_s and M_c.

Using a transformed section with n= 10, the direct stresses will be: $f_c = N/A_c$

and $f_s = N/A_s$

The flexural stresses will be:

$$f_c = \pm \frac{M_c\, t}{2I_c}$$

and $$f_s = \pm \frac{M_s\, c}{I_s}$$

Multiplying Equation (5) by E_c:

$$\frac{M_c}{I_c} = \frac{Nz}{nI_s + I_c} \quad \ldots\ldots\ldots (6)$$

Setting: $$B = \frac{1}{nI_s + I_c}$$

Then: $$\frac{M_c}{I_c} = NzB \quad \ldots\ldots\ldots (7)$$

From (5) and (7): $$\frac{M_s}{I_s} = n\frac{M_c}{I_c} = nNzB \quad \ldots\ldots (8)$$

The stresses at critical points across the section are, therefore, given by the following equations:

$$f_{ct} = \frac{N}{A_c} - NzBt/2 \quad \ldots\ldots (9)$$

$$f_{cb} = \frac{N}{A_c} + NzBt/2 \quad \ldots\ldots (10)$$

$$f_{st} = \frac{N}{A_s} + NznBc \quad \ldots\ldots (11)$$

$$f_{sb} = \frac{N}{A_s} - NznBc \quad \ldots\ldots\ldots\ldots\ldots\ldots\ldots\ldots \quad (12)$$

To relate the differential contaction "Δ" to the shear forces "N", which it induces, consider Equation (4):

$$\Delta = \frac{f_s + f_c}{E_s} = \frac{N/A_s + NznBc}{E_s} + \frac{N/A_c + NzB\ t/2}{E_s/n}$$

$$= \frac{N}{E_s}\left(z^2 nB + \frac{1}{A_s} + \frac{n}{A_c}\right)$$

Therefore:

$$N = \frac{E_s \Delta}{\frac{1}{A_s} + \frac{n}{A_c} + z^2 nB} \quad \ldots\ldots\ldots\ldots (13)$$

The differential contraction used in the above theory to determine the temperature stresses could also be caused by a temperature differential between the steel and the concrete. However this theory would be applicable only if the steel beam and the concrete slab each had constant temperatures across their respective cross-sections.

If the steel and concrete are free to expand or contract independently, with the same contraction coefficient, α_s, and if there is a temperature differential of "T" degrees between them, the difference in expansion or contraction per unit length is:

$$\Delta = \alpha_s \times T \quad \ldots\ldots\ldots\ldots\ldots\ldots\ldots\ldots \quad (14)$$

When the coefficients of expansion of concrete and steel are different, temperature stresses are present at any temperature other than that at which the concrete set. If the difference between the concrete setting temperature and the actual temperature of the beam at any time is "T" degrees, and if the steel and concrete are free to expand or contract independently, then their difference in length per unit of length is:

$$\Delta = (\alpha_s \alpha_c)\ T \quad \ldots\ldots\ldots\ldots\ldots\ldots\ldots \quad (15)$$

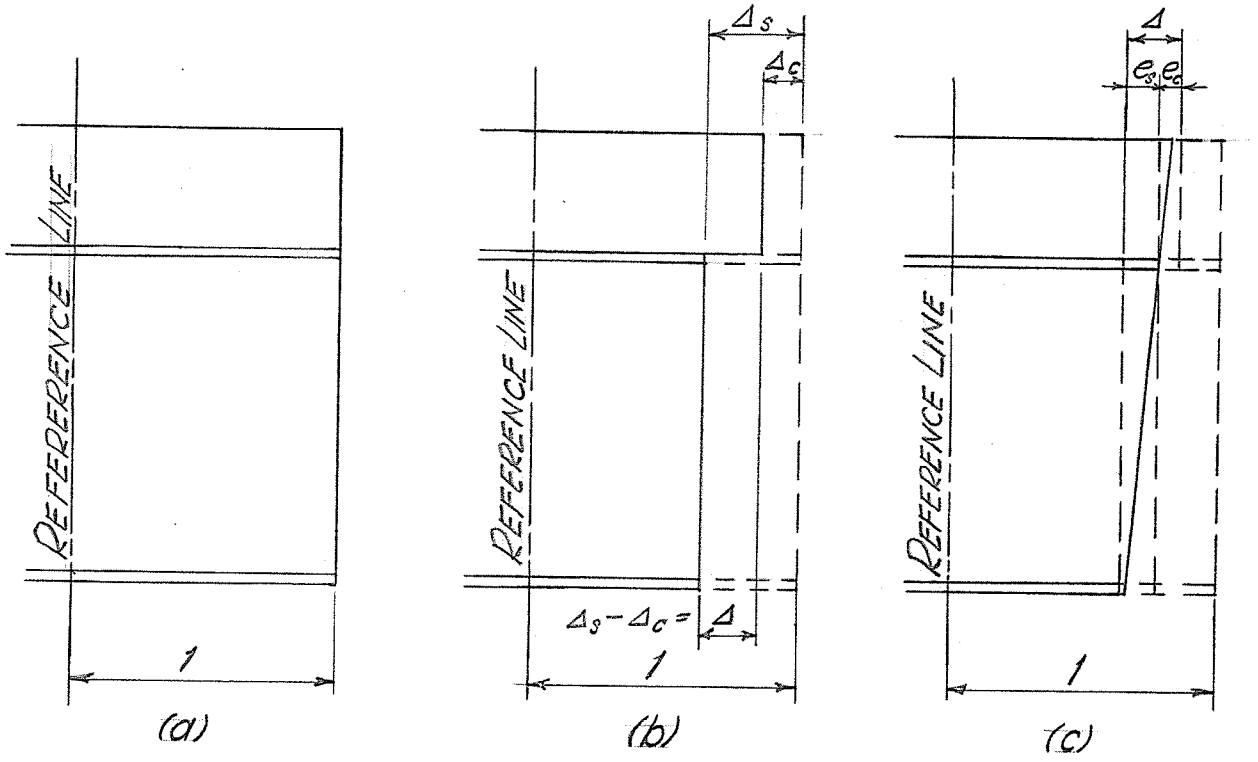

STRAIN DIAGRAM

FIG. 1

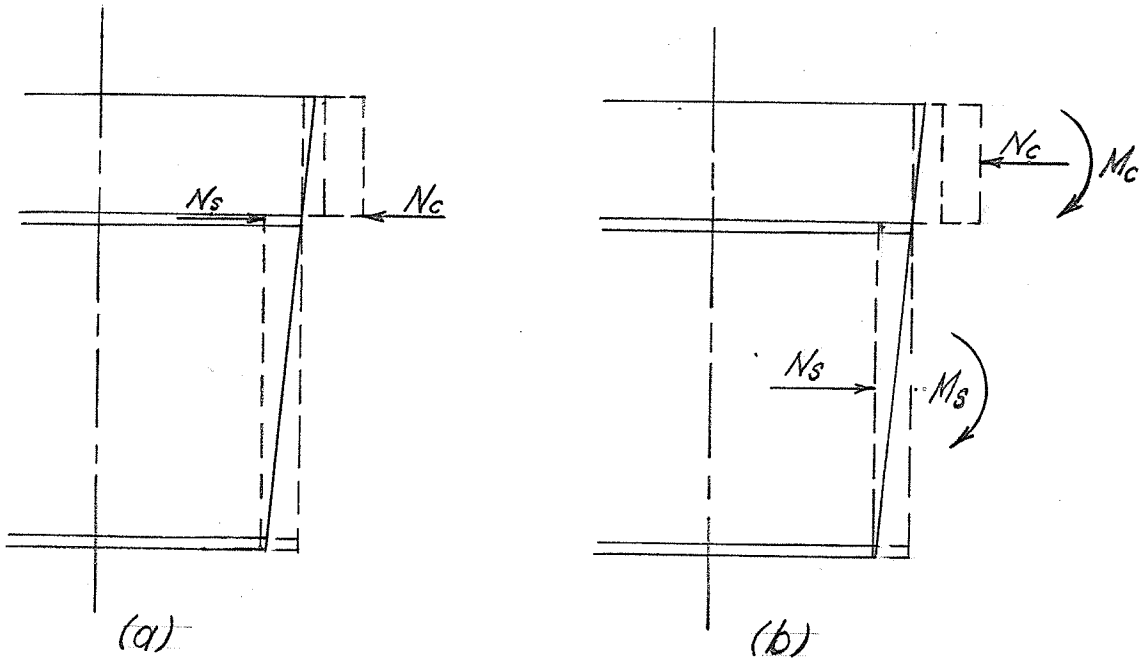

STRESS DIAGRAM

FIG. 2

It can be seen, therefore, that by using equations (9) to (15) one is able to calculate the stress at any point in a composite beam, due to a temperature differential between the slab and the steel beam or due to the fact that the slab and the beam have different thermal expansion coefficients.

Since "Δ" from equations (14) and (15) is a unit deflection, it can be seen from equation (13) that N is a force per unit of length. Furthermore, since a random cross-section was used to determine the value of N, this force must be a constant shear force along the steel-concrete interface over the whole length of the beam. This constant shear force, then, must produce a constant moment over the whole span of the beam, of: $M = N \times Z$. This constant moment, in turn, produces a similar stress distribution over any cross-section through the beam.

CHAPTER III

EXPERIMENTAL PROCEDURE

Design and Construction of Beam

In choosing the size of the steel beam and the dimensions of the concrete slab for the test unit, an attempt was made to approximate the scaled down proportions of an average composite bridge girder and slab unit. The average composite dimensions were determined from several examples shown in the "Alpha Construction Engineering Handbook".[4] The slab thickness was purposely made greater than the scale-down thickness to cause the slab to cool more slowly and possibly accentuate the stresses produced.

The steel beam selected was a 14 x $6\frac{3}{4}$ WF 30 with a cross-section as shown in Fig. 3(b). Fig. 3(a) shows an elevation of the steel beam, the span of which was 24'-0 centre to centre of supports. A slab 5 in. thick by 3'-6 wide was used.

The properties of the composite section are shown in Fig. 4. The beam was designed, using the transformed section method, as follows:

Steel Beam: 14 WF30 $d = 13.86$ in. $A = 8.81$ in.^{2}

$I_S = 289.6$ in.^{4} $S_S = 41.8$ in.^{3}

Concrete Slab: $A_C = 42 \times 5 - 210$ in.^{2}

$I_C = 210 \times 5^2/12 = 437.5$ in.^{4}

$n = E_S/E_C = 10$

Location of Composite N.A.:

To locate the composite neutral axis, the moment of the transformed concrete area about the steel neutral axis was used.

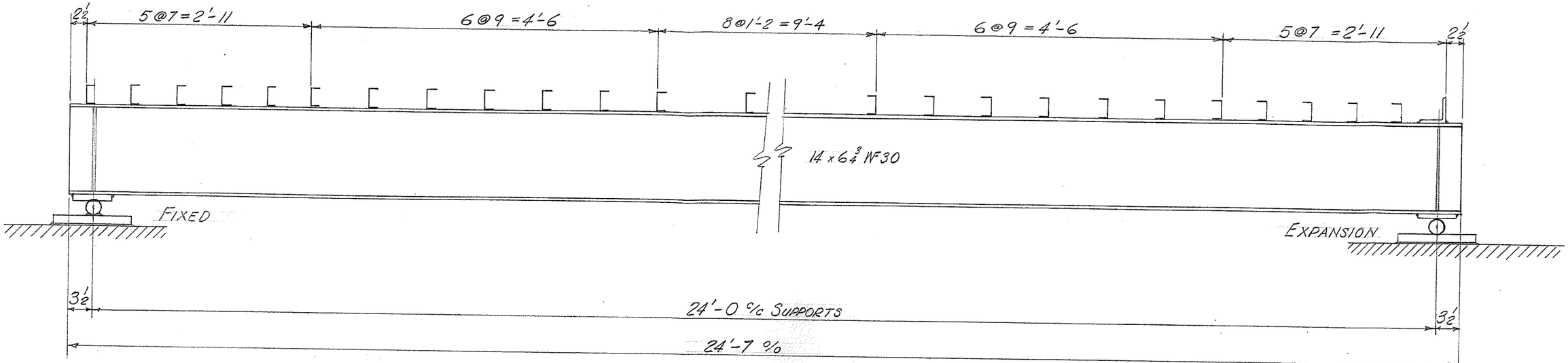

ELEVATION OF BEAM

SCALE: ¾"=1'-0

(a)

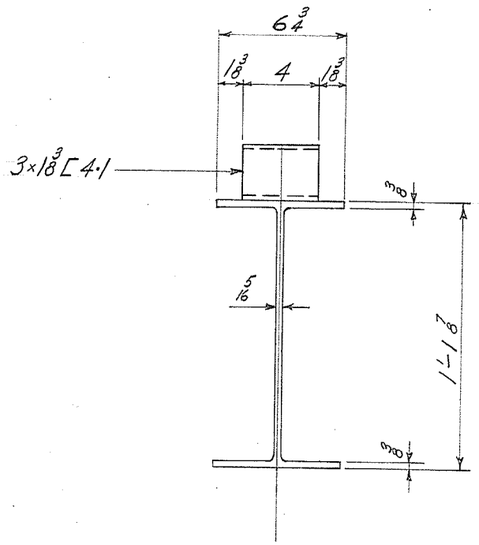

TYPICAL INTERIOR SECTION

SCALE: 1½"=1'-0

(b)

DETAIL OF STEEL BEAM

FIG. 3

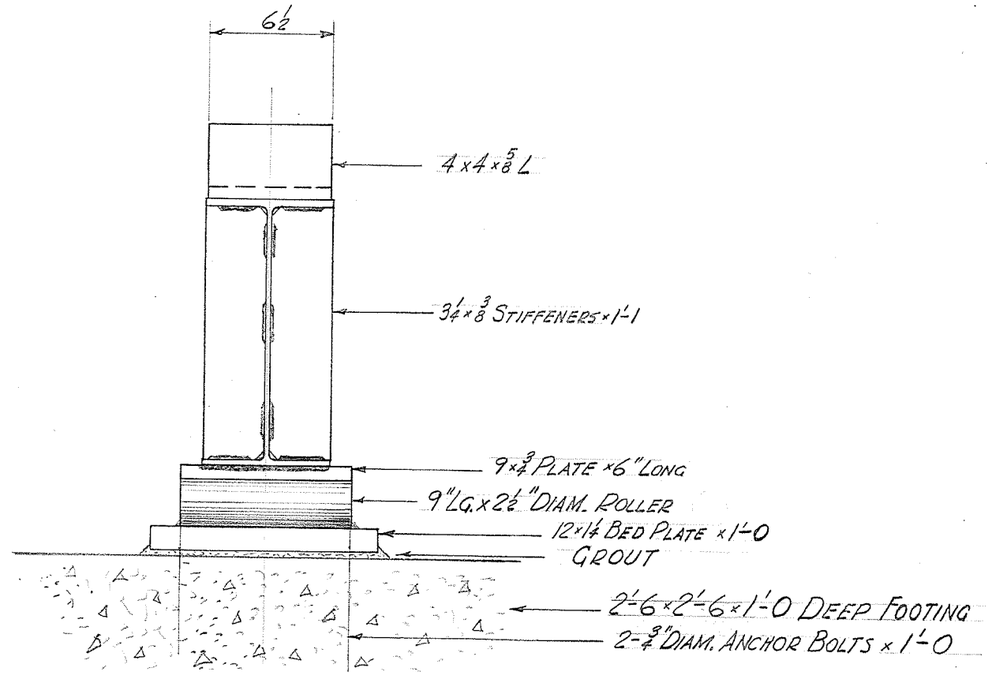

SECTION AT EXPANSION END

SCALE: 1½"=1'-0

(c)

210/10 = 21.0 21.0 (2.5 / 6.93) = 21 x 9.43 = 198.0

8.81
29.81

198.0/29.81 = 6.64 in.

The composite neutral axis is, therefore, located 6.64 inches above the steel neutral axis as shown in Fig. 4.

Determination of Composite Moment of Inertia:

Concrete I	= 43.75
$A_c \ d_1^2 = 21.0(2.79)^2$	= 163.6
Steel I	= 289.6
$A_s \ d_2^2 = 8.81 \ (6.64)^2$	= 390.0
Composite I	= 886.95 $in.^4$

Determination of the Section Moduli:

$$S_{ct} = \frac{886.95 \times 10}{5.29} = 1678 \text{ in.}^3$$

$$S_{cb} = \frac{886.95 \times 10}{0.29} = 30600 \text{ in.}^3$$

$$S_{st} = 886.95/0.29 = 3060 \text{ in.}^3$$

$$S_{sb} = 886.95/13.57 = 65.5 \text{ in.}^3$$

Determination of Maximum Allowable Moments and Load:

The maximum allowable moments on the beam to prevent over-stressing of the steel or the concrete are:

Steel: $M_s = f_s \times S_{sb} = 20 \times 65.5 = 1310$ in.kips = 109.0 ft.kips

Concrete: $M_c = f_c S_{ct} = 1.0 \times 1678 = 1678$ in.kips = 140.0 ft.kips

The erection of temporary shoring to carry the dead load until the concrete sets is seldom practical. When no shoring is used, the composite beam has to be designed to carry the total live load plus dead load. The beam used in this test was, therefore, designed and

constructed on this basis.

The dead load of the beam is: 30 + 10 + (210 x 150/144) = 0.259 kips/ft. This dead load caused a moment of:

$$M_{dl} = 0.259 \times 24^2/8 = 18.7 \text{ ft.kips}$$

This moment causes a stress at the bottom of the beam of:

$$f_s = M_{dl}/I_s = 18.7 \times 12/41.8 = 5.37 \text{ kips/in.}^2$$

The remaining allowable stress in the bottom of the beam is:

$$20 - 5.37 = 14.63 \text{ kips/in.}^2$$

The remaining composite beam moment value is then:

$$M = f_s \times S = 14.63 \times 65.5 = 959 \text{ in.kips} = 79.9 \text{ ft.kips}$$

The allowable uniform live load is then:

$$W = 8M/L^2 = 8 \times 79.9/24^2 = 1.11 \text{ kips/ft.}$$

The total load reaction for the beam is then:

$$R_t = (1.11 + 0.26) \times 12 = 16.45^K$$

The live load reaction is:

$$R_l = 1.11 \times 12 = 13.3^K$$

Design of Shear Connectors

To determine the shear connector spacing for a composite beam, it is necessary to calculate the maximum shear per inch along the steel-concrete interface. To do this, the value of Q/I must be calculated for the composite section; where Q is the moment of the transformed concrete area about the composite neutral axis. For the section used, this was found to be:

$$Q/I_{comp} = \frac{21.0 \times 2.79}{886.95} = 0.066 \text{ /in.}$$

To determine the shear value of one shear connector, the design formulae given in "Shear Connector Design Data"[2]

were used. A 3 C 4.1 by $4\frac{1}{2}$ in. long was chosen as the shear connector size.

The useful shear capacity of one such shear connector, assuming 3,000 psi concrete, was then determined to be:

$$Quc = 182\ (h + \tfrac{1}{2}t')\ W'\ \sqrt{f'c} = 182(0.462)4.5(\sqrt{3000}) = 21{,}100 \text{ lb.}$$

From "Public Roads - Volume 28, No. 1"[5] the useful capacity of a shear connector divided by its design capacity is given by:

$$Quc/Qdes = \frac{Spl}{Sc} \times \frac{fyp}{fs'}\ (1 + CsCm) - Cm$$ for a beam without shoring. $\frac{Spl}{Sc}$ is the ratio of the elastic section modulus to the plastic section modulus for the beam. Its value was determined from Table 2, Page 12 of the above reference and was approximately 1.45 for the slab and beam section used.

The factor Cm is the dead load beam moment divided by the live load moment and in this case was determined to be:

$$Cm = \frac{Mdl}{Mll} = \frac{18.7}{79.9} = 0.234$$

For the section, the factor $Cs = \frac{Sc}{Ss}$ was determined to be:

$$Cs = \frac{65.5}{41.8} = 1.57$$

Substitution of these values in the above equation gives:

$$Quc/Qdes = 1.45(\tfrac{33}{20})\ (1 + 0.234 \times 1.57) - 0.234 =$$

$$(1.45 \times 1.65 \times 1.367) - 0.234 = 3.270 - 0.234 = 3.036$$

The shear lug design value was, therefore, determined to be:

$$Qdes = \frac{21.1}{3.036} = 6.97^{k} \quad \text{say, } 7^{k}$$

The following table was then set up to determine the theoretical shear lug spacing for the beam.

Distance From R_1	Shear	Q/I	Shear/In.	Lug Value	Theoretical Spacing
0'-0	13.3	0.066	0.877	7^k	8.0"
3'-0	9.98	"	0.658	"	10.6"
6'-0	6.65	"	0.439	"	15.9"
9'-0	3.32	"	0.219	"	32.0"
12'-0	0.00	"	0.000	"	--

The shear values used in this table were obtained from the live load shear diagram for the beam. The shear per inch at the steel-concrete interface is equal to the total shear multiplied by Q/I. The theoretical spacing is the shear lug value divided by the shear per inch determined above. The actual shear connector spacing shown in Fig. 3(a) was obtained by staying within the limitations of the above theoretical spacing. Fig. 3(c) and Fig. 7(b) show the 4 x 4 x 5/8 angle that was used to replace the last shear connector over the expansion support. This heavy angle was used to determine whether or not a heavy, stiff shear connector at the end of the span affected the shear distribution along the top of the steel beam.

Design of Slab

The slab was designed to sustain a uniformly distributed live load approximately three times as great as that for which the beam was designed. This was done so that if it were ultimately desired to load the beam to failure, the slab would not fail transversely.

The uniform design load for the beam was

calculated to be 1.11 kips/ft. The design live load chosen for the slab was 3.0 kips/ft. For a 3'-6 slab, this corresponded to a load of 30/3.5 = 0.857 kip/ft.^{2} The slab dead load was 5/12 x 50 = 0.063 kips/ft.^{2} The total design load for the slab was, therefore, 0.857 + 0.063 = 0.920 kips/ft.^{2}.

The slab was treated as two cantilevers supported over the beam centre line. The maximum slab moment was then:

$$M_{sl} = 0.920 \times 1.75^2/2 = 1.41 \text{ ft. kips}$$

This moment necessitated a steel area per foot of slab length of:

$$A_R = \frac{M_{sl}}{f_s j d_s} = \frac{1.41 \times 12}{20 \times 0.866 \times 3.5} = 0.279 \text{ in.}^2$$

This steel area was supplied by number 4 reinforcing bars spaced at 8 inches, which provided a steel area of 0.29 in.^{2}/ft. of slab.

Ample longitudinal reinforcing was supplied by 8 number 4 bars. These bars provided an excess over the theoretically required temperature steel area, which was:

$$A_R = 0.002 \times 42 \times 5 = 0.42 \text{ in.}^2$$

The area actually provided was 1.57 in.^{2} This excess was provided in an attempt to avoid cracking of the slab due to the wide temperature variation. In addition to this longitudinal steel, a 3/8 in. diameter deformed rod was placed $\frac{3}{4}$ in. from the top of the slab over the beam centre line. This rod was suitably prepared and strain gauges were cemented to it at five points.

Fig. 5 shows the slab reinforcing used

As was the concrete slab, the supporting pier

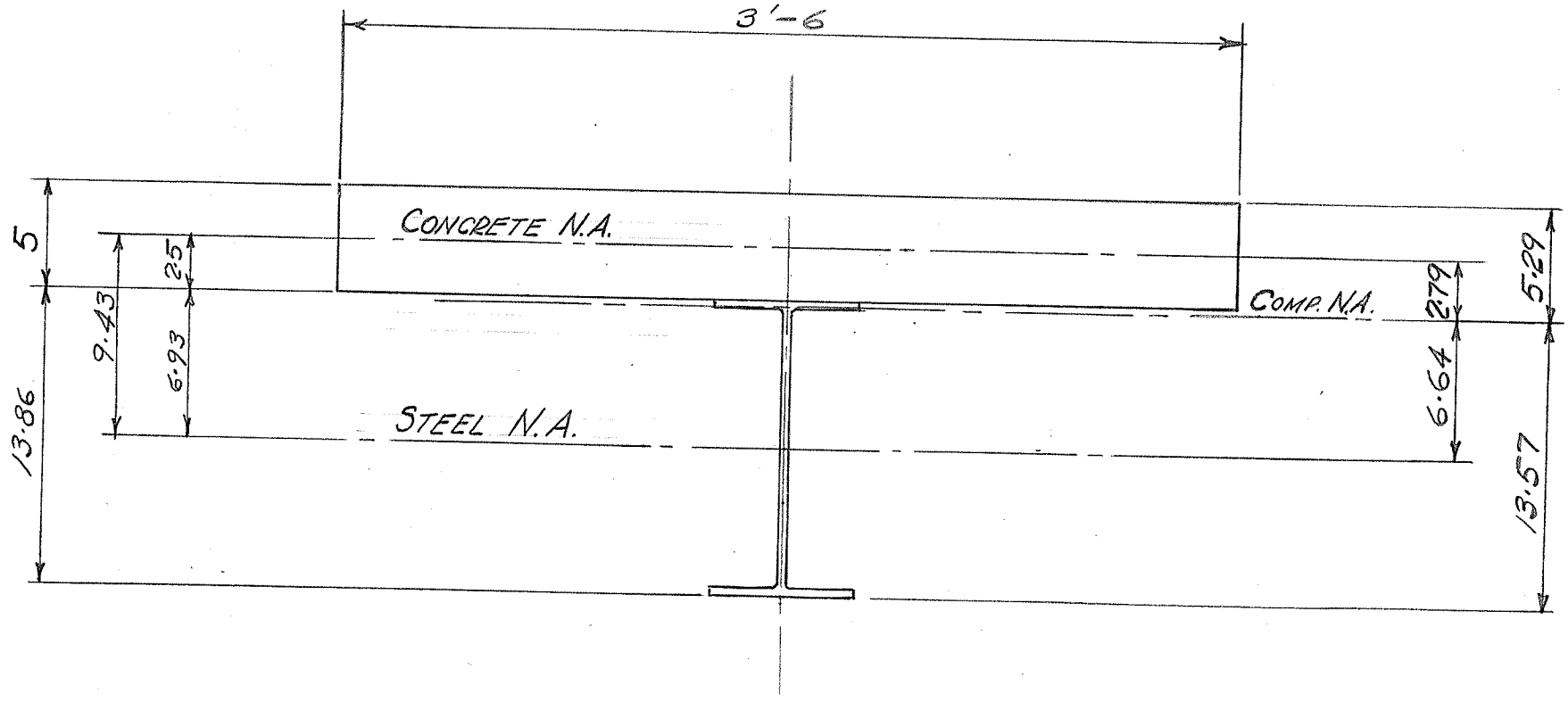

DIMENSIONS OF COMPOSITE SECTION

FIG. 4

members were designed to support the dead load plus approximately three times the live load that the beam was designed to carry. The reaction value for which the pier members were designed was

$$((3 \times 1.11) / 0.26) \times 12 = 43.1 \text{ kips}$$

As illustrated in Fig. 3, the beam was supported on 2'-6 square footings 1'-0 deep. One end of the beam rested on a $2\frac{1}{2}$ in. diameter rocker and the other on a $2\frac{1}{2}$ in. diameter roller. To prevent the introduction of moments at the supports, due to longitudinal components of the reactions, the bed plates were milled and carefully levelled on $\frac{1}{2}$ in. of grout.

As was mentioned previously, it is usually uneconomical to temporarily shore the girders until the composite bridge slab sets. To make the problem as realistic as possible, the slab was supported on the steel beam until it set. To accomplish this, special frames as shown in Fig. 6 were used to support the concrete forms. Eleven of these 2 in. x 4 in. frames were constructed from a template. The use of a template insured greater accuracy and uniformity of slab dimensions. Theframes were bolted together with 3/8 in. diameter carriage bolts. This again provided greater accuracy of assembly, greater strength, and more ease in dismantling the forms.

Fig. 7 and Fig. 8 show the steps followed in placing the steel beam, constructing the forms, and pouring the slab. Fig. 7(a) shows the steel beam before construction of the forms. Fig. 7(b) and Fig. 7(c) show the expansion and fixed beam supports respectively. Fig. 7(b)

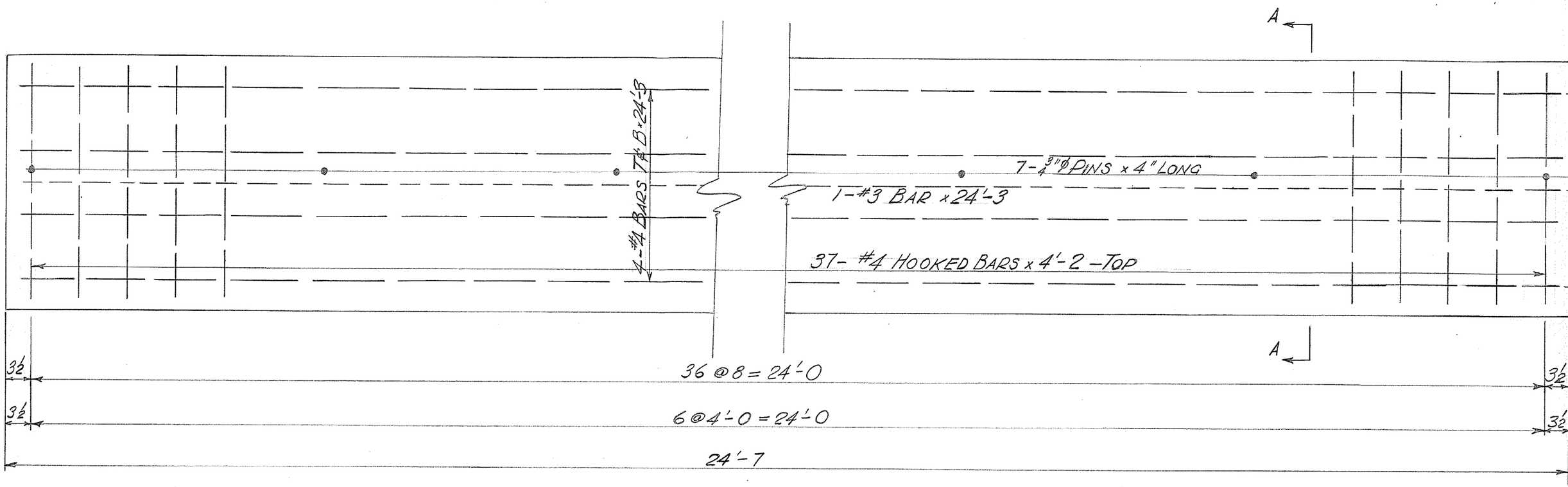

PLAN OF CONCRETE SLAB REINFORCING

SCALE: 3/4" = 1'-0

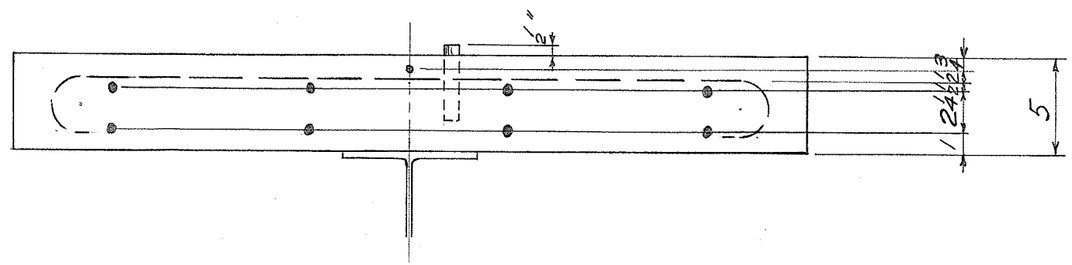

SECTION A-A

SCALE: 1½" = 1'-0

FIG. 5

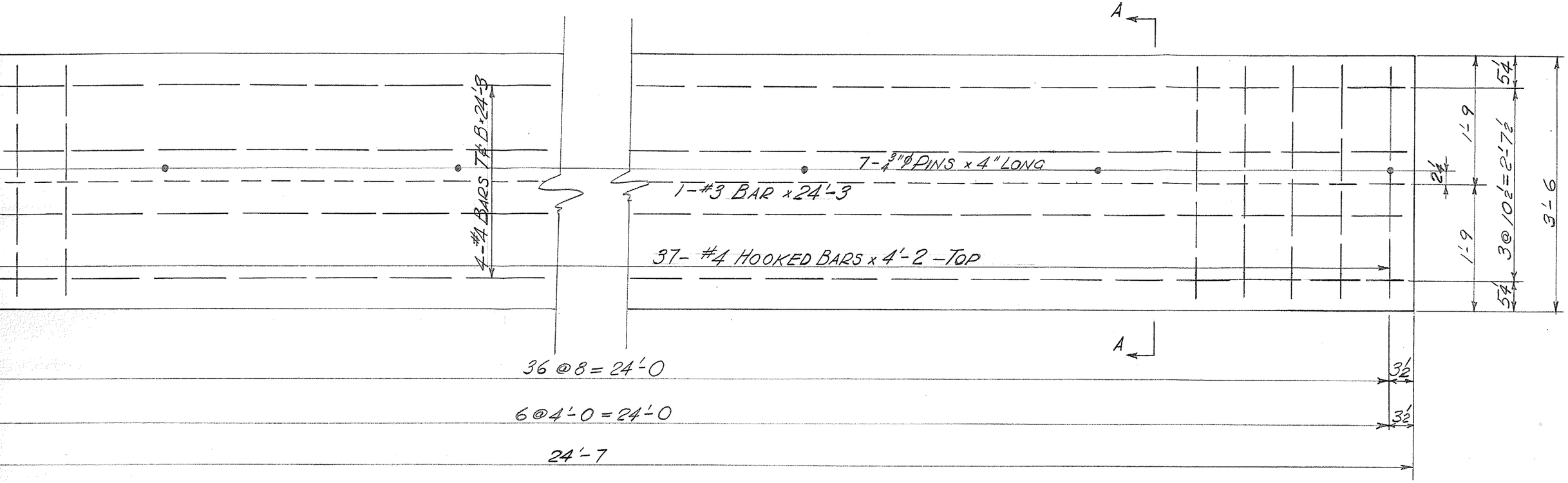

PLAN OF CONCRETE SLAB REINFORCING

SCALE: 3/4"=1'-0

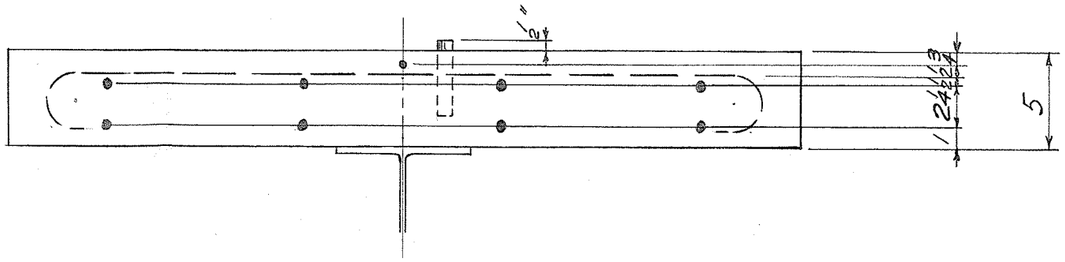

SECTION A-A

SCALE: 1½"=1'-0

FIG. 5

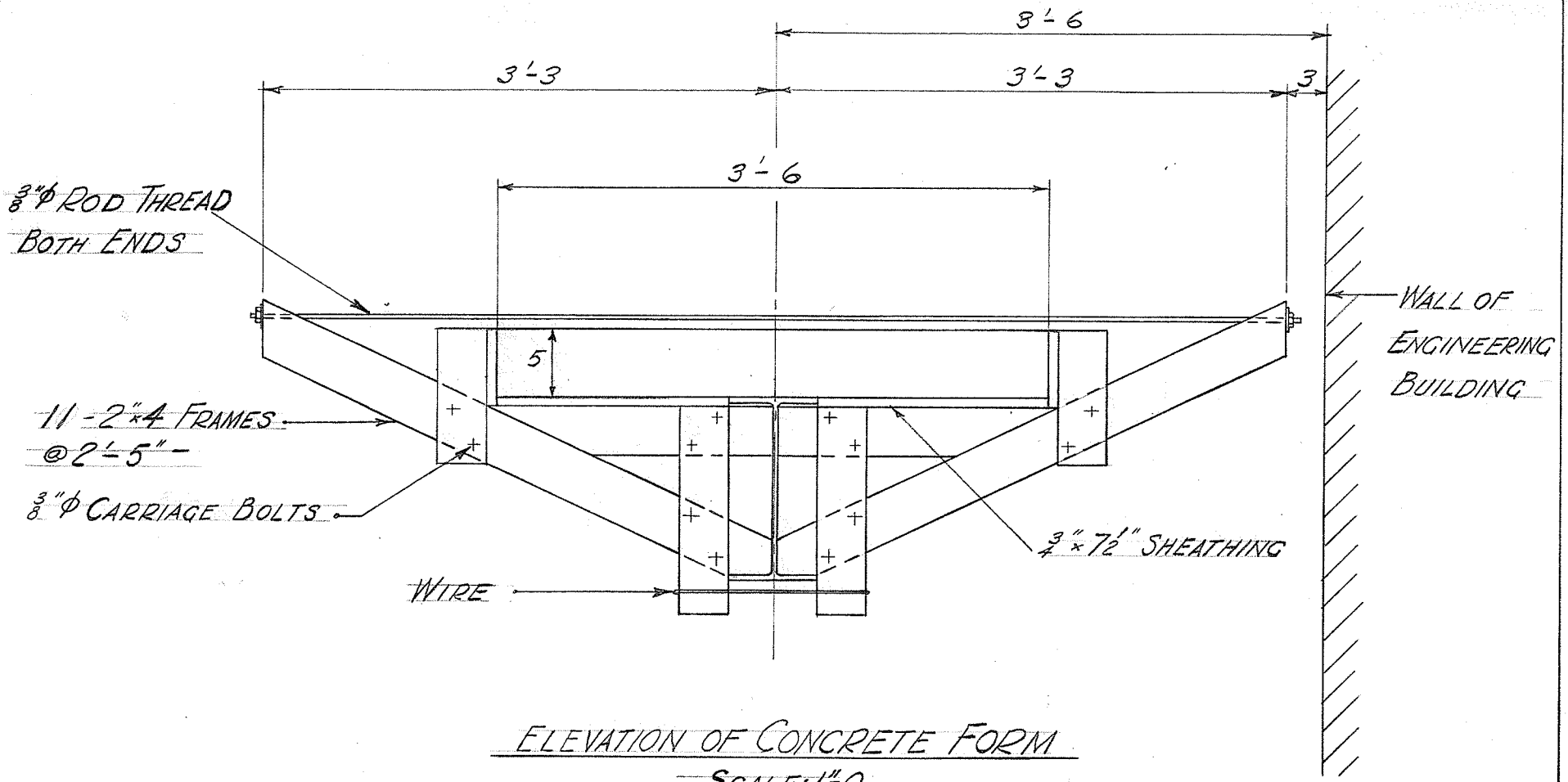

ELEVATION OF CONCRETE FORM
SCALE: 1"=0

FIG. 6

(81)

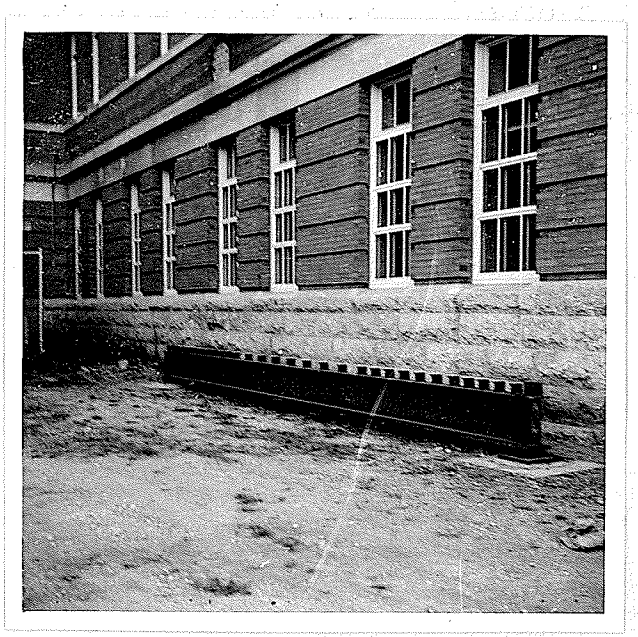

(a)

(b)

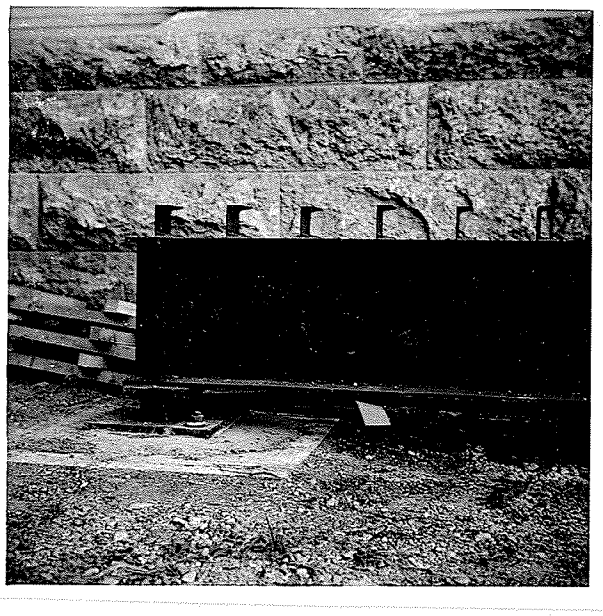

(c)

(d)

Steps in Construction of Beam-Slab Unit

Fig. 7

(a)

(b)

(c)

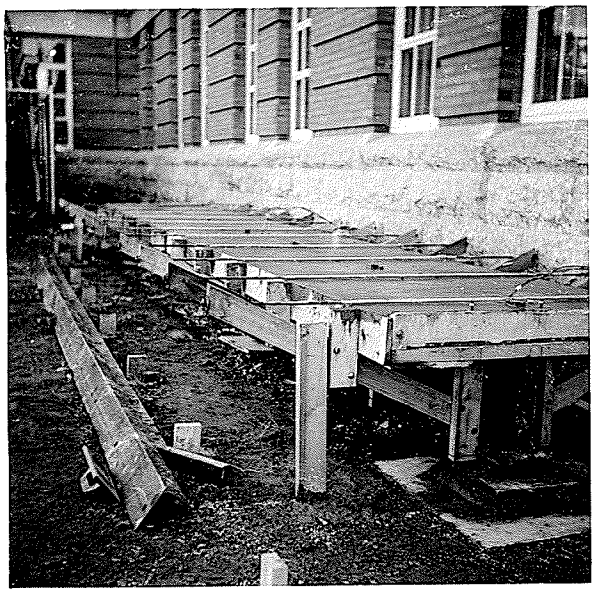

(d)

Steps in Construction of Beam-Slab Unit

Fig. 8

also shows the 4 x 4 x 3/8 in. angle used to replace the regular end channel shear lug at the expansion end.

Two views of the triangular frames in position on the beam are shown in Fig. 7(d) and 8(a). Fig. 8(b) shows the forms after the sheathing was in position and had been oiled. The reinforcing steel is shown in position in Fig. 8(c). This picture also shows the 3/8 in. diameter bar to which the strain gauges were cemented and the wooden blocks used to leave access to this bar after the slab was poured. The necessary pins, thermocouples, and bolts are shown in position in the concrete.

The concrete used was a transit mix 3,500 p.s.i. concrete. Two 6 in. diameter test cylinders were taken and loaded to failure after 28 days. The results of these compression tests are shown on Page 47 and indicate an average 28 day compressive strength of 4,675 p.s.i.

A one foot long beam and slab section was poured at the same time as the composite beam. Fig. 16(a) shows this section which was to be used to carry dummy strain gauges. This section was poured by suspending the steel beam section over the slab as the picture illustrates. However, it was later felt that the temperature distribution in this section would be different than that in the beam being tested. This section was, therefore, destroyed and a one foot long section of exactly the same cross-section as the composite beam constructed, in the same manner, to replace it. In a further attempt to obtain the same temperature distribution in this section and the section being tested, the ends of the beam and slab were

ENGINEERING BUILDING

7 PANELS @4'-0=28'-0

A

A

PLAN OF ENCLOSING BUILDING

SCALE: $\frac{3}{4}$"=1'-0

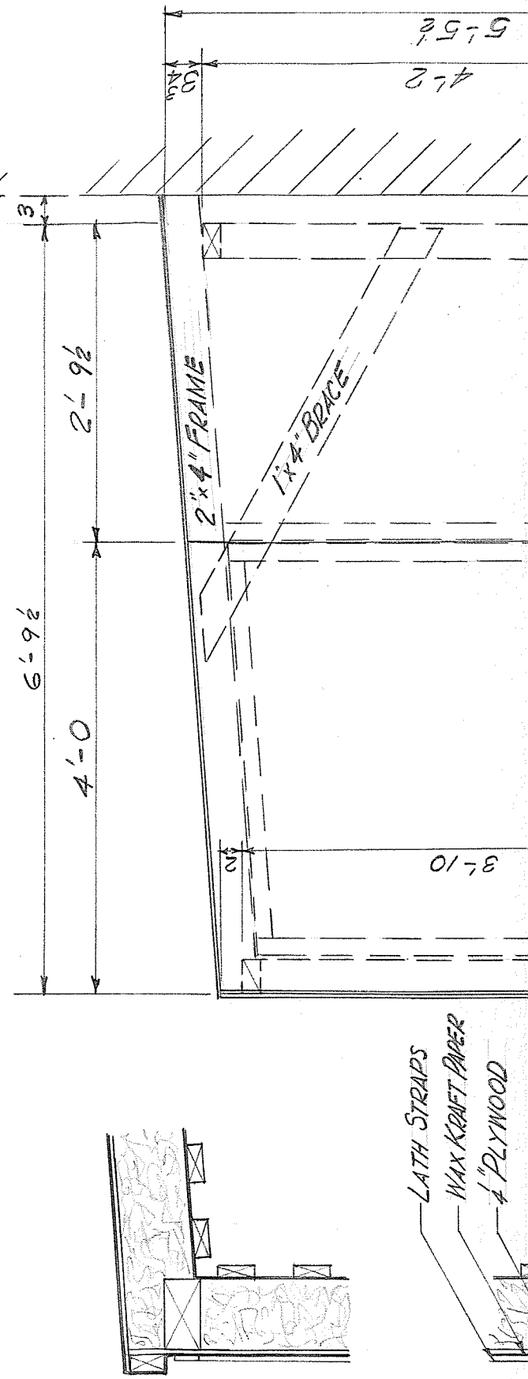

FIG. 9

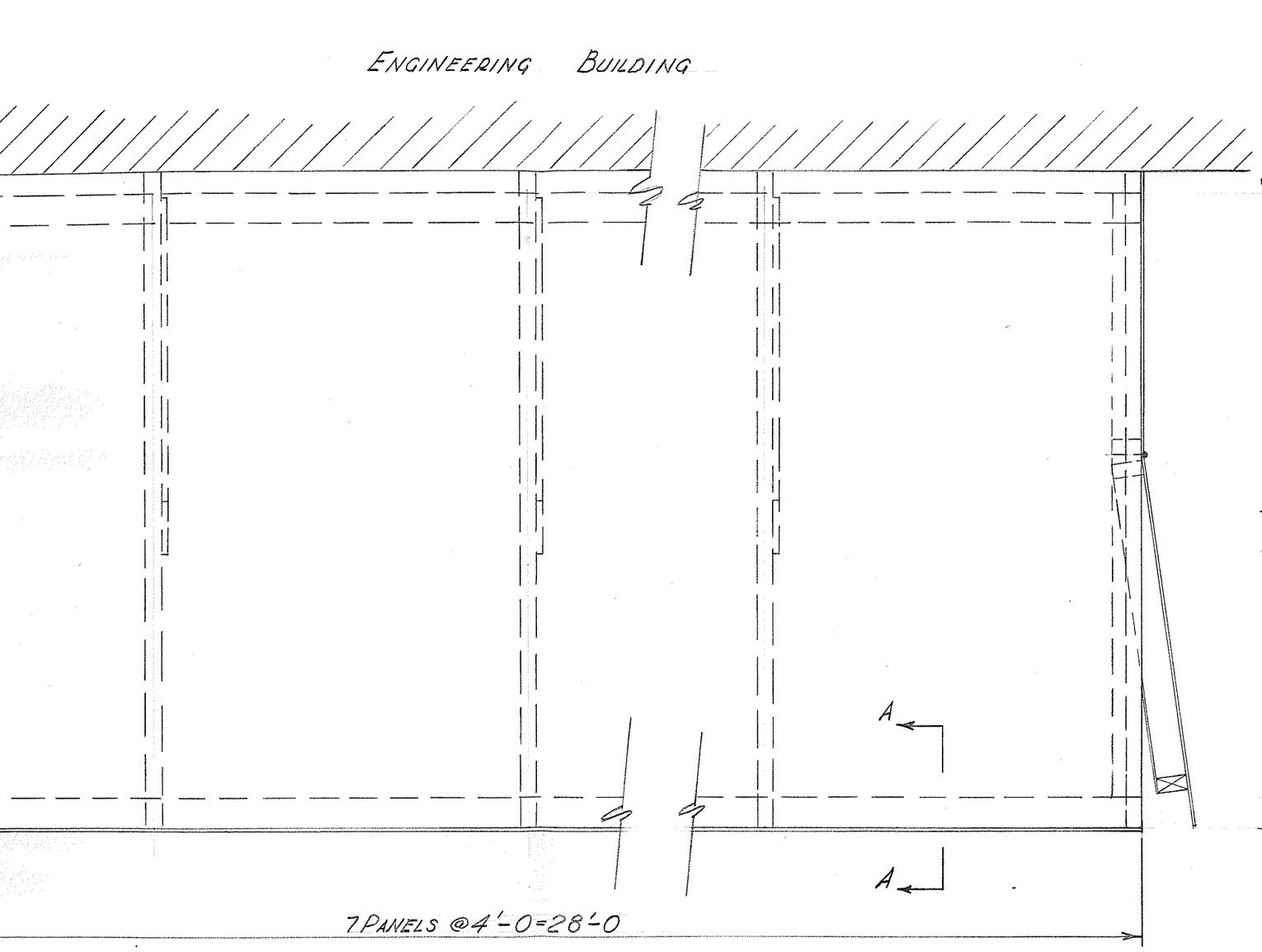

PLAN OF ENCLOSING BUILDING
SCALE: 3/32" = 1'-0

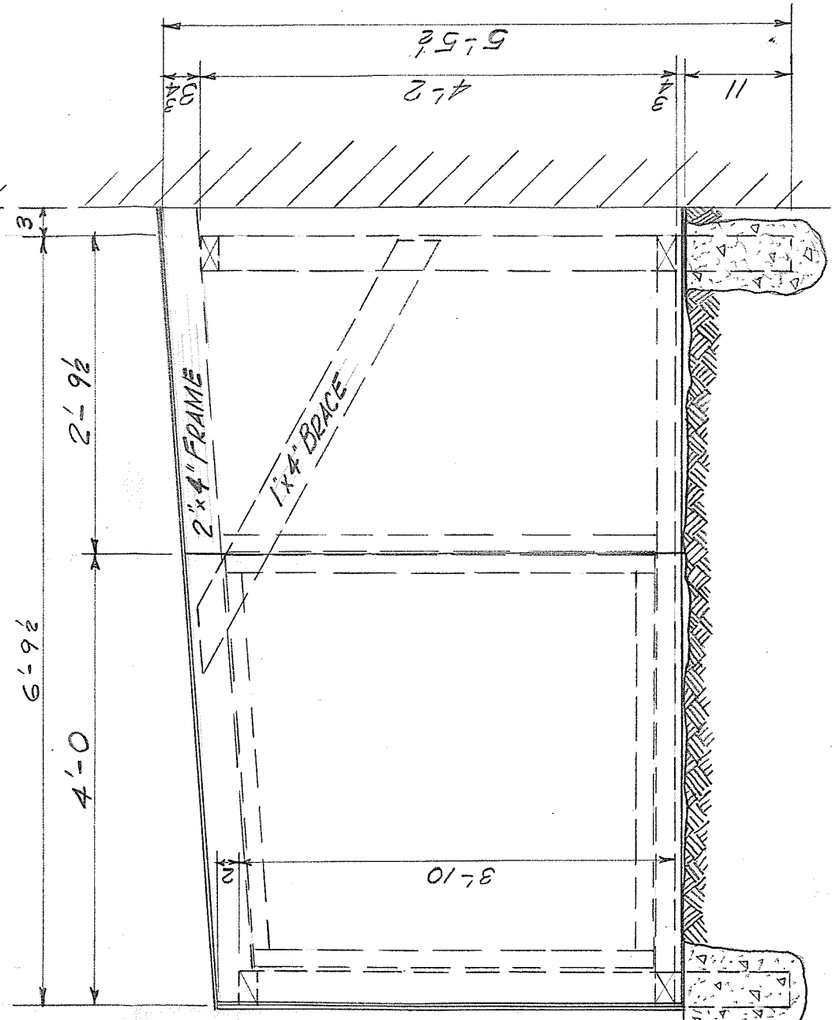

END ELEVATION
SCALE: 3/32" = 1'-0

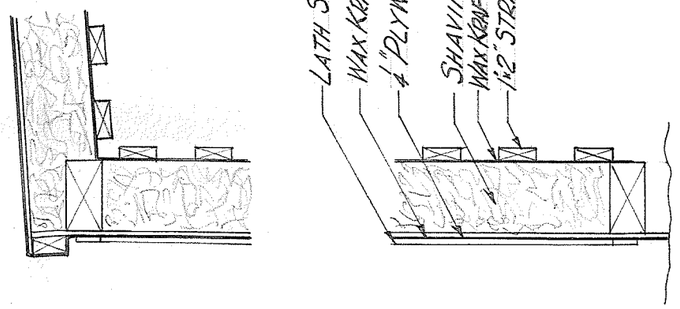

SECTION A-A
SCALE: 1½" = 1'-0

FIG. 9

insulated with fibreglass insulation. Fig. 16(b) and Fig. 16(c) show this section located at the end of the actual beam with the insulation in position.

For the purpose of measuring beam deflections, $\frac{3}{4}$ in. diameter pins 4 in. long were set in the slab at 4 foot intervals over the span. The location of the bars is shown in Fig. 5. In addition, 3/8 in. diameter bolts were set over each support. These bolts were later to hold small bearing plates supporting the two 6 x 4 x 3/8 in. angles used for measuring the deflections. Fig. 10(d) shows these angles resting on the bearing plate at the fixed support. Six thermocouples were also embedded in the concrete: three over the expansion support and three at midspan.

Construction of Enclosing Building and Heating Facilities

After the beam construction was completed, a hut 7'-0$\frac{1}{2}$ wide x 28'-0 long was built over it. Fig. 9 shows the dimensions and details ofconstruction of the hut. Two doors approximately 4'-0 by 4'-0 were located, one at either end of the hut, as illustrated in the drawing.

For the foundation of the hut, 2 x 4's 1'-0 long were set in concrete. The 2 x 4 frame was then constructed and sheathed with $\frac{1}{4}$ in. plywood. The plywood was covered by medium weight wax kraft paper strapped on the outside. The insulation consisted of shavings, and in a few places, of fibreglass bats held in place by a second layer of wax kraft paper strapped to the studs and rafters by 1" x 2" strapping. To help insulate the building, soil was banked up approximately a foot high around it.

(a)

(b)

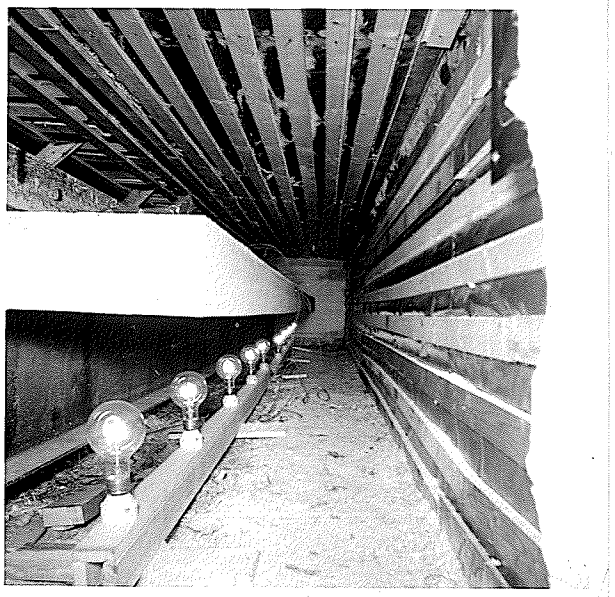

(c)

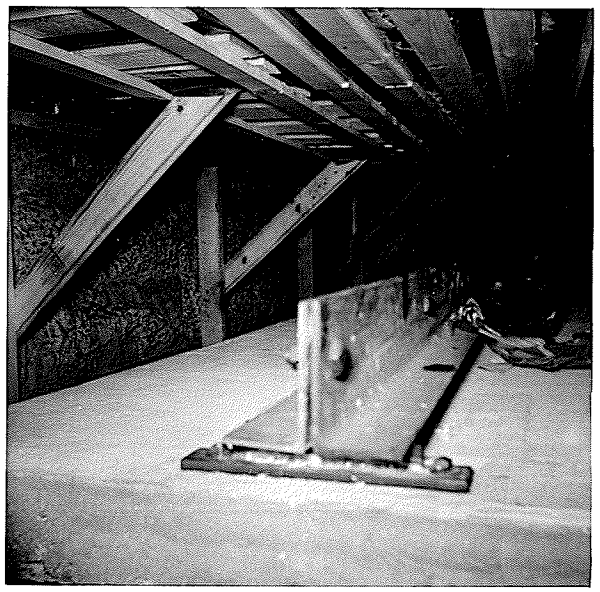

(d)

Views of Enclosing Building

Fig. 10

The construction of the doors was similar to that of the walls and roof. Figs. 10(a) and (b) show two exterior views of the building, while Figs. 10(c) and (d) show interior views.

To heat the building, eighteen 250 watt-120 volt heat lamps were used. The lamps were arranged in six banks of three. It was possible to turn each bank on separately. The lamp sockets were fastened to frames made from $\frac{3}{4}$ in. sheathing. As shown in Fig. 11, the lamps were located in two rows of nine, at a 2'-9 spacing. The frames were set on the ground directly under the edges of the slab. To circulate the air in the hut, two fans were used, one at either end of the beam. Fig. 10(c) shows the lamps operating along one side of the beam.

Instrumentation

For a rapid, accurate determination of the temperature, at various points in the steel beam and the concrete slab, ten copper-constantin thermocouples were positioned on the beam-slab unit as illustrated in Fig. 13. Thermocouples one, two, and three were embedded in the slab over the expansion support at depths of 4 in., $2\frac{1}{2}$ in., and 1 in. respectively. Thermocouples 4, 5 and 6 were similarly located in the slab at the midpoint of the span. The purpose of these six couples was to obtain a reliable determination of the temperature distribution in the slab as it cooled. Gauges 3 and 6 were also used to determine the temperatures of the strain gauges located $\frac{3}{4}$ of an inch below the top of the slab. Thermocouple 7 was located on the 1'-0 long unstressed slab-beam section at the steel

UNSTRESSED SECTION

COMPOSITE BEAM

3'-6"

8 @ 2'-9" = 22'-0"

DISTRIBUTION OF HEAT LAMPS

SCALE: 3/4" = 1'-0"

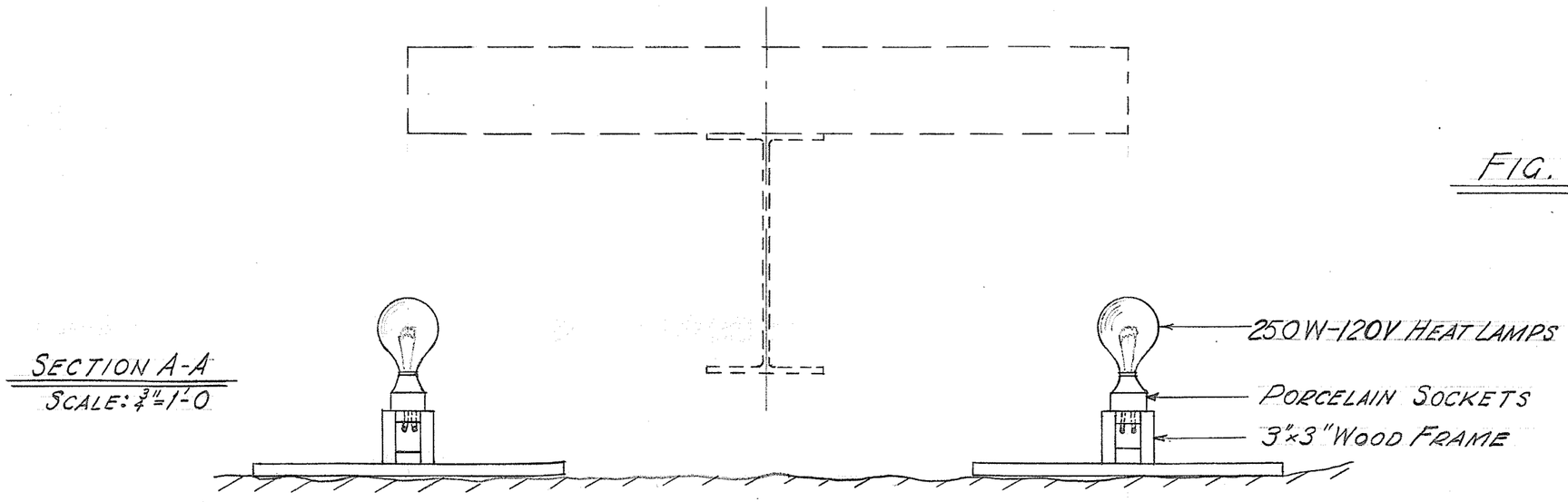

SECTION A-A

SCALE: 3/4" = 1'-0"

FIG. 11

UNSTRESSED SECTION

COMPOSITE BEAM

8 @ 2'-9 = 22'-0

DISTRIBUTION OF HEAT LAMPS
SCALE: 3/4" = 1'-0

FIG. 11

SECTION A-A
SCALE: 3/4" = 1'-0

250W-120V HEAT LAMPS

PORCELAIN SOCKETS

3"x3" WOOD FRAME

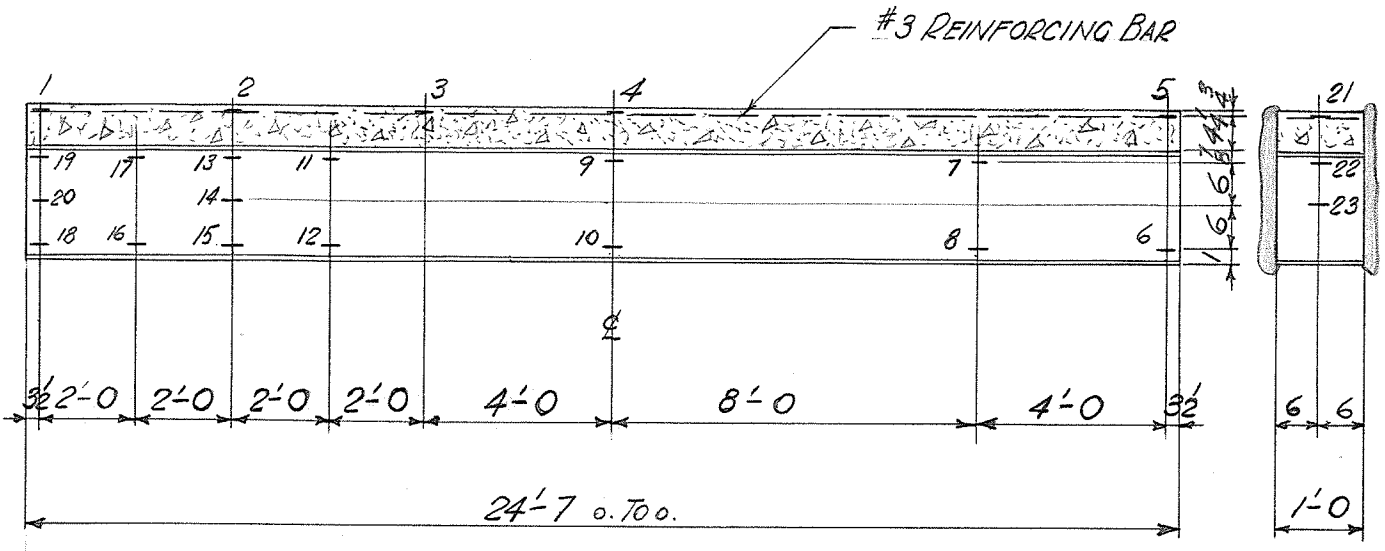

STRAIN GAUGE DISTRIBUTION

FIG. 12

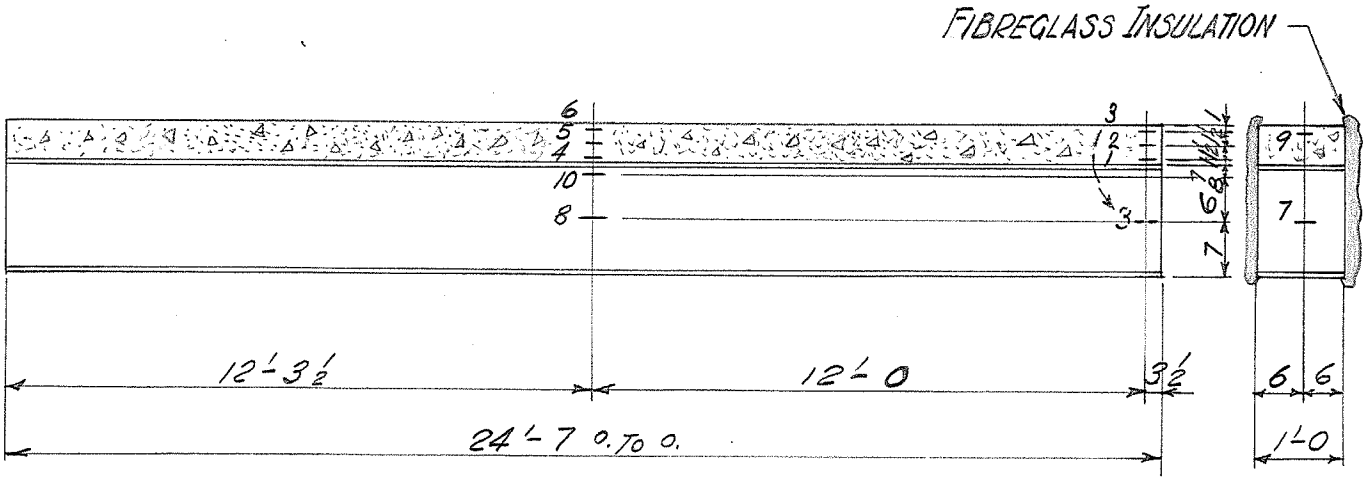

THERMOCOUPLE DISTRIBUTION

FIG. 13

neutral axis. In the corresponding position at the mid-span of the composite beam, thermocouple number 8 was located. After several tests had been run, and the slab temperature distribution determined, thermocouple number 3 was cut off and relocated at the steel neutral axis over the expansion support. These latter three couples were used to determine the temperatures of all the strain gauges at or below the steel neutral axis, it being assumed that the temperature of the steel beam would be constant below this neutral axis.

Thermocouple 9 was located 1 in. below the top of the slab in the unstressed section to determine the temperature of the strain gauge located in the same position. Number10 was located on the web of the steel beam just below the top flange at the midpoint of the span. It was used to determine the temperatures of the gauges in the corresponding positions along the beam.

The method of applying the thermocouples was to dip the junction of the two wires in varnish and to cover it with a thin layer of electricians tape. The thermocouples in the slab were then simply embedded in the concrete, while those on the beam were taped to it and covered with fibre glass insulation. Fig. 14(b) shows thermocouples 8 and 10 before the fibreglass was applied.

The leads were all brought together with the strain gauge leads and run into the Engineering building through a window. Where the leads were exposed between the hut and the window, they were insulated with fibreglass and wrapped in a metallic cover.

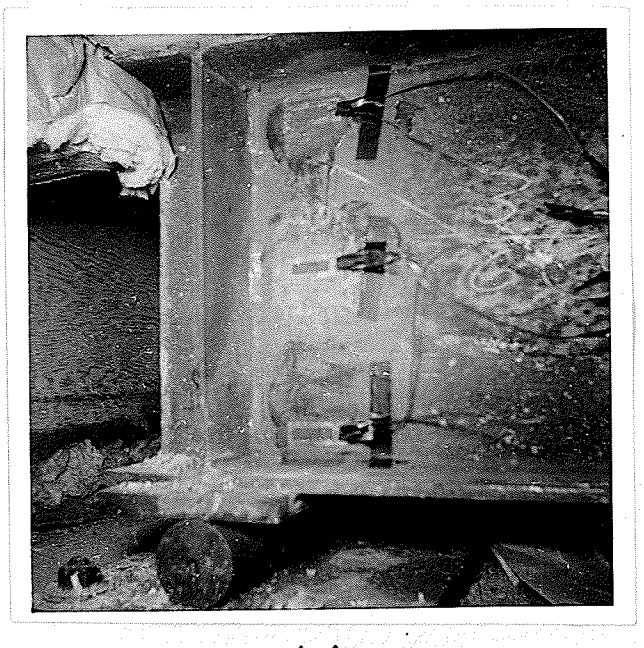

(a)

(b)

(c)

Strain Gauges and Thermocouples Located on Steel Beam

Fig. 14

Inside the Engineering building, the leads were connected to a multiple switch as shown in Fig. 15. Two different cold junction thermocouples were connected to the two-way switch on the potentiometer, to facilitate the reading of temperatures above or below the cold junction temperature. Otherwise, the cold junction leads would have had to have been reversed each time. The cold junction temperature was maintained at 32°F by placing the thermocouples in a $\frac{1}{4}$ in. diameter glass tube and submerging them in a thermos of ice water as illustrated. A potentiometer was used to measure the voltage set up in the thermocouple circuit by the temperature difference and a chart used to convert that voltage reading to the corresponding temperature reading.

Baldwin SR-4 strain gauges were used for measuring strains. The 20 active gauges used were located as shown in Fig. 12. Gauges 1 to 5 were cemented to a 3/8 in. diameter reinforcing rod embedded $\frac{3}{4}$ in. below the top of the slab over the beam centre line. Gauges that could be cemented directly to concrete, were not available at the time this test was done. However, it was felt to be a reasonable assumption that the steel rod would be strained very nearly the same amount as the concrete and that the concrete strains could, therefore, be obtained in this manner. The purpose of the slab strain gauges was to determine the longitudinal strain distribution. The gauges located at various points along the beam web just above the bottom flange and just below the top flange were used to measure the longitudinal strain distribution in the beam

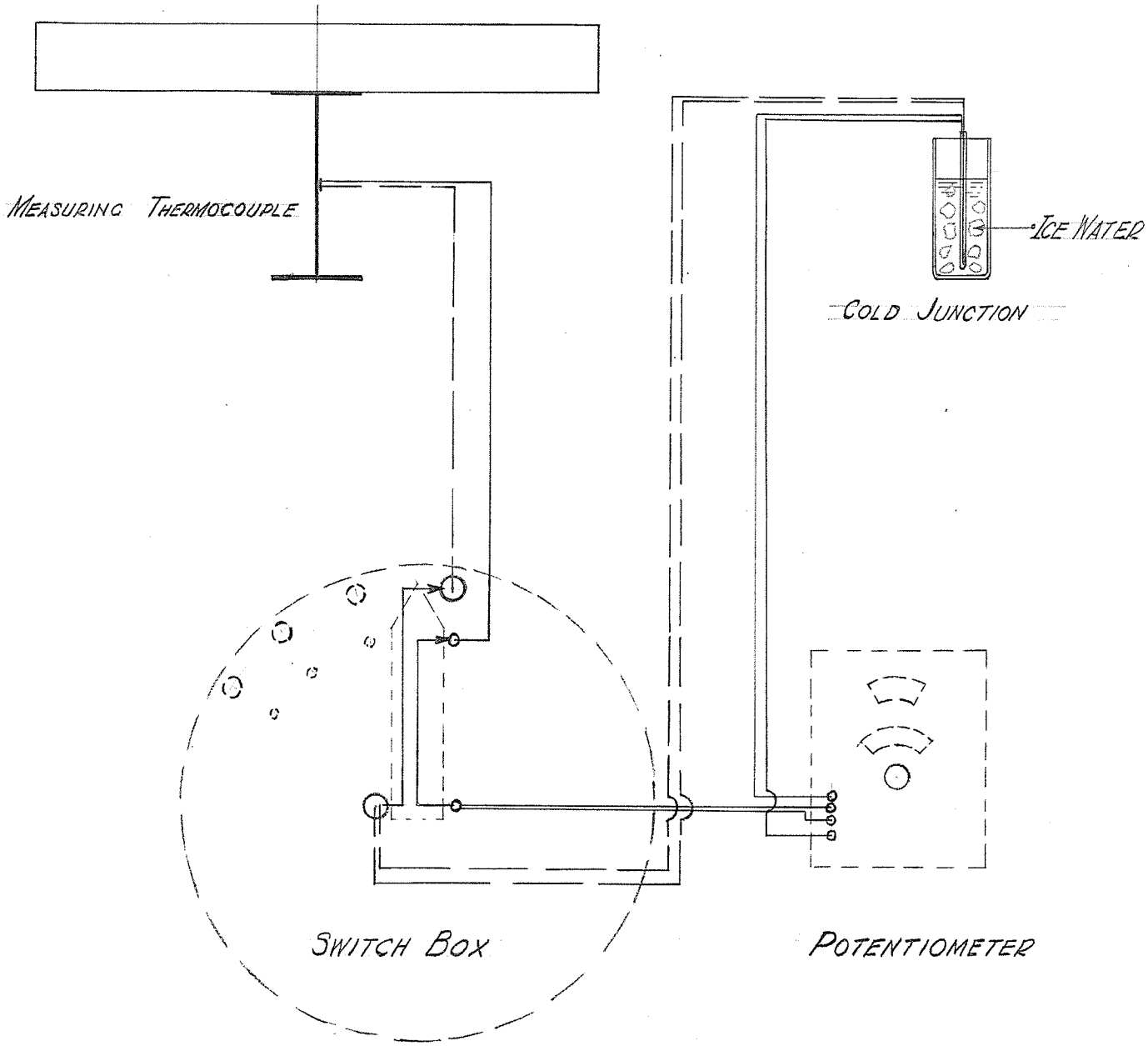

THERMOCOUPLE CIRCUIT

FIG. 15

at these locations. At the section over the expansion support and the section 4 feet from it, gauges were located at the steel neutral axis. It was attempted to determine the strain distribution over a vertical section at these locations.

Since electrical resistance strain gauges are very sensitive to temperature change, it is necessary to balance each active gauge against an unstrained gauge that is kept at the same temperature as the active gauge. This eliminates apparent strain due to a change in the temperature of the active gauge. For this reason, the unstressed beam and slab section was constructed and 3 dummy gauges located on it as shown in Fig. 16(c) in positions corresponding to the positions of the active gauges on the composite beam.

Before applying a gauge, the beam was carefully cleaned off, using an emery stone in a portable $\frac{1}{4}$ in. drill. The location was then carefully cleaned with solvent and the gauge applied with a liberal coat of glucose cement. Originally, the strain gauge leads were of varying lengths depending on the location of the gauge. Later, however, it was realized that the change in resistance of the leads as their temperatures changed, would cause apparent strains in the gauges. It was necessary, therefore, to splice in extra lengths of wire, tomake all the leads the same length, in order to eliminate this condition.

(a)

(b)

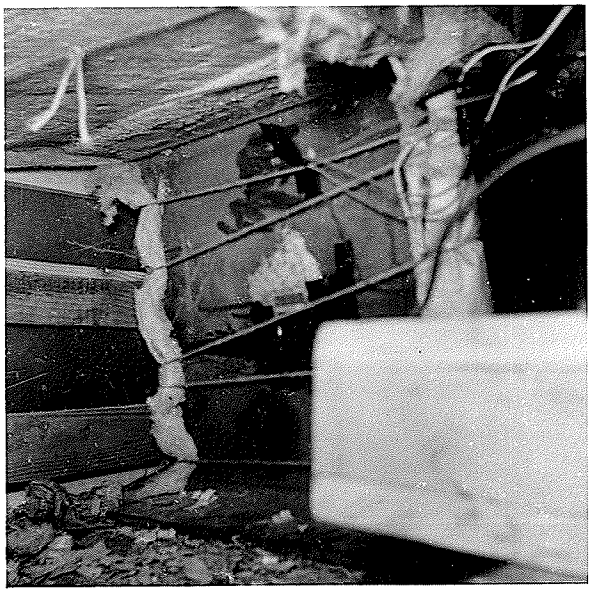

(c)

Unstressed Beam Section

Fig. 16

Fig. 14(a) and Fig. 14(b) show gauges located on the beam web at the expansion support and at the mid-span respectively.

Fig. 14(c) shows a general view of the strain gauges located on the beam web and of their leads. Although the picture shows the leads taped to the web, they were later laid on the ground to decrease their temperature fluctuations.

The strain gauge leads were run into the Engineering building with the thermocouple leads and connected to the standard multiple switch box used in the Engineering laboratory. A three-way switch was used to switch the three dummy gauges to permit the balancing of any active gauge against it's corresponding dummy gauge.

The Baldwin SR-4 strain measuring potentiometer used in the Engineering laboratory was used for measuring strain in micro inches per inch. Fig. 17 shows a schematic diagram of the strain gauge circuit.

The apparatus used for obtaining the strain and temperature readings is shown in Fig. 18. Fig. 18(a) shows the thermocouple reading potentiometer on the right and the cold junction thermos at the top. The large circular multiple switch on the box at the left was used for switching in the different thermocouples.

The Baldwin SR-4 strain indicating potentiometer is shown at the right of Fig. 18(b). The multiple switch is shown at the left of this picture. The balancing rheostats used to balance each gauge at a certain initial reading can be seen on the face of the box.

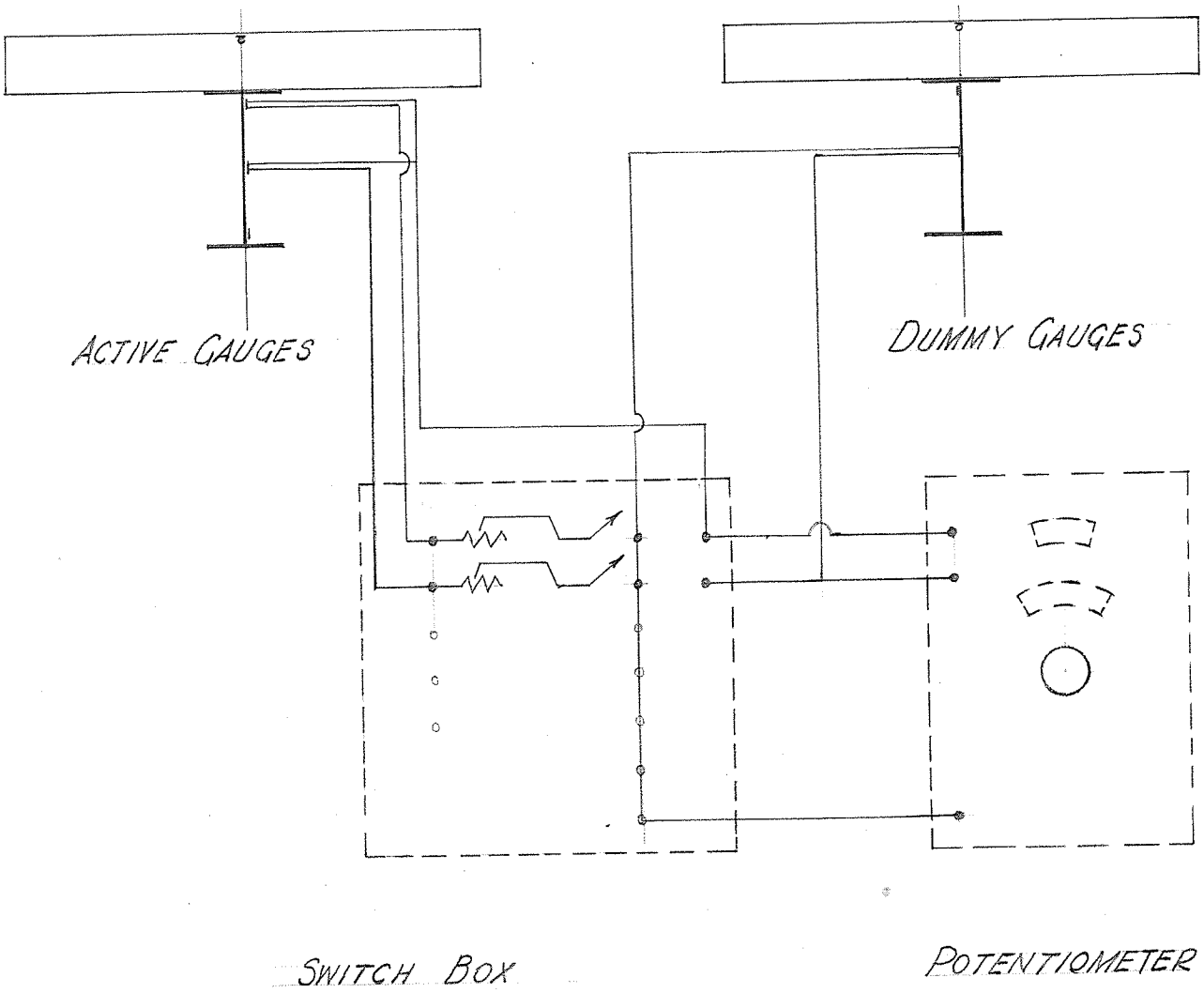

STRAIN GAUGE CIRCUIT

FIG. 17

(a)

(b)

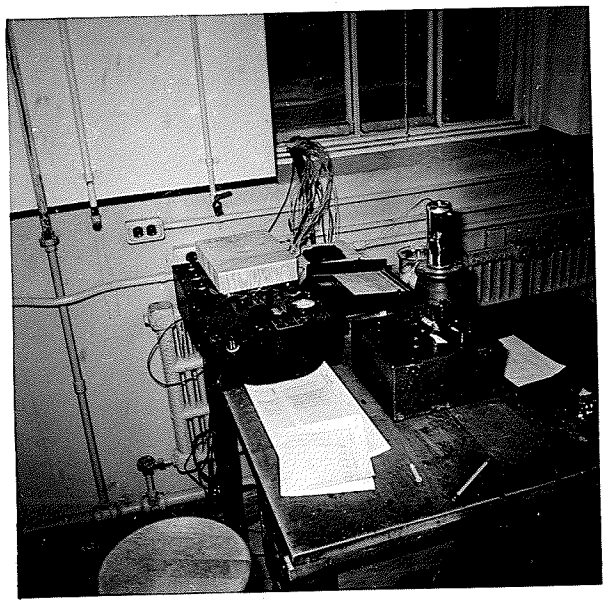

(c)

Strain Gauge and Thermocouple Measuring Apparatus.

Fig. 18

The smaller three-way switch on the box at the top of the picture was the one used to switch in the different dummy gauges.

Fig. 18(c) shows a general view of the strain and temperature measuring apparatus with the thermocouple and strain gauge leads going out the window in the background.

As was mentioned previously, two 6 x 4 x 3/8 in. angles bolted with their long legs back to back were supported on top of the slab on a knife edge at one end and a roller at the other. Three sixteenth in. diameter holes were drilled through the outstanding leg of one of these angles at seven points directly over $\frac{3}{4}$ in. diameter pins, which had been previously set in the concrete. These pins had machined tops, but were not set perfectly level. An Ames dial, reading to one thousandths of an inch, was securely fastened to a flat wooden block as shown in Fig. 19. Strain readings were taken by setting the wooden block flat on the outstanding leg of the angle, and allowing the actuating stem of the dial to extend through the hole and rest on the top of the pin, as the figure illustrates.

Test Procedure

One complete cycle of heating and cooling of the beam-slab unit was possible. In this cycle, the beam could be rapidly heated and then rapidly cooled, or these steps could be done in reverse.

Initially, several tests were done including

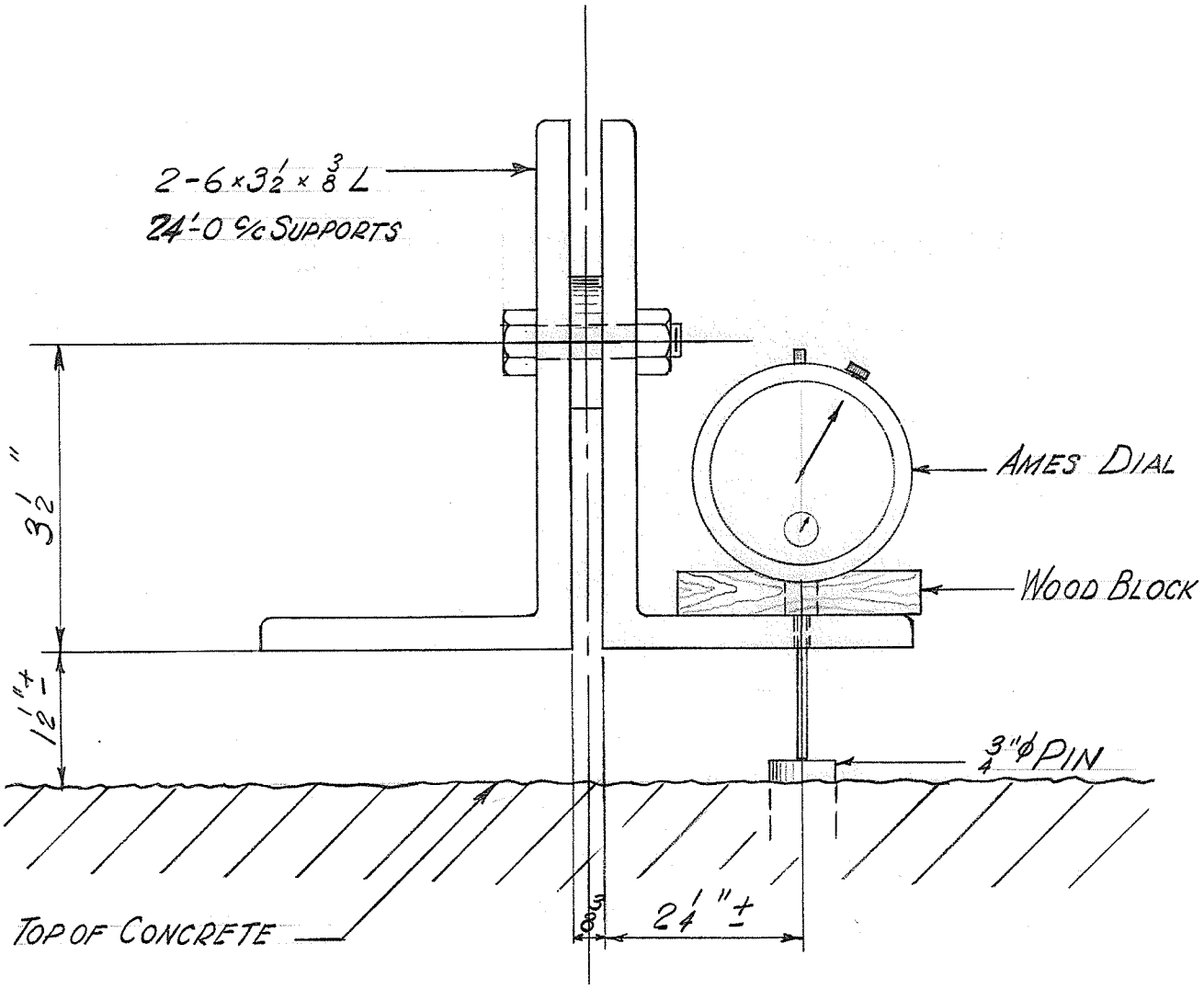

DEFLECTION MEASURING DEVICE

SCALE: HALF SIZE

FIG. 19

only the rapid cooling part of this cycle. These tests furnished incomplete results which were not tabulated as part of this thesis. Tests 1 and 2 were then done, starting with the rapid cooling part of the cycle, followed by the rapid heating portion. The third, and final, test employed the rapid heating cycle first with the rapid cooling cycle following it.

For tests 1 and 2, the doors of the building were closed and the heat lamps were turned on approximately fifteen hours before the start of the test. During this time, two electric fans were used to circulate the air in an effort to obtain a uniform temperature throughout the beam and slab unit and the unstresses section. Fifteen minutes before the first readings were taken, the heat lamps were turned off while the fans were left running. Two sets of initial deflection, strain gauge, and thermocouple readings were taken and averaged to establish the initial conditions.

The doors of the building were then opened and strain gauge, thermocouple, and deflection readings recorded at approximately twenty minute intervals for the first $2\frac{1}{2}$ or 3 hours. Readings were then taken at longer intervals for another hour or two or till the maximum deflection was passed.

The beam was then allowed to cool completely with the doors left open and a set of readings was taken after approximately 24 hours. The doors were then closed and the lamps turned on. Reading of strain gauges, thermocouples, and deflection were again recorded at approximately

20 minute intervals and later at half-hour and one hour intervals for five or six hours. A final set of readings was then taken approximately 48 hours after the beginning of the test. The beam had returned very closely to its initial condition of temperature by this time.

The procedure of the third test was very similar to that of the first two except that the order of carrying out the two parts of the cycle was reversed.

Determination of Temperature Difference-Apparent Strain Relationship

As has been pointed out, when strain readings for an active gauge are obtained by balancing against a similar dummy gauge, the strain readings will be correct only if both gauges are at the same temperature. Otherwise, there will be a difference in resistance and, therefore, an apparent strain, due to the temperature difference.

Because it was impossible during this test to keep each active gauge at the same temperature as it's corresponding dummy gauge, it was necessary to conduct a test to determine the relationship between an active-dummy gauge temperature difference and the apparent strain it produced. The apparatus used for this test is illustrated in Fig. 20. Four gauges attached to a 6'-0 long unstrained section of beam which was maintained at room temperature, were used as active gauges. The dummy gauge was cemented to a small $\frac{1}{2}$ in. thick section of a 4 in. steel beam. The dummy section was placed in a glass container with a fahrenheit thermometer and was covered

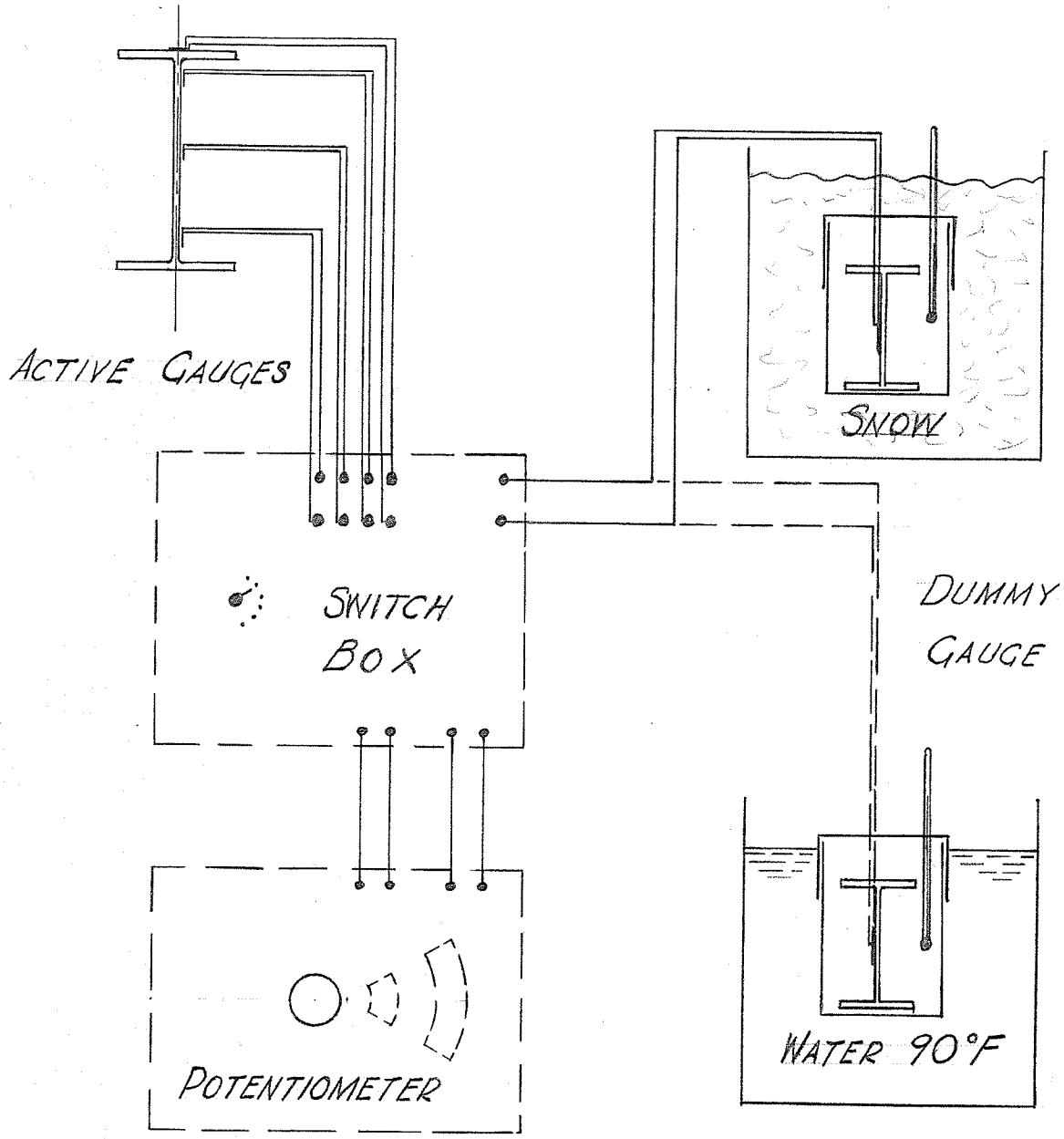

APPARATUS FOR DETERMINING TEMPERATURE DIFFERENCE —APPARENT STRAIN RELATIONSHIP FOR STRAIN GAUGES

FIG. 20

with a cardboard top. With the dummy gauge and the active gauges at room temperature, strain readings were taken for each active gauge. The dummy section, in it's container, was then placed in a tub of snow and allowed to cool. When the strain readings stopped changing, the thermometer was read and a second set of strain readings recorded. The container was then removed from the tub and the dummy gauge allowed to return to room temperature. Again, when the readings stopped changing, strain and temperature readings were recorded. The dummy section, in it's container, was then immersed in a tub of water at 90°F. Another set of temperature and strain readings was taken at this temperature before the dummy section was removed and cooled to room temperature for a last set of readings.

The results of this test are shown in Table II From these results, the curves shown in Fig. 23 were drawn and an approximate temperature difference-apparent strain relationship determined. Although the actual relationship is probably not linear, this approximate relationship was determined to give a quick method of correcting for gauge temperature differences in the composite beam tests.

Determination of Approximate Difference in Expansion Coefficients For Steel and for a Plain Sample of The Concrete Used in the Slab Construction

As was stated in the introduction, the thermal expansion coefficient of concrete varies depending on the type of aggregate. Although the concrete expansion

coefficient is different for plain and reinforced concrete, it was desired to check the difference in expansion coefficients for steel and for the concrete used. To check this, the following test was done.

At the same time as the slab was poured, a plain concrete specimen, approximately 4 feet in length, was poured. A greased stick $\frac{3}{4}$ in. square was embedded in the top of the specimen and later removed leaving a groove. Fig. 21(a) shows this specimen after pouring. One quarter in. diamter bolts were also embedded in the ends of the concrete specimen. After the concrete had set, $1\frac{1}{2}$ in. by $2\frac{1}{2}$ in. plates were bolted to either end. A 3/8" diamter deformed reinforcing rod was threaded on one end, machined round on the other and rigidly fastened to the plate by two nuts on the threaded end. The other end was allowed to protrude through a 3/8 in. diameter hole in the plate at the other end.

An Ames dial reading to five ten thousandths of an inch was rigidly clamped to the rod as shown in Fig. 21(b) so that the actuating stem rested on the plate. The whole assembly was placed on a movable wagon.

With the specimen at room temperature, the Ames dial was read and the temperature was recorded. The assembly was carefully moved to an unheated room and allowed to cool to a uniform temperature. The temperature and Ames dial were again read. The outside door was then opened and the room was cooled even more. The readings were then recorded a third time. Care had to be taken in moving the specimen since the slightest disturbance

(a)

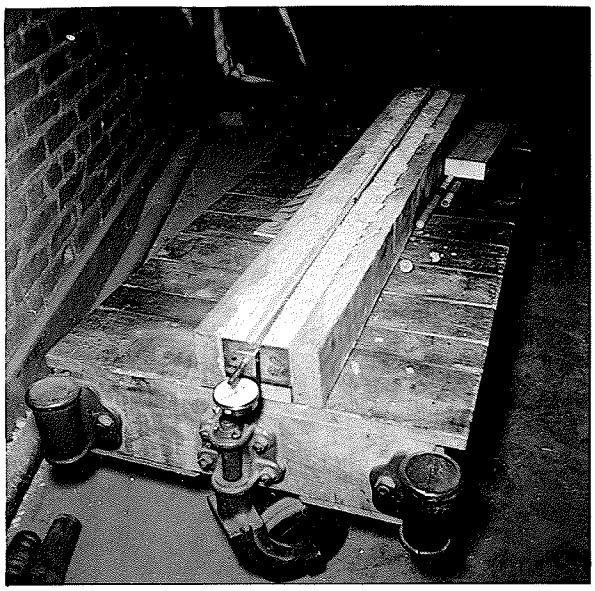

(b)

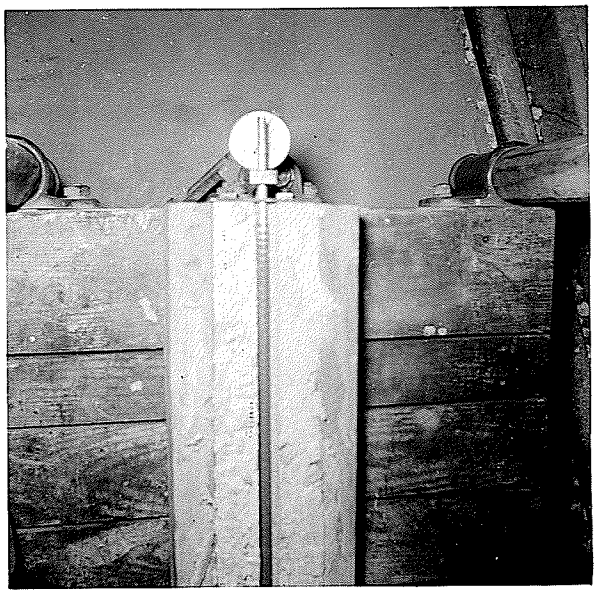

(c)

Apparatus for Determining Approximate Difference

In Expansion Coefficients for Steel

And for Concrete Used.

Fig. 21

changed the dial reading. The results of this test are shown on Page 48 and illustrated graphically in Fig. 22.

The length of the rod between the fixed end and the Ames dial clamp was greater than the length of the concrete specimen. However, it was felt the contraction of the rod in this extra length would be balanced by the contraction in the actuating stem of the Ames gauge and no correction was made.

Fig. 21 (c) shows a view of the specimen on the moveable wagon. The fahrenheit thermometer used for measuring the temperature can be seen on top of the specimen.

CHAPTER IV

RESULTS AND CALCULATIONS

Results

The results for tests 1, 2 and 3 are listed in tables IV TO VIII

Several incomplete tests were run, but their results were inacurrate and are, therefore, not shown.

The dummy gauge columns, in the tables of strain gauge readings, give the number of the dummy gauge against which each active gauge was balanced. The thermocouple readings were obtained in millivolts of electrical potential. A conversion chart was used to change these readings to degrees fahrenheit, and they were tabulated in this form. The tabulated deflection readings were obtained by subtracting the initial dial reading for the given point from each successive reading.

The tabulated slab temperature was obtained from the average of thermocouples 2 and 5, while the steel temperatures in the tables were obtained from thermocouples 3 and 8. Two of the graphs of deflection and temperature difference vs time and those of strain gauge readings vs time were broken with respect to the time axis. This was done to prevent excessive length of the time scale.

TABLE I

Results of Compression Tests on Sample Cylinders of Concrete Used in Slab Construction

Date of Pouring October 16, 1957

Date of Test November 13, 1957

Specimen	Diameter (in.)	Area ($in.^2$)	Ultimate Load(lb.)	Ultimate Strength(psi)
1	5.98	28.1	125,030	4,450
2	5.93	27.2	133,250	4,900

Average 28 day strength = $\frac{4450 + 4900}{2}$ = 4,675 psi

TABLE II

RESULTS OF TEST TO DETERMINE DIFFERENCE IN EXPANSION CO-EFFICIENTS FOR STEEL AND FOR A PLAIN SAMPLE OF THE CONCRETE USED IN THE CONSTRUCTION OF THE SLAB.

Length of Specimen - 47.85 in.

	Temperature	Dial Reading
Test No. 1	68° F	0.1509
	30° F	0.1538
	22.5° F	0.1553
Test No. 2	68.5° F	0.1511
	60° F	0.1521
	51° F	0.1525
Test No. 3	67° F	0.1524
	45° F	0.1541
	36° F	0.1549

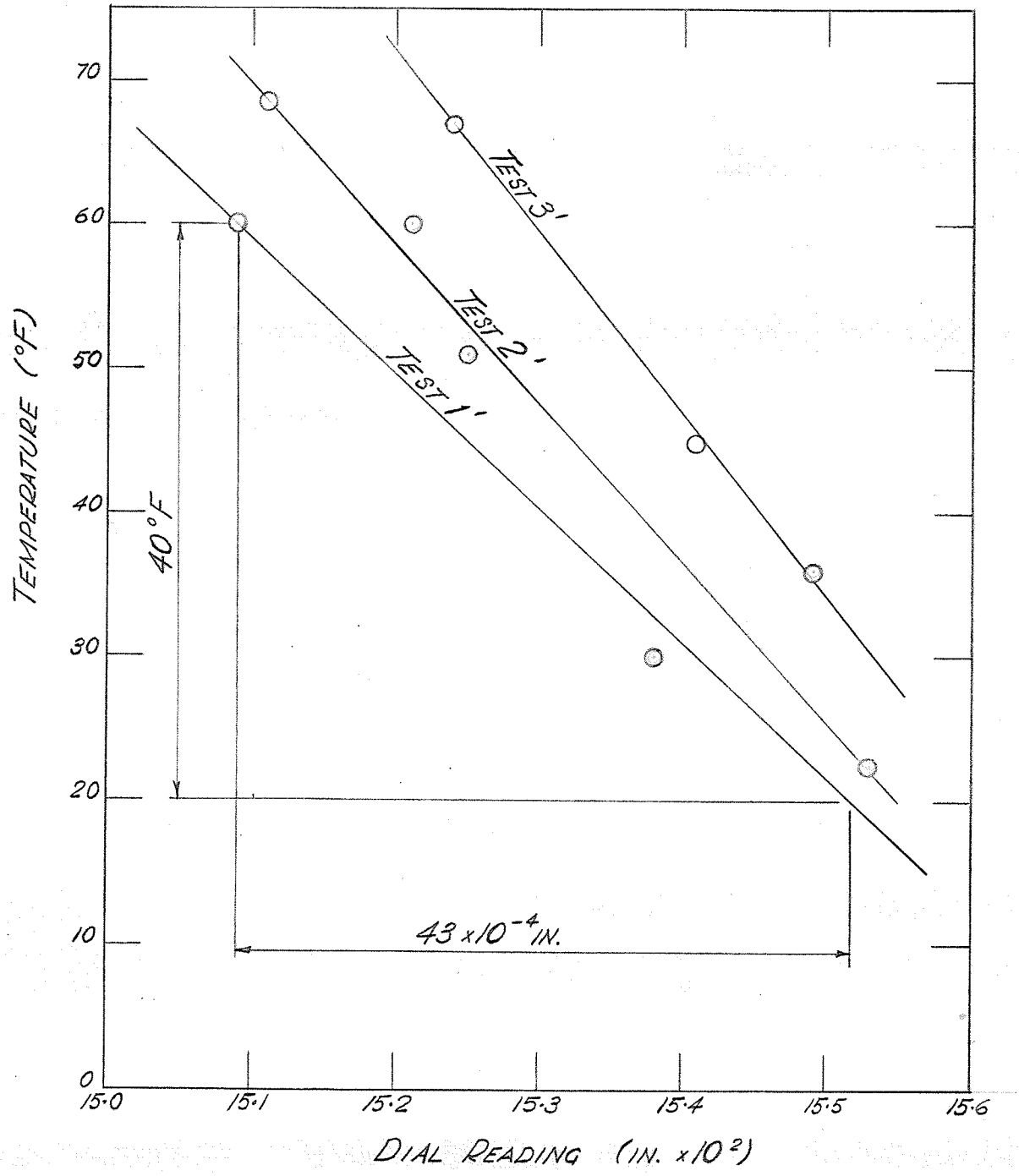

PLOT OF TEMPERATURE VS DIFFERENCE IN EXPANSION FOR STEEL AND FOR PLAIN SAMPLE OF CONCRETE USED IN TEST SLAB

FIG. 22

TABLE III

RESULTS OF TEST TO DETERMINE APPARENT STRAIN CAUSED BY A TEMPERATURE DIFFERENCE BETWEEN ACTIVE AND DUMMY GAUGES

Active Gauge	Temperature	Dummy Gauge Temp.	Strain Reading	Temp. Difference	Apparent Strain
1	66.5°F	61.5°F	8482	+ 5°F	0
2	-	-	8491	-	0
3	-	-	10548	-	0
4	-	-	10531	-	0
1	66.0°F	32.0°F	8540	+34°F	+0058 Micro in/in.
2	-	-	8549	-	+0058
3	-	-	10605	-	+0057
4	-	-	10590	-	+0059 Av +0058
1	66.5°F	59.5°F	8461	+ 7°F	+0021
2	-	-	8473	-	+0018
3	-	-	10528	-	+0020
4	-	-	10511	-	+0020 Av +0020
1	66.5°F	90.0°F	8417	-23.5°F	-0065
2	-	-	8428	-	-0063
3	-	-	10480	-	-0068
4	-	-	10465	-	-0066 Av -0066
1	66.5°F	68.5°F	8467	-2°F	-0015
2	-	-	8475	-2°F	-0016
3	-	-	10530	-	-0018
4	-	-	10515	-	-0016 Av. -0016

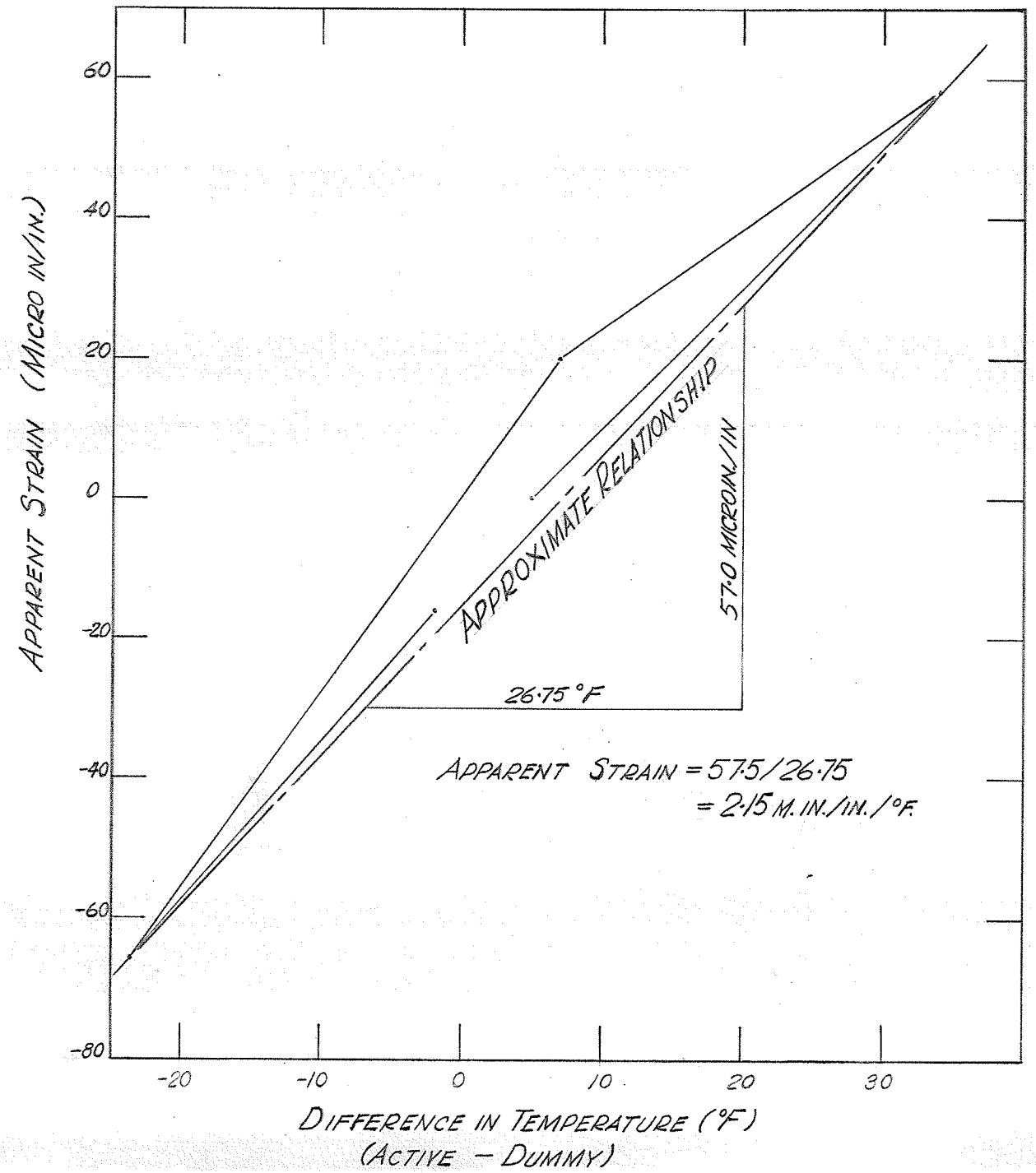

APPARENT STRAIN
VS
DIFFERENCE IN TEMPERATURE
BETWEEN ACTIVE & DUMY GAUGES

FIG. 23

TABLE IV

TEST 1 - STRAIN GAUGE AND TEMPERATURE READINGS

Active Gauge	Dummy Gauge	0	5 m.	20 m.	35 m.	55 m.	1h-15m.	1h-35m	2h-0m	3h-0m	4h-0m	5h-15m
1	21	999	991	1011	1011	1018	1014	1000	990	980	970	961
2	21	1000	1020	1049	1050	1059	1055	1066	1071	1081	1083	1083
3	21	1021	1024	1065	1070	1092	1080	1108	1104	1119	1125	1129
4	21	1049	1056	1009	1091	1117	1103	1121	1119	1125	1121	1121
5	21	1020	1020	1040	1039	1061	1042	1050	1045	1045	1072	1091
6	23	990	970	957	961	933	902	920	910	921	933	941
7	22	985	960	972	983	988	980	1001	1034	1025	1043	1034
8	23	1003	989	979	980	943	928	925	925	953	953	940
9	22	990	943	1012	998	1012	1034	1038	1050	1085	1110	1075
10	23	1035	961	982	963	951	947	940	940	953	949	946
11	22	999	916	979	970	975	1013	1020	1017	1055	1065	1079
12	23	1028	975	968	948	938	963	961	967	975	962	972
13	22	999	930	950	921	945	968	981	979	1003	993	1019
14	22	998	938	950	911	927	942	952	953	970	967	1000
15	23	950	885	832	812	801	802	811	820	815	800	820
16	23	941	866	803	783	762	765	772	785	778	761	775
17	22	975	940	978	959	972	990	1014	1019	1033	1039	1065
18	23	1028	942	890	863	840	837	847	855	847	833	847
19	22	1090	875	912	857	871	871	881	880	869	845	860
20	22	997	870	880	821	829	830	848	850	850	840	863
Thermocouple												
1		119°	118°	109°	101°	94.5°	88.5°	81°	76.5°	60°	47.5°	34°
2		119°	118.5°	116°	110°	103°	97°	90°	84°	67°	53°	38°
3		115°	91°	55.5°	43°	38°	36°	35°	33.5°	28°	21°	16.5°
4		124°	122°	116°	109.5°	105.5°	100°	95°	90.5°	77.5°	67°	55°
5		-	-	-	-	-	-	-	-	-	-	-
6		123°	120°	116°	111°	108°	103.5°	99°	94.5°	81°	70°	57.5°
7		108°	88°	62°	48°	44°	41°	39°	36.5°	32°	29°	24°
8		103°	89.5°	75°	61.5°	56°	53°	48°	46°	40°	31.5°	29.5°
9		106°	104.5°	101.5°	95°	91°	86.5°	80°	76°	60°	48°	27°
10		120°	106°	91°	82°	78°	73.5°	69.5°	66.5°	56°	46.5°	26.5°

TABLE IV (Cont'd

Active Gauge	27h-0m	27h-20m	27h-35m	27h-55m	28h-15m	28h-40m	29h-0m	29h-40m	30h-30m	25h-0m
1¢	985	974	967	985	988	980	980	975	971	980
2	1110	1099	1088	1099	1092	1076	068	1055	1049	993
3	1142	1127	1112	1120	1111	1090	080	1066	1058	1020
4	1191	1074	1068	1071	1067	1046	035	1020	1009	1041
5	1159	1129	1120	1128	1120	1104	098	1084	1079	1023
6	924	940	933	943	950	959	959	962	971	1008
7	1049	1058	1047	1040	1041	1037	029	1021	1016	971
8	902	942	973	1001	1020	1027	024	1029	1030	1039
9	1170	1163	1107	1132	1112	1110	099	1089	1072	949
10	921	970	1000	1025	1040	1048	050	1051	1057	1096
11	1111	1119	1101	997	1085	1071	065	1053	1046	959
12	980	1110	1027	1041	1051	1056	054	1049	1052	1052
13	1045	1060	1047	1044	1042	1032	036	1028	1019	963
14	1049	1069	1062	1066	1061	1050	048	1033	1019	949
15	798	840	865	884	901	911	915	919	925	974
16	778	824	853	876	892	901	903	902	912	969
17	1123	1126	1112	1104	1086	1092	081	1075	1061	966
18	884	920	940	960	972	983	987	990	1000	1072
19	905	930	942	945	949	949	951	948	952	976
20	970	1009	1029	1031	1028	1031	029	1020	1012	984
Thermocouple										
1	-4.5°	-1.5°	3.5°	9°	13.5°	17.5°	23°	27°	32°	119.5°
2	-4.5°	-4°	-1.5°	3°	7°	10°	15.5°	20°	28°	116°
3	1.5°	19°	29.5°	33°	39°	43°	48°	54°	59.5°	126°
4	3°	5.5°	10°	14°	18.5°	22°	27°	31.5°	35°	126.5°
5	-	-	-	-	-	-	-	-	-	-
6	3°	5°	5.5°	8°	11°	14.5°	18°	23°	29°	120°
7	5.5°	19°	27°	32°	35°	39.5°	43°	48°	53°	116°
8	4°	25°	32°	40.5°	46°	51°	56°	62°	69°	135°
9	-3.5°	-2°	0°	4°	8°	11°	16.5°	22°	28°	108°
10	4°	19.5°	25.5°	32°	32.5°	37°	41°	47°	54.5°	134°

TABLE V

TEST 1 - DEFLECTION READINGS

Time (From 10:45)	Av.Conc. Temp.	Av.Steel Temp.	Diff.	Deflection (in.)						
				$\frac{1}{0}$	$\frac{2}{0}$	$\frac{3}{0}$	$\frac{4}{0}$	$\frac{5}{0}$	$\frac{6}{0}$	$\frac{7}{0}$
0	121.5°	109°	12.5°	0	.036	.057	.068	.063	.052	.001
10	120.5°	90°	30.5°	.002	.101	.156	.177	.156	.100	.002
30	108°	56°	52°	0	.121	.195	.224	.204	.133	.006
45	107°	49.5°	57.5°	0	.136	.219	.248	.222	.140	.006
65 1h- 5m	102°	46°	56°	.001	.135	.220	.247	.220	.140	.008
90 1h- 30m	97°	41.5°	55.5°	0	.136	.217	.246	.218	.138	.008
115 1h- 55m	91°	40°	51°	.002	.118	.191	.217	.193	.122	.007
195 3h- 15m	76°	34°	42°	.001	.122	.194	.214	.192	.120	.007
255 4h--15m	63°	26°	37°	.005	.109	.176	.196	.177	.110	.006
325 5h- 25m	48°	23°	25°	.005	.070	.105	.117	.103	.064	.003
27h- 0m(1:45)	-1°	3°	-4°	.008	.019	.025	.030	.025	.023	-0.001
27h- 25m(2:10)	1°	22°	-21°	.006	-.013	-.025	.030	.025	.023	-0.001
27h- 45m(2:30)	4°	31°	-27°	.002	-.031	-.054	-.060	-.046	-.031	-.004
28h--05m(2:50)	8°	37°	-29°	.001	-.041	-.071	-.076	-.063	-.037	-.006
28h- 25m(3:10)	9.5°	42.5°	-33°	.002	-.046	-.080	-.087	-.072	-.047	-.006
28h- 45m(3:30)	12.5°	47°	-34.5°	.002	-.051	-.086	-.096	-.078	-.052	- .006
29h- 15m(4:00)	17.5°	52°	-34.5°	.001	-.056	-.093	-.103	-.084	-.055	-.007
29h- 45m(4:30)	22°	58°	-36°	.001	-.057	-.097	-.115	-.087	-.058	-.008
30h- 35m(5:20)	29.5°	63.5°	-34°	0	-.033	-.061	-.066	- .055	-.037	-.005
50h- 0m(12:45)	123°	130.5°	-7.5°	.001						

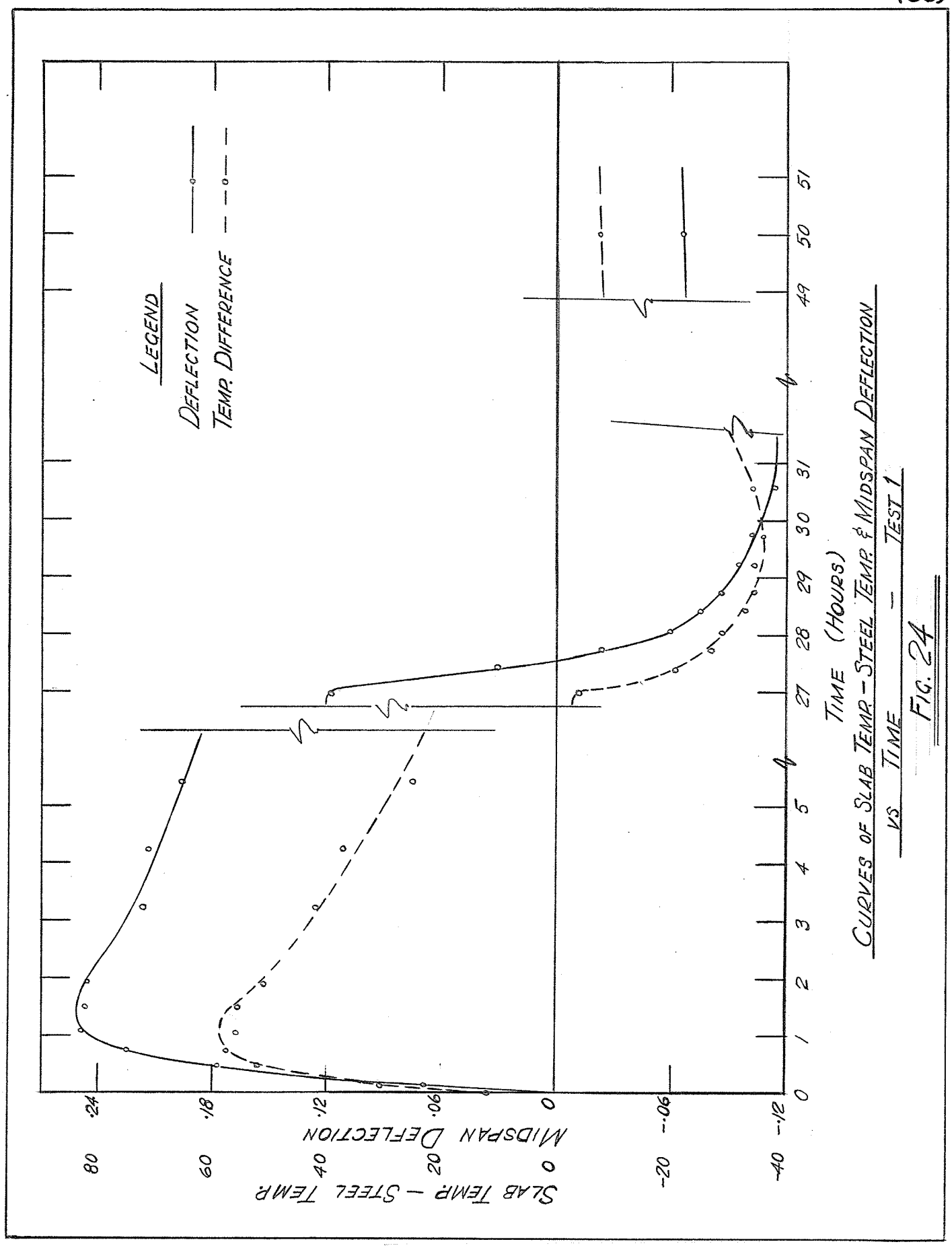

CURVES OF SLAB TEMP – STEEL TEMP & MIDSPAN DEFLECTION VS TIME – TEST 1

FIG. 24

TABLE VI

TEST 2 - STRAIN GAUGE AND TEMPERATURE READINGS

Active Gauge	Dummy Gauge	0m	15m	30m	45m	1h-5m	1h-25m	1h-45m	2h-15m	3h-25m	6h-20m
1	21	1017	997	1012	1010	1011	1009	1023	1010	987	972
2	21	972	965	980	984	997	1000	1012	1015	1002	1003
3	21	977	972	995	992	1012	1025	1029	1036	1024	1018
4	21	1018	999	1020	1023	1043	1052	1048	1049	1032	1009
5	21	971	936	940	955	980	965	945	980	932	960
6	23	999	969	925	899	898	870	890	913	909	916
7	22	893	880	900	905	921	900	942	950	931	924
8	23	980	937	900	848	858	835	869	884	862	875
9	22	876	874	897	895	903	915	947	961	959	971
10	23	951	925	871	836	838	829	851	863	850	867
11	22	883	912	904	930	937	928	962	976	974	985
12	23	942	918	890	880	869	860	879	899	892	911
13	22	918	900	894	914	909	904	924	949	941	960
14	22	921	914	900	913	900	891	910	935	931	950
15	23	962	921	882	885	856	838	863	861	870	869
16	23	968	911	872	872	847	828	849	849	860	861
17	22	895	909	902	935	931	930	955	970	979	1006
18	23	890	937	882	871	854	849	842	853	860	880
19	22	972	930	973	929	911	899	909	913	906	920
20	22	947	895	866	872	848	842	860	840	874	911
Thermocouple											
1		121.5°	121°	111°	103°	97.5°	91°	84°	77.5°	62.5°	43.5°
2		120°	120°	119°	109°	103.5°	98°	91°	84°	67°	45.5°
3		122.5°	82°	67.5°	59°	52°	47°	44°	42°	37°	32.5°
4		127.5°	125°	121.5°	106.5°	103°	97.5°	92.5°	86.5°	73°	54°
5		–	–	–	–	–	–	–	–	–	–
6		122°	122°	118.5°	107°	103.5°	99°	94°	88.5°	74°	54°
7		116°	91°	74°	64.5°	60°	55.5°	53°	49.5°	44°	37°
8		126°	92°	72.5°	61.5°	58.5°	54°	52.5°	49.5°	44°	37.5°
9		112.5°	111°	106°	101.5°	97°	92°	86°	80°	66°	45.5°
10		126.5°	107.5°	93°	84.5°	79°	75°	72°	67.5°	58°	45°

TABLE VI (Cont'd)

Active Gauge	7h-55m	23h-20m	23h-40m	27h-55m	28h-45m	30h-20m	33h--35m
1	988	1012	1022				
2	1099	1041	1052				
3	1021	1039	1051				
4	1003	969	987				
5	973	1059	1060				
6	916	945	960				
7	928	1032	1033				
8	870	897	932				
9	976	1091	1071				
10	859	863	911				
11	981	1089	1072				
12	901	931	962				
13	949	1061	1054				
14	944	1051	1043				
15	865	867	909				
16	858	882	922				
17	999	1122	1105				
18	873	887	921				
19	918	1009	1012				
20	783	670	670				
Thermocouple							
1	37°	24.5°	27°	60.5°	72.5°	81.5°	93°
2	37.5°	24.5°	25.5°	54.5°	67.5°	76°	88.5°
3	28°	25.5°	40°	85.5°	94°	100°	105.5°
4	45.5°	28°	29.5°	62.5°	74°	84°	95.5°
5	-	--	-	-	-	-	-
6	45.5°	26.5°	28°	52.5°	65°	75°	87°
7	32°	28°	24°	78°	87°	92.5°	97°
8	32°	27°	46.5°	94°	103.5°	110°	112.5°
9	39°	26°	27°	53°	67°	74.5°	85.5°
10	39°	27.5°	41°	79°	91°	99°	105.5°

TABLE VII

TEST 2 - DEFLECTION READINGS

Time From 9:55	Av.Conc. Temp.	Av.Steel Temp.	Diff.	Deflection 1	2	3	4	5	6	7
0	124.5°	124.5°	0	0	0	0	0	0	0	0
25m	124°	71°	53°	∕0.002	∕.055	.088	.095	.080	.053	-.055
40m	110.5°	60°	50.5°	∕0.007	.115	.174	.201	.174	.115	∕0.010
1h- 5m	106.5°	55.5°	51°	.006	.146	.231	.252	.225	.141	.013
1h-25m	101°	50.5°	50.5°	.007	.150	.239	.263	.233	.155	.013
1h-45m	96°	48°	48°	.005	.150	.240	.264	.235	.155	.014
2h- 5m	92°	47°	45°	.006	.142	.228	.252	.224	.150	.013
2h-25m	84°	45°	39°	.005	.135	.215	.239	.213	.143	.012
3h-35m	72°	40.5°	31.5°	.005	.117	.185	.208	.187	.116	.010
6h-35m	50.5°	35°	15.5°	.003	.083	.134	.148	.135	.082	.007
8h-05m	41.5°	30°	11.5°	.004	.077	.124	.136	.123	.076	.006
23h-30m	26°	35°	-9°	∕.001	.056	.093	.097	.094	.056	.003
23h-50m	28.5	51.5	23	-.002	∕.007	∕.018	∕.016	∕.017	∕.009	∕.006
24h-15m				-.003	-.022	-.036	-.038	-.034	-.025	-.007
24h-55m				-.006	-.047	-.076	-.081	-.072	-.049	-.009
25h-40m				-.006	-.053	-.087	-.097	-.085	-.053	-.011
27h- 5m				-.003	-.057	-.092	-.100	-.090	-.057	-.011
28h-55m	68.5°	99°	-30.5°	-.003	-.054	-.085	-.098	-.085	-.055	-.011
30h-30m	77.5°	105°	-27.5°	-.005	-.049	-.080	-.092	-.079	-.050	-.010
32h-40m	86°	107.5°	-21.5°	-.004	-.046	-.077	-.087	-.075	-.046	-.008

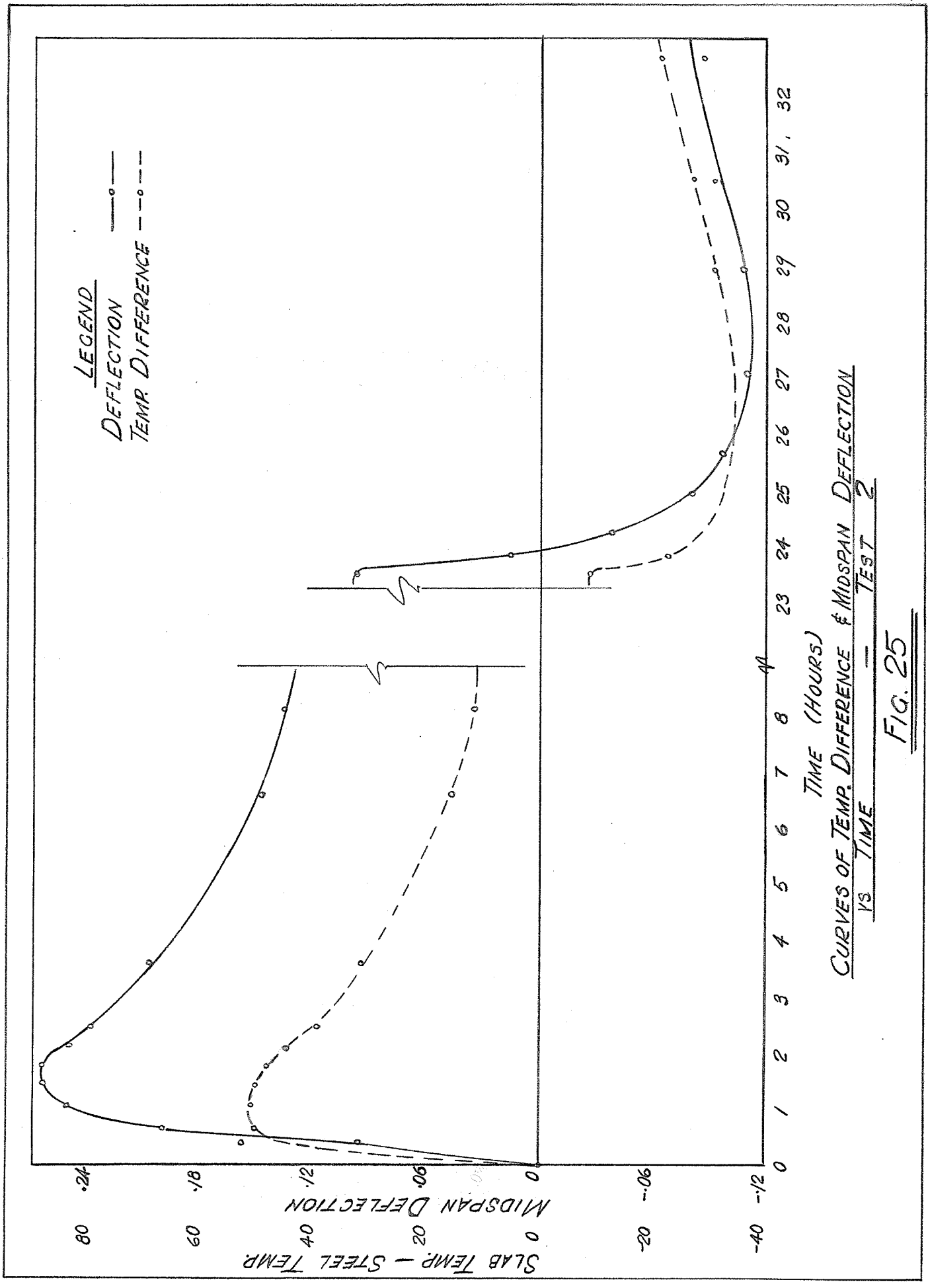

CURVES OF TEMP. DIFFERENCE & MIDSPAN DEFLECTION VS TIME — TEST 2

FIG. 25

TABLE VIII

TEST 3 - DEFLECTION READINGS

Active Gauge	Dummy Gauge	0	5m	25m	45m	1h-5m	1h-25m	1h-45m	2h-5m	2h-25m	2h-45m
1	21	002	007	004	980	987	990	986	981	979	986
2	21	008	011	001	987	990	990	983	979	971	976
3	21	016	020	018	990	992	990	983	977	970	974
4	21	989	000	991	966	972	971	965	961	958	963
5	21	994	986	982	962	972	976	976	972	974	980
6	23	990	017	030	044	055	060	070	078	090	094
7	23	990	018	005	012	017	015	022	029	035	038
8	23	998	041	080	111	125	127	135	139	147	149
9	23	998	999	981	980	974	968	971	971	972	972
10	23	004	054	086	112	125	127	136	141	148	150
11	23	000	010	996	996	942	988	989	991	991	991
12	23	019	060	080	099	100	099	099	101	102	099
13	23	005	021	017	021	018	015	018	020	021	020
14	23	004	021	019	028	023	021	024	024	027	024
15	23	010	056	087	112	120	124	129	131	137	136
16	23	012	056	091	114	121	123	121	129	131	130
17	23	997	002	987	987	980	974	974	974	976	972
18	23	001	046	071	091	100	102	108	114	119	119
19	23	989	015	020	031	031	035	040	048	052	054
20	23	998	032	043	055	053	053	059	061	065	065
Thermocouple											
1		31.5	32	36	38	41	43.5	46	46.5	51.5	53.5
2		32	32	32.5	35	37	38.5	41	43.5	46	48
3		27	39.5	51.5	58	63	65	68.5	71	73	74.5
4		32	33.5	36.5	39	43.5	45	47.5	50.5	53	55.5
5		32.5	33	34	35	37.5	38.5	41	43.5	46	48
6		33	32.5	34	35	36.5	38.5	40	43	44	47
7		29.5	38.5	47	52.5	57	60	62.5	64	66.5	67.5
8		27	47	58	66.5	71.5	74	77	80	82.5	84
9		31.5	31.5	32	33	35	37	37.5	41	43	46
10		30	41.5	48	54.5	59	62	64.5	68	70.5	72

TABLE VIII(Cont'd)

Active Gauge	3h-15m	4h-35m	25h-0m	25h-20	25h-40	26h-5	26h-35	27h-5	27h-35	28h-35	40h-0
1	981	981	925	934	941	949	952	951	934	935	958
2	970	966	865	880	887	894	904	912	899	909	956
3	966	959	880	892	909	419	930	939	927	934	977
4	959	962	925	944	961	963	975	980	963	970	985
5	980	983	871	870	860	872	859	958	837	824	968
6	099	098	049	983	920	907	900	891	871	870	026
7	040	040	991	955	960	962	966	965	943	938	003
8	150	146	074	997	940	909	900	900	880	879	027
9	972	966	872	874	901	910	920	927	911	915	979
10	151	151	072	996	969	948	939	931	911	914	009
11	987	995	891	907	921	938	943	951	930	935	969
12	103	101	991	948	932	930	928	923	908	912	994
13	022	027	936	934	940	955	963	961	942	943	975
14	025	029	945	952	950	952	962	952	933	935	978
15	140	148	051	012	976	965	962	951	935	935	986
16	131	140	045	002	965	954	948	945	926	929	982
17	972	970	908	921	941	959	972	973	976	979	982
18	121	129	085	031	005	992	989	980	981	982	999
19	071	072	057	041	041	040	039	029	025	019	978
20	066	070	029	001	993	990	991	987	984	984	989
Thermocouple											
1	57	68	104.5	99.5	95.5	89.5	83	77.5	72.5	66.5	32
2	51.5	63.5	101	99.5	97	92.5	88	81.5	76	69.5	32
3	76.5	85.5	108.5	77	65	59	52.5	48	44	41	29
4	59.5	71	108.5	103	97	91	86.5	80.5	76	69.5	37
5	52.5	63	103.5	103	100	95.5	91	86.5	81	76.5	37.5
6	50	62	101.5	99	96	93	89	84	80	72.5	37
7	70	78	101	81	68.5	62	57	54	50.5	46.5	33
8	86.5	95	114	73	58.5	55	50	46	43	39	32
9	48	60	95	95	91	88	84	78	75	6615	32.5
10	75	84.5	111.5	95	80	75.5	72	65	62.5	55.5	34.5

TABLE IX

TEST 3 - DEFLECTION READINGS

Time	Conc. Temp.	Steel Temp	Diff.	Deflection (in.) 1	2	3	4	5	6	7
0	32°	27°	+5°	0	0	0	0	0	0	0
10m	33°	43°	-10°	-.002	-.043	-.071	-.081	-.065	.041	-.005
30m	34°	54.5°	-20.5°	-.003	-.075	-.122	-.136	-.119	-.76	-.009
50m	35°	62.5°	-27.5°	-.005	-.093	-.151	-.166	-.144	-.092	-.011
1h-10m	37.5°	67.5°	-30°	-.005	-.105	-.169	-.187	-.164	-.105	-.012
1h-30m	38.5°	69.5°	-31.5°	-.005	-.111	-.178	-.198	-.172	-.111	-.013
1h-50m	41°	73°	-32°	-.005	-.113	-.182	-.204	-.179	-.115	-.014
2h-10m	43.5°	75.5°	-32°	-.006	-.115	-.187	-.208	-.182	-.118	-.014
2h-30m	46°	78°	-32°	-.006	-.116	-.189	-.209	-.183	-.119	-.014
2h-50m	48°	79°	-31°	-.006	-.116	-.189	-.209	-.185	-.118	-.014
3h-20m	52°	81.5°	-29.5°	-.006	-.116	-.188	-.209	-.185	-.119	-.014
4h-50m	63.5	90.5	-27	-.005	-.112	-.181	-.203	-.178	-.115	-.014
25h- 5m	102.5°	112°	-95°	-.002	-.080	-.131	-.147	-.128	-.080	-.007
25h-25m	101.5°	75°	+26.5°	.001	-.013	-.030	-.044	-.041	-.030	-.001
25h-50m	96.5°	62°	+34.5°	.004	+.033	.045	.044	.036	.023	+.006
26h-10m	92°	57°	35°	+.007	+.049	.068	.072	.059	.037	.007
26h-40m	89.5°	51.5°	38°	.008	.055	.080	.086	.071	.045	.008
27h-10m	84°	47°	37°	.005	.056	.083	.089	.076	.047	.008
27h-40m	78.5°	43.5°	35°	.005	.053	.079	.086	.074	.046	.008
28h-40m	73°	40°	33°	.005	.047	.071	.075	.064	.040	.007
41h-00m	35°	30.5°	+45°	+.002	-.004	-.009	-.008	-.006	-.004	+.002

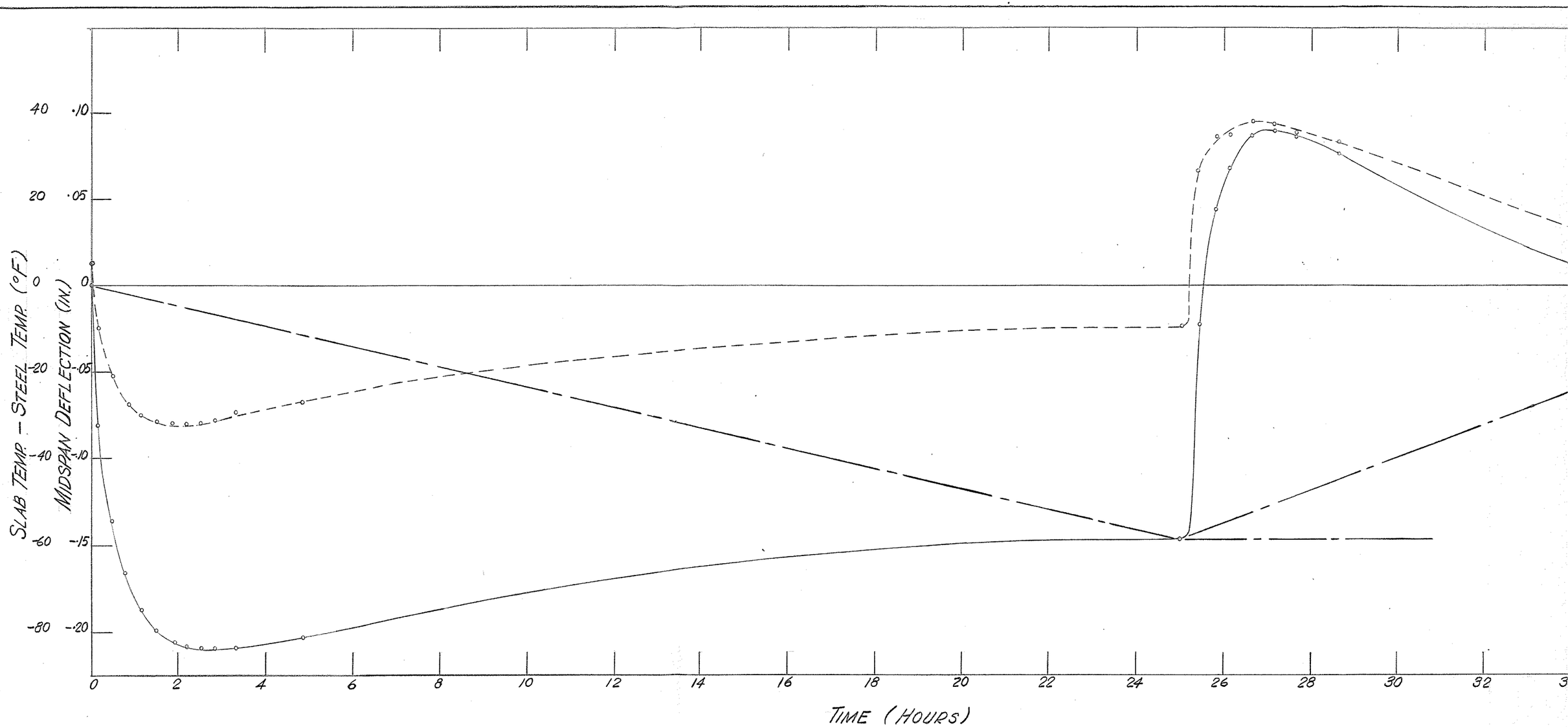

CURVES OF SLAB TEMP. – STEEL TEMP. & MIDSPAN DEFLECTION VS TIME – TEST 3

FIG. 26

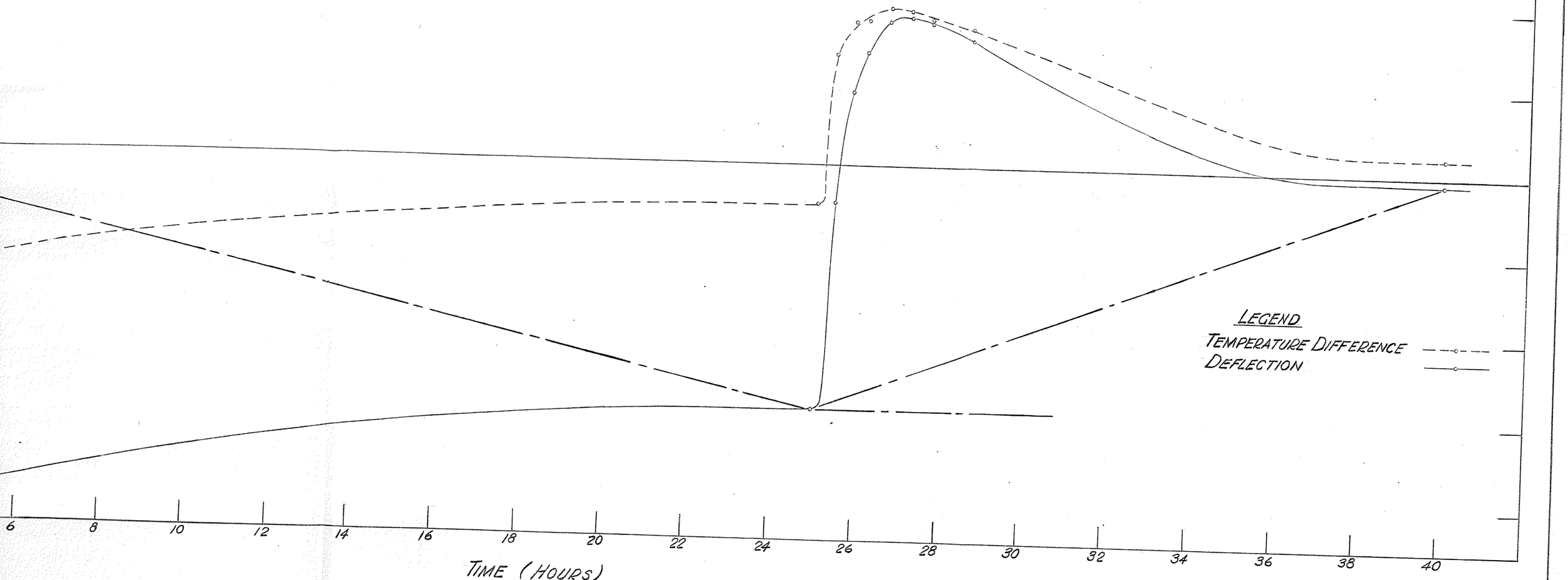

CURVES OF SLAB TEMP. – STEEL TEMP. & MIDSPAN DEFLECTION VS TIME – TEST 3

FIG. 26

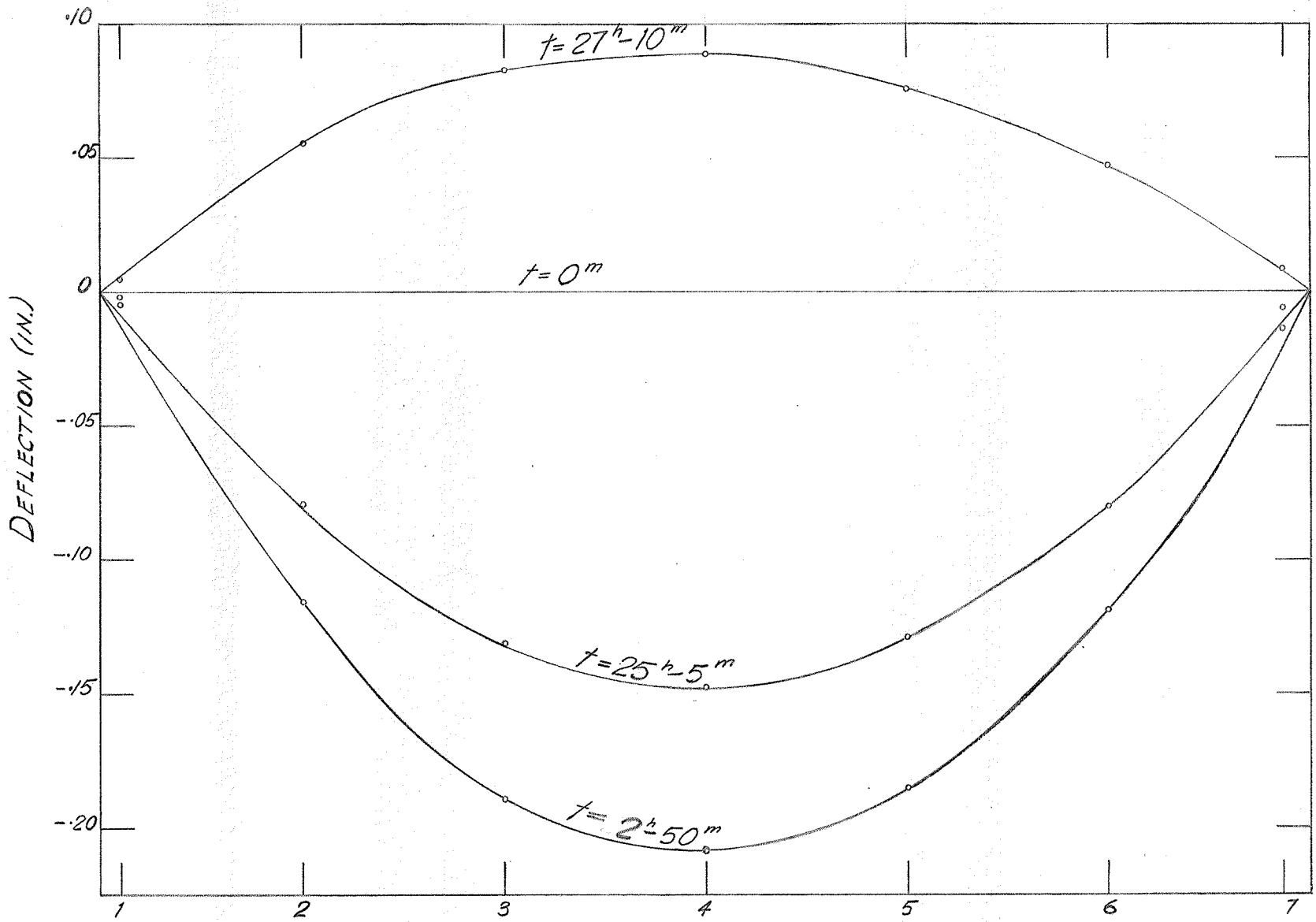

TYPICAL DEFECTION DIAGRAMS
FOR BEAM-SLAB UNIT — TEST 3

FIG. 27

CALCULATIONS

Calculations are shown for Test 3 only. Curves of midspan deflection and slab temperature minus steel temperature vs time were shown for Tests 1 and 2.

CALCULATIONS TO DETERMINE DIFFERENCE IN EXPANSION COEFFICIENTS FOR STEEL AND FOR A PLAIN SAMPLE OF CONCRETE USED IN SLAB

From Fig. 22, the total contraction difference per degree fahrenheit for Test 1' = $43 \times 10^{-4}/40 = 1.075 \times 10^{-4}$ in/°F. Similarly, for Test 2', this value is 0.89×10^{-4} in/°F and for Test 3', it is 0.802×10^{-4} in./°F. The average of these three test values is 0.924×10^{-4} in/°F. The unit contraction difference per degree fahrenheit is then:

$$0.924 \times 10^{-4}/47.85 = 1.93 \times 10^{-6} \text{ per } ^{\circ}F$$

where 47.85 in. = length of sample. Assuming the coefficient of expansion for steel is 6.5×10^{-6} per °F, the thermal expansion coefficient for a plain sample of the concrete used in the slab must have been $(6.5 - 1.93) \times 10^{-6} = 4.57 \times 10^{-6}$/°F.

CALCULATIONS FOR TEST TO DETERMINE APPARENT STRAIN CAUSED BY A TEMPERATURE DIFFERENCE BETWEEN ACTIVE AND DUMMY GAUGES

The calculations to determine the apparent strain read on an active gauge, due to the fact that it is at a different temperature than it's balancing dummy gauge, are shown in Fig. 23.

CALCULATION OF THEORETICAL STRESS CAUSED BY A 100° TEMPERATURE DIFFERENTIAL BETWEEN THE STEEL BEAM AND THE CONCRETE SLAB.

Assuming that the concrete slab remained at a constant temperature while the steel beam cooled by 100°F throughout, the unit contraction of the steel relative to the concrete slab would be:

$$\Delta = \alpha T = 6.5 \times 10^{-6} \times 100 = 6.5 \times 10^{-4} \text{ in./in.}$$

Assume that for the section: n = 10

From Fig. 4: $Z = 6.64 + 2.79 = 9.43$ in.

For the section: $B = \frac{1}{nI_s + I_c} = \frac{1}{10(289.6) + 437.5} = \frac{1}{3333.5} = 3.0 \times 10^{-4}$

Therefore, the equivalent shear force along the steel-concrete interface, due to the temperature difference, would be:

$$N = \frac{E_s}{\frac{1}{A_s} + \frac{n}{A_c} + Z^2 nB} = 6.5 \times 10^{-4} \times 30 \times 10^6 / \frac{1}{8.81} + \frac{10}{210} +$$

$(9.43)^2 \times 10 \times 3.040^{-4} = 45.500$ lb./in.

The resulting stresses would then be:

$$f_{ct} = \frac{N}{A_c} - NzB\ t/2 = \frac{4.55 \times 10^4}{210} - 4.55 \times 10^4 \times 3.0 \times 10^{-4} \times$$

$$9.43 \times 2.5 = 216 - 322 = 106 \text{ p.s.i. tension}$$

$f_{cb} = 216 + 322 = 538$ p.si. compression

$$f_{st} = \frac{N}{A_s} + NzBc = \frac{4.55 \times 10^4}{8.81} + 4.55 \times 10^4 \times 3.0 \times 10^{-4} \times 9.43 \times$$

$$6.93 = 5160 + 892 = 6052 \text{ p.s.i.}$$

$f_{sb} = 5160 - 892 = 4268$ p.s.i.

The equivalent moment caused by the two shear forces "N" acting at the steel-concrete interface would be:

$M = M_s + M_c = Nz = 9.43 \times 4.55 \times 10^4 = 4.29 \times 10^5$ in.lb.
This moment is shown being applied to the real beam in Fig. 28. The equivalent conjugate beam for this loading is as shown in the figure.

The uniform conjugate load is:

$$\frac{4.29 \times 10^5}{30 \times 10^6 \times 886.95} = 1.611 \times 10^{-5} \text{ per in.}$$

Each conjugate reaction for this load is then:

$$144 \times 1.611 \times 10^{-5} = 2.32 \times 10^{-3} \text{ radians.}$$

The real beam deflection diagram is the conjugate beam bending moment diagram and has ordinates as calculated below:

$\delta_4 = 2.32 \times 10^{-3} \times 48 - 1.611 \times 10^{-5} \times 48^2/2 = 9.27 \times 10^{-2}$ in.

$\delta_8 = 2.32 \times 10^{-3} \times 96 - 1.611 \times 10^{-5} \times 96^2/2 = 14.82 \times 10^{-2}$ in.

$\delta_{12} = 2.32 \times 10^{-3} \times 144 - 1.611 \times 10^{-5} \times 144^2/2 = -16.68 \times 10^{-2}$ in.

The theoretical deflection diagram for this temperature difference is shown in Fig. 29.

CALCULATION OF ACTUAL DEFLECTION DUE TO SLAB-STEEL TEMPERATURE DIFFERENCE

From Fig. 26, for a temperature difference between the slab and the steel beam of zero (at 25 hours 5 minutes) the midspan deflection was -0.145 in. This deflection must have been due only to the difference in expansion coefficients for the beam and for the slab. The total concrete temperature change, giving rise to this deflection, was: $101.5^\circ - 32^\circ = 69.5^\circ$

The maximum beam deflection was -0.209 in. This deflection occurred at 2 hours 50 minutes. At this time, the temperature of the slab was 48°.

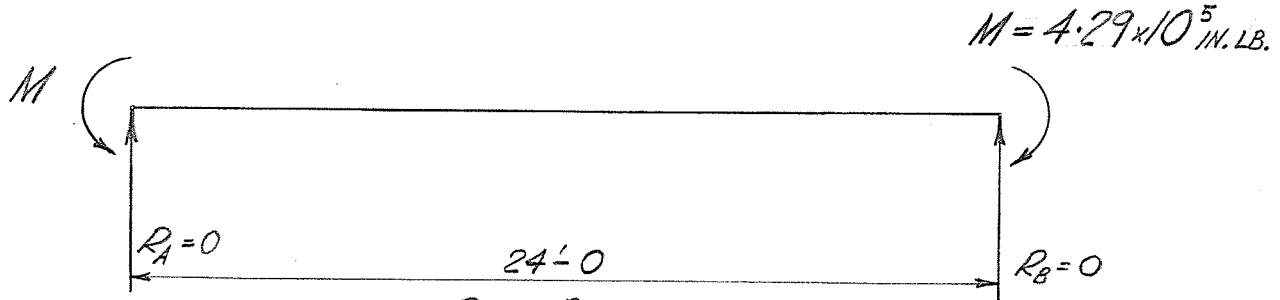

REAL BEAM

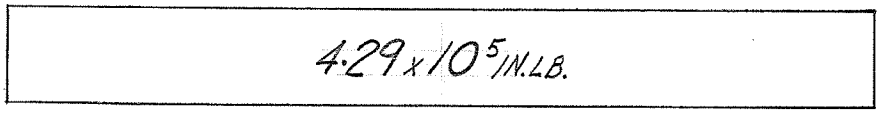

B.M. DIAGRAM

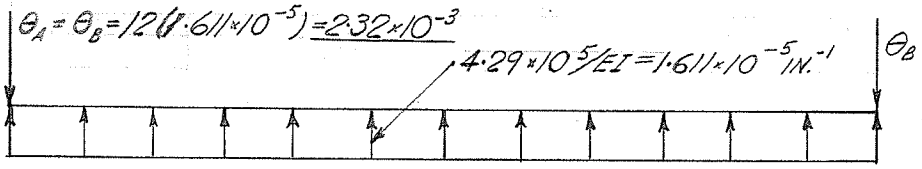

CONJUGATE BEAM

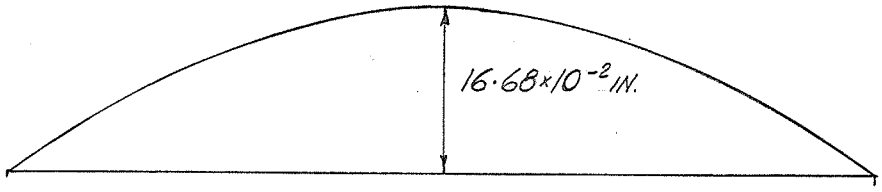

DEFLECTION DIAGRAM

DETERMINATION OF DEFLECTION DIAGRAM

FIG. 28

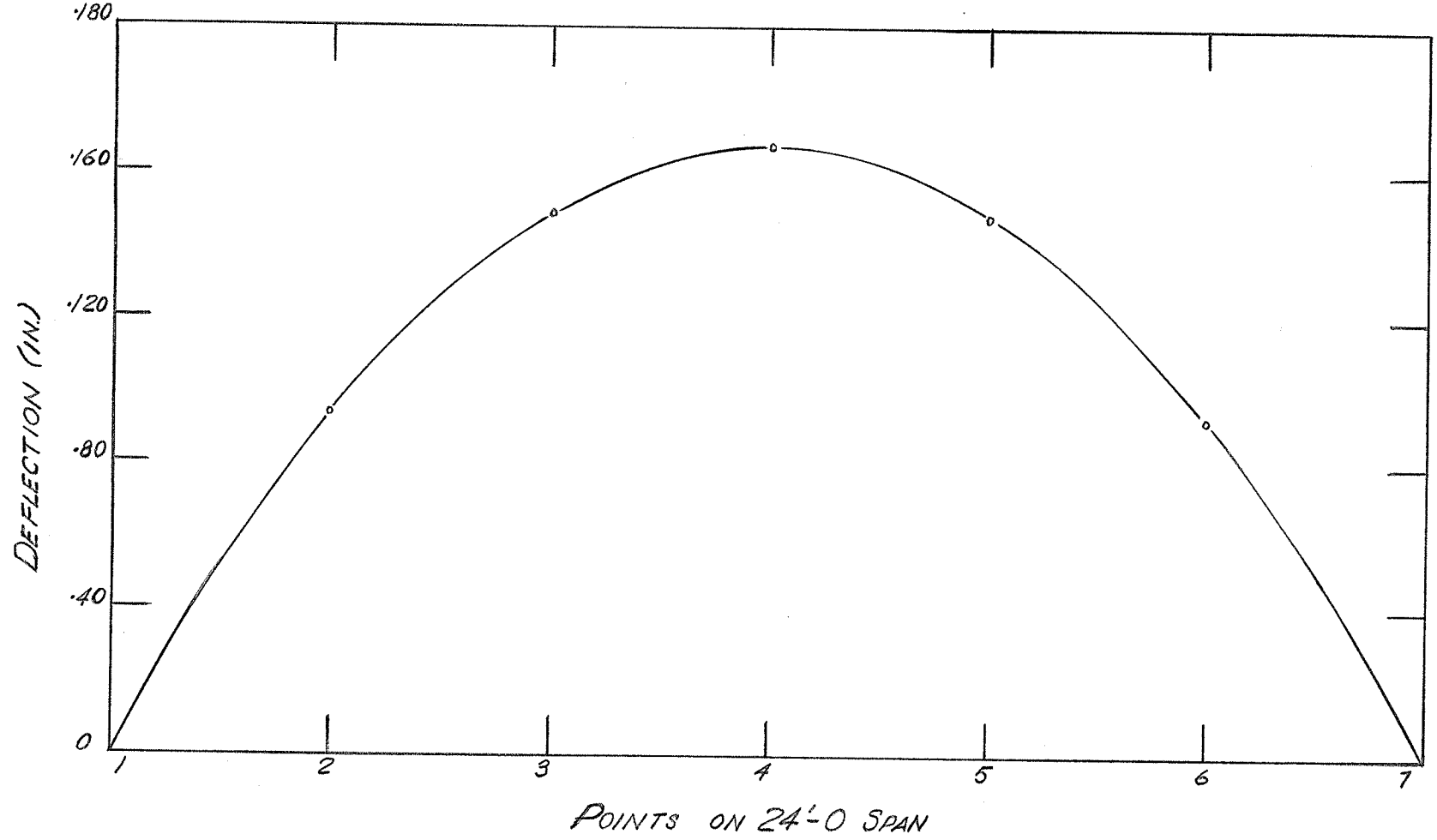

THEORETICAL DEFLECTION FOR 100° TEMPERATURE DIFFERENTIAL BETWEEN STEEL AND CONCRETE

FIG. 29

The deflection caused by a difference in expansion coefficients varies directly as the shear force "N", which in turn varies directly as the change in temperature of the beam-slab unit. It was, therefore, assumed that the deflection varies linearly with the temperature change. The equivalent deflection at 2 hours 50 minutes, due to the difference in expansion coefficients must, therefore, have been:

$$\left(\frac{48-32}{69.5}\right) \times 0.145 = 0.0334 \text{ in.}$$

The deflection at this time, caused by differential heating of the beam and slab, must then have been: 0.209 - 0.033 = 0.176 in. The temperature difference between the slab and the beam at this time was 32°.

Using similar calculations and reasoning, the deflection due to differential cooling, at 27 hours 10 minutes must have been 0.198 in. This deflection was due to a temperature differential of 37°. The equivalent deflection due to a 32° temperature differential would be:

$$\frac{32}{37} \times 0.198 = 0.1715 \text{ in.}$$

This provides an agreement within $\frac{.0045}{0.176} \times 100 = 2.5\%$.

However, the theoretical deflection due to a 32° temperature differential is $\frac{32}{100} \times 0.167 = 0.0535$ in.

-DETERMINATION OF STRAIN READINGS FOR PLOTTING STRAIN-TIME GRAPH

The strain gauge readings had to be corrected for the effect of active-dummy gauge temperature difference.

To illustrate this correction, consider the strain reading for gauge 10 at a time of 25 hours 0 minutes in Test 3. Table VIII shows that the temperature of the active gauge at this time was 114° (thermocouple 8). The temperature of dummy gauge 23 at this time was read by thermocouple 7 and was 101°. From Fig. 23, the approximate apparent strain due to a temperature difference between an active gauge and it's corresponding dummy gauge was determined to be 2.15 microin./in. per °F temperature difference.

In this case, the temperature difference was 114° - 101° = 13°. The strain correction to be applied to the gauge reading was, therefore: $\pm$ 13 x 2.15 = $\pm$ 28 microin./in. The plus sign was determined from the fact that, as indicated in Fig. 23, the correction is positive when the active gauge is warmer than the dummy gauge.

The actual gauge reading at this time was 1072. The corrected reading was, therefore, 1072 + 28 = 1100. The initial corrected reading for this gauge was 999. The corrected strain reading for this time, then, was 1100 - 999 = +101 microin./in. In this case, the plus sign indicates tension in the beam at the gauge point. A negative strain indicates compression.

These strain values were determined for 14 different gauges, as shown in Tables X to XVI, at each time and plotted in Figs. 30, 31, 32.

Some of the dummy gauge temperatures had to be determined by interpolating between thermocouple temperatures. For example, the temperatures for gauge 15 were taken as the average of the temperatures of thermocouples

8 and 3 since gauge 15 was approximately half way between these points.

TABLE X

TEST 3 - CORRECTED STRAIN READINGS

Time	Gauge 9 Reading	Temp Diff.	Corr.	Corr. Rdg.	Strain	Gauge 10 Reading	Temp. Diff.	Corr.	Corr. Rdg.	Strain
0	998	0.5	1	999	0	1004	-2.5	-5	999	0
5m	999	3	6	1002	+003	1054	8.5	18	1072	+73
25m	981	1	2	982	-017	1086	11	24	1110	+111
45m	980	2	4	982	-15	1112	14	30	1142	+143
1h- 5m	974	2	4	978	-21	1125	14.5	31	1156	+157
1h-25m	968	2	4	972	-27	1127	14	30	1157	+158
1h-45m	971	2	4	970	-29	1136	14.5	31	1167	+168
2h- 5m	971	4	9	980	-19	1141	16	34	1175	+176
2h-25m	972	4	9	981	-18	1148	16	34	1182	+183
2h-45m	972	5	11	983	-16	1150	16.5	35	1185	+186
3h-15m	972	5	11	983	-16	1151	16.5	35	1186	+187
4h-35m	966	6.5	14	980	-19	1151	17	36	1187	+188
25h- 0m	872	10.5	23	895	-104	1072	13	28	1100	+101
25h-20m	874	14	30	905	-94	996	-8	-17	979	-20
25h-40m	901	11.5	25	926	-73	969	-10	-22	947	-52
26h- 5m	910	13.5	29	939	-60	948	-7	-15	933	-66
26h-35m	920	15	32	952	-47	939	-7	-15	924	-75
27h-05m	927	11	24	951	-48	931	-8	-17	914	-85
27h-35m	911	12	26	937	-62	911	-7.5	-16	895	-104
28h-35m	915	9	19	934	-65	914	-7.5	-16	898	-101
40h- 0m	979	1.5	3	982	-17	1009	-1	-2	1007	+8

TABLE XI

TEST 3 - CORRECTED STRAIN READINGS

Time	Gauge 13 Reading	Temp. Diff.	Corr.	Corr. Rdg.	Strain	Gauge 15 Reading	Temp. Diff.	Corr.	Corr. Rdg.	Strain
0	005	0.5	1	006	0	010	-2.5	-5	005	0
5m	021	3	6	027	21	056	8.5	18	074	71
25m	017	1	2	019	13	087	11	24	111	106
45m	021	2	4	025	19	112	14	30	142	137
1h- 5m	018	2	4	022	16	120	14.5	31	151	146
1h-25m	015	2	4	019	13	124	14	30	154	149
1h-45m	018	2	4	022	16	129	14.5	31	160	155
2h- 5m	020	4	9	029	23	131	16	34	165	160
2h-25m	021	4	9	030	24	137	16	34	171	166
2h-45m	020	5	11	031	25	136	16.5	35	171	166
3h-15m	022	5	11	033	27	140	16.5	35	175	170
4h-35m	027	6.5	14	041	35	148	17	36	184	179
25h- 0m	936	10.5	23	959	-47	051	13	28	079	074
25h-20m	934	14	30	964	-42	012	-8	-17	995	-10
25h-40m	940	11.5	25	965	-41	976	-10	-22	954	-51
26h- 5m	955	13.5	29	984	-22	965	-7	-15	950	-55
26h-35m	963	15	32	995	-11	962	-7	-15	947	-58
27h- 5m	961	11	24	985	-21	951	-8	-17	934	-71
27h-35m	942	12	26	968	-38	935	-7.5	-16	919	-86
28h-35m	943	9	19	962	-44	935	-7.5	-16	919	-86
40h- 0m	975	1.5	3	978	-28	986	-1	-2	984	-21

TABLE XII

TEST 3 - CORRECTED STRAIN READINGS

Time	Gauge 14 Reading	Temp. Diff.	Corr.	Corr. Rdg.	Strain	Gauge 20 Reading	Temp. Diff.	Corr.	Corr. Rdg.	Strain
0	004	-2.5	-5	999	0	998	-2.5	-5	993	0
5m	021	8.5	18	039	40	032	7	15	022	29
25m	019	11	24	043	44	043	4.5	10	053	60
45m	028	14	30	058	59	055	5.5	12	067	74
1h - 5m	023	14.5	31	054	55	053	6	13	066	73
1h -25m	021	14	30	051	52	053	5	11	064	71
1h -45m	024	14.5	31	055	56	059	6	13	072	79
2h - 5m	024	16	34	058	59	061	7	15	076	83
2h -25m	027	16	34	061	62	065	6.5	14	079	86
2h -45m	024	16.5	35	059	60	065	7	15	080	87
3h -15m	025	16.5	35	060	61	066	6.5	14	080	87
4h -34m	029	17	36	065	66	070	7.5	16	086	93
25h- 0m	945	13	28	973	-26	029	7.5	16	045	52
25h-20m	952	-8	-17	935	-64	001	-4	-9	992	-1
25h-40m	950	-10	-22	928	-71	993	-3.5	-8	985	-8
26h- 5m	952	-7	-15	937	-62	990	-3	-6	984	-9
26h-35m	962	-7	-15	947	-52	991	-4.5	-10	981	-12
27h-05m	952	-8	-17	935	-64	987	-6	-13	974	-19
27h-35m	933	-7.5	-16	917	-82	984	-6.5	-14	970	-23
28h-35m	935	-1.5	-16	919	-80	984	-5.5	-12	972	-21
40h- 0m	978	-1	-2	976	-23	989	-4	-9	980	-13

TABLE XIII

TEST 3 - CORRECTED STRAIN READINGS

Time	Gauge 18 Reading	Temp. Diff.	Corr.	Corr. Rdg.	Strain	Gauge 19 Reading	Temp. Diff.	Corr.	Corr. Rdg.	Strain
0	001	-2.5	-5	996	0	989	+0.5	1	990	0
5m	046	7	15	061	65	015	-4.5	-10	005	15
25m	071	4.5	10	081	85	020	-5.5	-12	008	18
45m	091	5.5	12	103	107	031	-6.5	-14	017	27
1h- 5m	100	6	13	113	117	031	-6.5	-14	017	27
1h-25m	102	5	11	113	117	035	-7	-15	020	30
1h-45m	108	6	13	121	125	040	-6.5	-14	026	36
2h- 5m	114	7	15	129	134	048	-5	-11	037	47
2h-25m	119	6.5	14	133	137	052	-5.5	-12	040	50
2h-45m	119	7	15	134	138	054	-5	-11	-43	53
3h-15m	121	6.5	14	135	139	071	-5	-11	060	70
4h-35m	129	7.5	16	145	149	072	-3	-6	066	76
25h- 0m	085	7.5	16	101	105	057	+5	11	068	78
25h-20m	031	-4	-9	022	26	041	+18	39	080	90
25h-40m	005	-35	-8	997	1	041	+18	39	080	90
26h- 5m	992	-3	-6	986	-10	040	+17.5	38	078	88
26h-35m	989	-4.5	-10	979	-17	039	+17.5	38	077	87
27h- 5m	980	-6	-13	967	-29	029	+13	28	057	67
27h-35m	981	-6.5	-14	967	-29	025	+13.5	29	054	64
28h-35m	982	-5.5	-12	970	-26	019	+11	24	043	53
40h- 0m	999	-4	-9	990	-6	978	-1.5	-3	975	-15

TABLE XIV

TEST 3 - CORRECTED STRAIN READINGS

Time	Gauge 6 Reading	Temp. Diff.	Corr.	Corr. Rdg.	Strain	Gauge 1 Reading	Temp. Diff.	Corr.	Corr. Rdg.	Strain
0	990	-2.5	-5	985	0	002	1	2	004	0
5m	017	7	15	032	47	007	-0.5	-1	006	2
25m	030	4.5	10	040	55	004	1.5	3	007	3
45m	044	5.5	12	056	71	980	1	2	982	-22
1h- 5m	055	6	13	068	83	987	-1	-2	985	-19
1h-25m	060	5	11	071	86	990	0	0	990	-14
1h- 45m	071	6	13	084	99	986	1	2	988	-16
2h- 5m	078	7	15	093	108	981	-2	-4	977	-27
2h-25m	090	6.5	14	104	119	979	-0.5	-1	978	-26
2h-45m	094	7	15	109	124	986	-1	-2	984	-20
3h-15m	099	6.5	14	113	128	981	-0.5	-1	980	-24
4h-35m	098	7.5	16	114	129	981	-1	-2	979	-25
25h- 0m	049	7.5	16	065	80	925	2.5	5	930	-74
25h-20m	983	-4	-9	974	-11	934	0.5	1	935	-69
25h-40m	920	-3.5	-8	912	-73	941	3.5	8	949	-55
26h- 5m	907	-3	-6	901	-84	949	3.5	8	957	-47
26h-35m	900	-4.5	-10	890	-95	952	2.5	5	957	-47
27h- 5m	891	-6	-13	878	-107	951	3	6	957	-47
27h-35m	871	-6.5	-14	857	-128	934	1.5	3	937	-67
28h-35m	870	-5.5	-12	858	-127	935	3	6	941	-63
40h--0m	026	-4	-9	017	-132	958	-0.5	-1	957	-47

TABLE XV

TEST 3 - CORRECTED STRAIN READINGS

Time	Gauge 4 Reading	Temp. Diff.	Corr.	Corr. Rdg.	Strain	Gauge 5 Reading	Temp. Diff	Corr.	Corr. Rdg.	Strain
0	989	1.5	3	992	0	994	1	2	996	0
5m	000	1	2	002	10	986	-0.5	-1	985	-11
25m	991	2	4	995	3	982	1.5	3	985	-11
45m	966	2	4	970	-22	962	1	2	964	-32
1h- 5m	972	1.5	3	975	-17	972	-1	-2	970	-26
1h-25m	971	1.5	3	974	-18	976	0	0	976	-20
1h-45m	965	2.5	5	970	-22	976	1	2	978	-18
2h- 5m	961	2	4	965	-27	972	-2	-2	968	-28
2h-25m	958	1	2	960	-32	974	-0.5	-1	973	-23
2h-45m	963	1	2	965	-27	980	-1	-2	978	-18
3h-15m	959	2	4	963	-29	980	-0.5	-1	979	-17
4h-35m	962	2	4	966	-26	983	-1	-2	981	-15
25h- 0m	925	6.5	14	939	-53	871	2.5	5	876	-120
25h-20m	944	4	9	953	-39	870	0.5	1	871	-125
25h-40m	961	5	11	972	-20	860	3.5	8	868	-128
26h- 5m	963	5	11	974	-18	872	3.5	8	880	-116
26h-35m	975	5	11	986	-6	859	2.5	5	864	-132
27h- 5m	980	6	13	993	1	958	3	6	864	-136
27h-35m	963	5	11	974	-18	837	1.5	3	840	-156
28h-35m	970	6	13	983	-9	824	3	6	830	-166
40h- 0m	985	4.5	10	995	3	868	-0.5	-1	867	-29

TABLE XVI

TEST 3 - CORRECTED STRAIN READINGS

Time	Gauge 8 Reading	Temp. Diff.	Corr.	Corr. Rdg.	Strain	Gauge 16 Reading	Temp. Diff.	Corr.	Corr. Rdg.	Strain
0	998	-2.5	-5	993	0	1012	-2.5	-5	1007	0
5m	1041	7	15	1056	63	1056	7	5	1061	54
25m	1080	4.5	10	1090	97	1091	4.5	10	1101	94
45m	1111	5.5	12	1123	130	1114	5.5	12	1126	119
1h- 5m	1125	6	13	1138	145	1121	6	13	1134	127
1h-25m	1127	5	11	1138	145	1123	5	11	1134	127
1h-45m	1135	6	13	1148	155	1127	6	13	1140	133
2h- 5m	1139	7	15	1156	163	1129	7	15	1144	137
2h-25m	1147	6.5	14	1161	168	1131	6.5	14	1145	138
2h-45m	1149	7	15	1164	171	1130	7	15	1145	138
3h-15m	1150	6.5	14	1164	171	1131	6.5	14	1145	138
4h-35m	1146	7.5	16	1162	169	1140	7.5	16	1156	149
25h- 0m	1079	7.5	16	1095	102	1045	7;5	16	1061	54
25h-20m	997	-4	-9	998	-5	1002	-4	-9	993	-14
25h-40m	940	-3.5	-8	932	-61	965	-3.5	-8	957	-50
26h- 5m	909	-3	-6	903	- 90	954	-3	-6	948	-59
26h-35m	900	-4.5	-10	890	-103	948	-4.5	-10	938	-69
27h-05m	900	-6	-13	887	-106	945	-6	-13	932	-75
27h-35m	880	-6.5	-14	866	-127	926	-6.5	-14	912	-95
28h-35m	879	-5.5	-12	867	-126	929	-5.5	-12	917	-90
40h- 0m	1027	-4	-9	1018	+25	982	-4	-9	973	-34

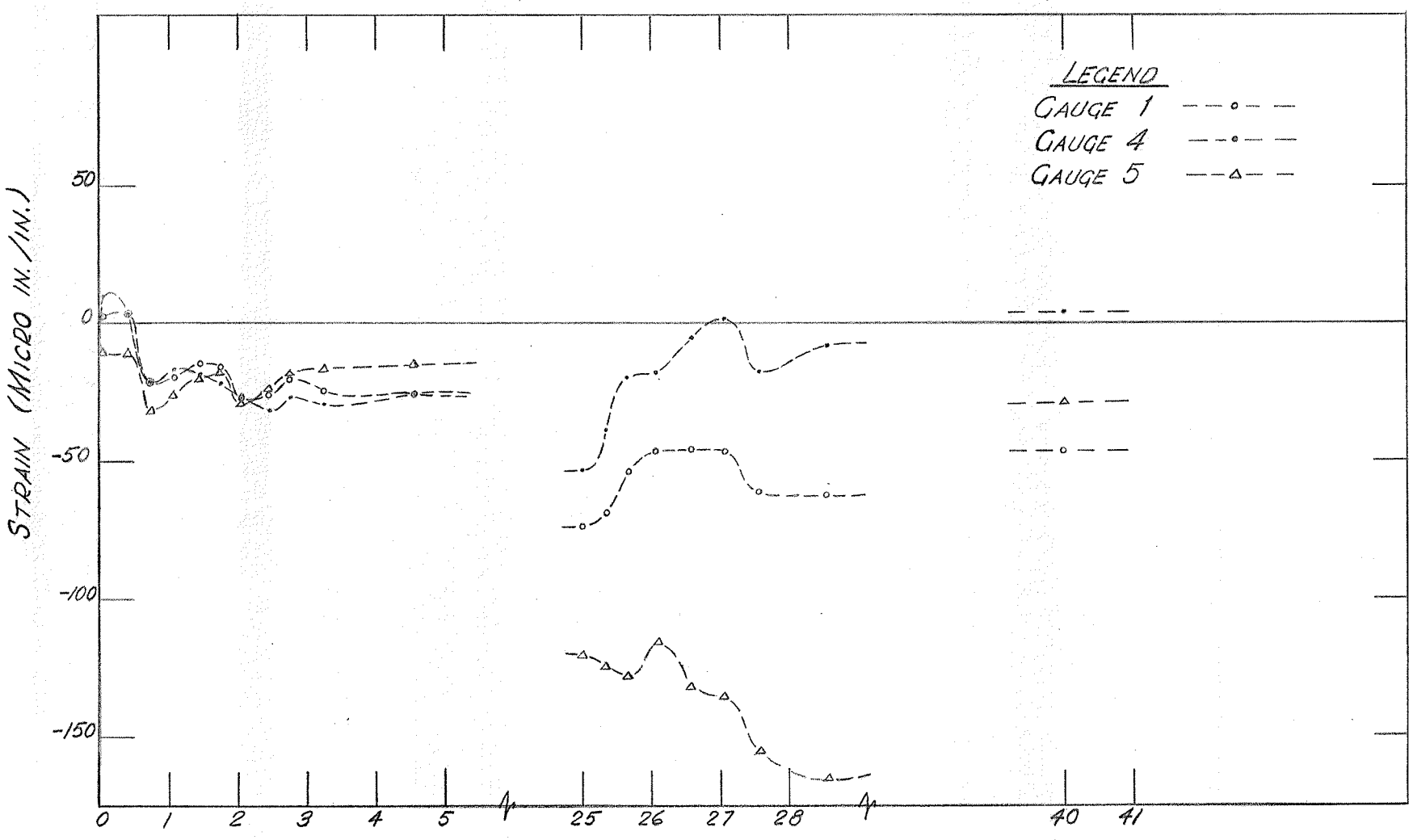

CURVES OF STRAIN VS TIME — TEST 3

FIG. 30

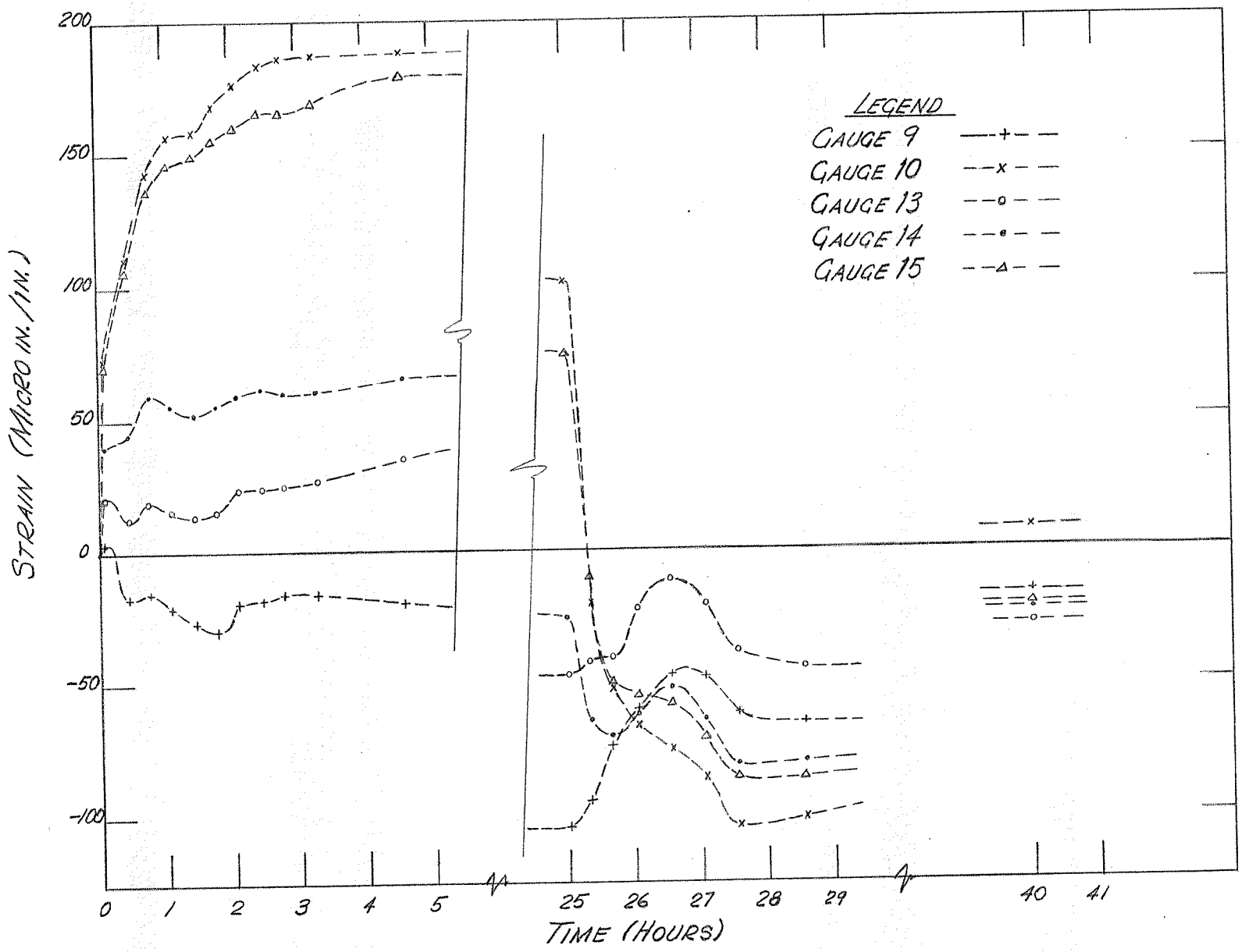

CURVES OF STRAIN VS TIME — TEST 3

FIG. 31

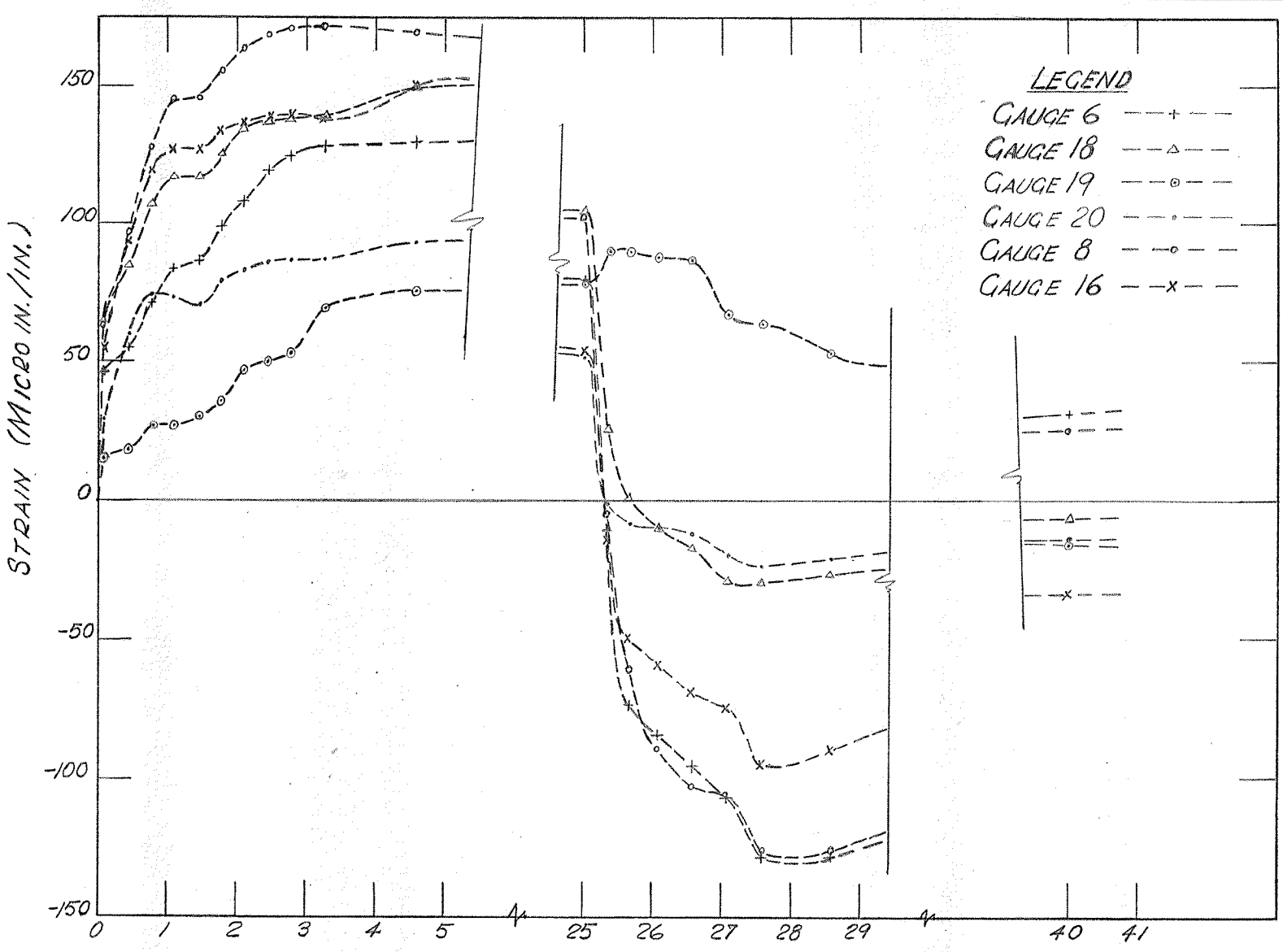

CURVES OF STRAIN VS TIME – TEST 3

FIG. 32

DETERMINATION OF STRESS DIAGRAMS FOR THE COMPOSITE BEAM

To determine the stress in a steel beam at a gauge location, the following formula was used:

$$f_s = E_s \times e_s$$

The beam stress at gauge 10 at a time of 25 hours-0 minutes in Test 3 was, therefore:

$f_s = 30 \times 10^6 \times 101 - 10^{-6} - 3030$ p.s.i. tension

The stresses at the different gauge points along the bottom of the beam web, and at the midspan cross-section, were calculated in this manner and listed in Table XVII. The resulting stress diagrams are shown in Fig. 33. The stresses listed are the maxima on the heating cycle, the stress at 25 hours, and the maxima on the cooling cycle.

CHECK ON MIDSPAN DEFLECTION

From Fig. 33, the bottom flange midspan stress at a time of 4 hours-35 minutes was 6,400 p.s.i.

Assuming composite action, the stress at the bottom of the beam is given by:

$$f_{sb} = M/S_{sb}$$

Therefore, the beam moment corresponding to this stress is:

$$M = 6{,}400 \times 65.5 = 420{,}000 \text{ in. lb.}$$

As calculated for the theoretical deflection for a 100° temperature differential, a beam moment of 429,000 in.lb. caused a deflection of 0.167 in. The corresponding midspan deflection for a moment of 420,000 in.lb. would then be:

$$\frac{420}{429} \times 0.167 = 0.164 \text{ in.}$$

The actual deflection at this time was 0.203 in. Therefore, the percent error between the midspan deflection, calculated from the bottom flange stress, and that actually measured was:

$$\frac{0.203 - 0.164}{0.164} = 23.8\%$$

The midspan deflections were similarly calculated at 25 hours and at 27 hours 35 minutes. The stresses corresponding to each deflection were also calculated by proportion. The results of these calculations are shown below.

Time	Calculated Defl.	Actual Defl.	Actual Stress	Calculated Stress	% Error
4h-35m	-0.164 in.	-0.203 in	6400 psi	7930 psi	23.8
25h- 0m	-0.093 "	-0.147 "	3800 "	6000 "	58
27h-35m	0.082 "	0.086 "	3200 "	3360 "	4.9

The deflection due to differential temperature at 4 hours 35 minutes was 0.176 in. The corresponding bottom flange stress must have been $\frac{0.167}{0.147} \times 3800 = 4320$ p.s.i

TABLE XVII

BEAM AND SLAB TEMPERATURE STRESSES

Gauge	-Time-		
	4h-35m	25h-0m	27h-35m
6	3870	2400	-3840
8	5075	3060	-3820
10	5650	3030	-3120
12	4111	150	-3660
14	1980	-780	-2460
15	5370	2220	-2580
16	4470	1620	-2860
18	4470	3150	-870
20	2800	1560	-690
1	-750	-2220	-2010
4	-780	-1590	-540
9	-570	-3120	-1950

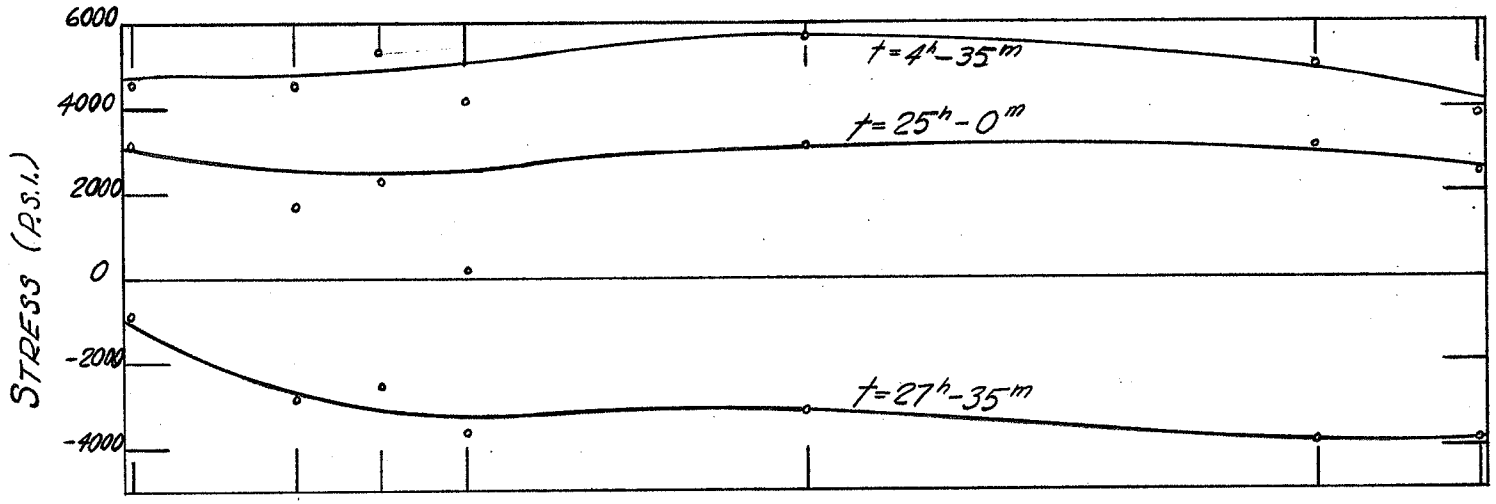

GAUGE LOCATIONS ON 24'-0 SPAN

LONGITUDINAL STRESS DISTRIBUTION - BOTTOM OF WEB

(a)

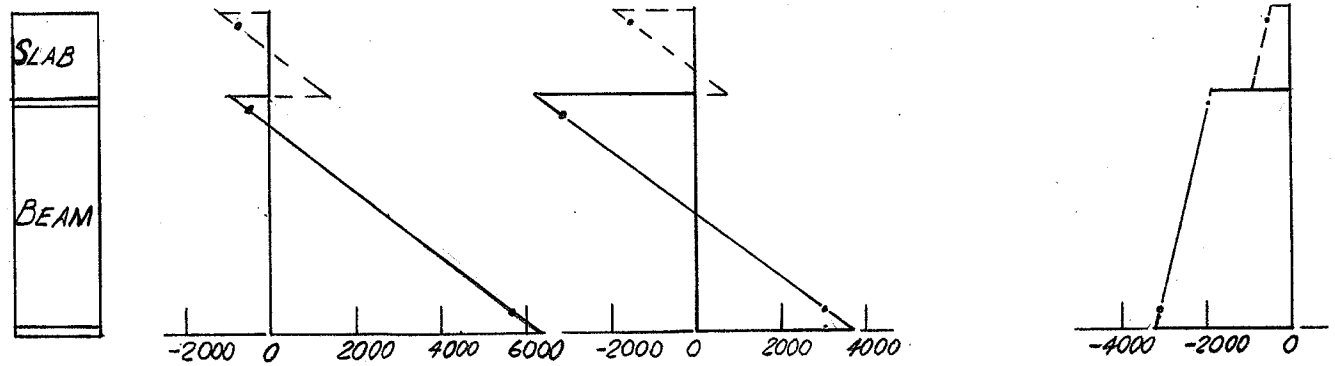

CROSS-SECTION $t=4^h-35^m$ $t=25^h-0^m$ $t=27^h-35^m$

STRESS DISTRIBUTION AT MIDSPAN

(b)

TEST 3 - STRESS DISTRIBUTION DIAGRAMS

FIG. 33

CHECK OF MIDSPAN DEFLECTION CAUSED BY DIFFERENCE IN EXPANSION COEFFICIENTS

The expansion coefficient for a plain sample of the concrete used in the slab was determined experimentally to be 4.57×10^{-6} per °F. In Test 3, the temperature rise in the slab, from a time of 25 hours 0 minutes, was 102.5 - 32 = 70.5°. The corresponding change in the steel temperature was 112 - 27 = 85°. The unit expansions caused by these temperature changes would be:

$$\Delta_s = 85 \times 6.7 \times 10^{-6} = 570 \times 10^{-6} \text{ in./in.}$$

$$\Delta_c = 70.5 \times 4.57 \times 10^{-6} = 322 \times 10^{-6} \text{ in./in.}$$

The differential unit expansion was, therefore, 248×10^{-6} in./in. The theoretical differential unit expansion for a 100° temperature differential was calculated to be 650×10^{-6}. The midspan deflection corresponding to this differential expansion was calculated to be 0.167 in. The deflection corresponding to a differential expansion of 248×10^{-6} in./in. is:

$$\frac{248}{650} \times 0.167 = 0.64 \text{ in.}$$

The actual deflection at this time was 0.147 in.

CHAPTER V

Discussion

At the outset of this thesis, the author was not aware of the great complexity of the problem. In addition, the construction of the beam-slab unit and the enclosing building consumed such a large portion of the allotted time that the time remaining for testing, and for interpreting the results, was rather limited. Therefore, although it was originally intended to check the theoretical solution to what appeared to be a simple problem involving differential expansion, this thesis is an exploratory investigation of the problem. It is hoped that the apparatus will be used to conduct future, more complete tests.

Factors Affecting Test Results

As was mentioned previously, the thickness of the concrete slab was purposely exaggerated in order to accentuate the effectof rapid temperature changes on the beam. An excessive amount of longitudinal reinforcing steel was used to prevent damaging of the concrete due to the large temperature changes it had to undergo. The amount of reinforcing used was nearly four times that actually required. This excess of steel would increase the expansion coefficient of the slab, making it closer to that of the beam. The stresses and deflections caused by a difference in expansion coefficients would, therefore, be reduced. Thus, these factors would tend to exaggerate the deflections due to differential rates of temperature

change and to have the opposite effect on those due to different expansion coefficients.

A great deal of difficulty was experienced in obtaining a uniform temperature throughout the actual beam and the unstressed section. At times, the heat lamps were turned off, in various locations, in an attempt to equalize temperatures. However, the ends of the beam and the dummy section were always colder than the centre portion of the unit. On the cooling part of the cycle, when the doors were opened, draughts caused rapid temperature fluctuations and variations, which probably affected strain gauge and thermocouple readings.

The thermocouples which were located on the steel beam were taped to the steel section and covered with a layer of fibre glass insulation to protect them from the influence of the air. However, even with this protection, a temperature drop in these thermocouples of several degrees was noted almost immediately, when the heat lamps were turned off. The use of a lighter colored insulating material and possibly some sort of reflector might have reduced, or eliminated, this effect.

Deflection Readings

The deflection readings yielded the best results in the tests. However, some error was apparent in these readings; this error having three sources. The first source was in not placing the Ames dial exactly flat, and in exactly in the same position on the angle each time. In addition, the actuating stem of the dial had a threaded

extension which often became loose and had to be tightened. The actual possible error from these two sources was of the order of two to three thousandths of an inch. This was indicated by taking two sets of readings, one right after the other.

The third source of error was in the expansion of the angles used in obtaining the deflection readings. One support for these angles was a knife edge, while the other was a roller.

Because of this, there was differential contraction and, therefore, relative movement between the angles and the slab. As a result, the actuating stem of the Ames dial did not bear on exactly the same points, each time, on the pins set in the concrete. Since the tops of these pins were not perfectly level, errors in the deflection readings resulted. The maximum relative movement occurred at the expansion support. The maximum variation measured here in Test 3, was 0.022 in. However, 0.020 in. of this was actual deflection since the point was actually located 6 in. from the expansion support. The probable error from this source is, therefore, not known exactly but is estimated at a maximum of 0.005 in.

The accuracy of these deflection readings is illustrated by the close symmetry of the typical beam deflection diagrams shown in Fig. 27. The deflection diagram corresponding to a time of 2 hours 50 minutes corresponds almost exactly to the theoretical deflection curve for a 100^{o} temperature differential.

To relate the deflection readings to the slab and beam temperatures, curves of midspan deflection and of slab temperature minus steel temperature were plotted against time, as the beam went through a complete heating and cooling cycle.

Fig. 24 shows these curves plotted for Test 1. The deflection curve should return to zero after a complete cooling and heating cycle. This was not the case for Test 1. However, the final deflection of -0.066 can be largely attributed to the fact that the concrete was warmer than the steel by 12.5 degrees at the beginning of the test and colder by 7.5 degrees at the conclusion.

The curves for Test 2 are shown in Fig. 25 and are very similar to those for Test 1. However, this test was not carried to completion since no readings were obtained right at the end of the cycle.

Fig. 26 shows the midspan deflection and temperature differential curves for Test 3. In this case, to give a better picture of the variations of deflection and temperature, the complete time scale is shown.

The curves resembled very closely, those for tests 1 and 2, except that in this test, the rapid heating portion of the cycle preceeded the rapid cooling part. In the previous two tests the reverse was true.

The very close similarity in the shapes of the two curves indicates that a large part of the beam deflection is due to differential cooling and heating of the beam and slab. The deflection curve can actually be broken up

into two parts; that due to differential rates of temperature change, and that due to a difference in expansion coefficients. The dividing line separating the deflections due to these different causes is shown in Fig. 26. This line begins at zero deflection and zero time, and drops at a uniform rate to a deflection of -0.147 in. at 25^h-0^m. At this point, the heating part of the cycle is finished and a new horizontal base line can be drawn as shown. The new dividing line then returns uniformly, to very nearly the original deflection base line. These dividing lines represent the deflection curves that would result if the heating and cooling cycles were allowed to occur very gradually. They represent, therefore, the deflections due only to different expansion coefficients. These deflections vary linearly with the temperature change of the unit (that of the slab in this case). The ordinates between the dividing lines and the actual deflection curve represent the deflections due to temperature differential.

The effect of the part of the deflection due to different expansion coefficients can be seen from the temperature difference and deflection curves. In every case, the maximum deflection curve lags behind the maximum temperature difference curve, on the time scale. This further indicates that the deflection was made up of two components, one of which increased gradually from zero to a maximum on one part of the cycle and then gradually decreased back to zero on the next.

Since the rate of change of the slab temperature

is rapid at first and gradually decreases to zero at 25 hours, or on the cooling cycle at 40 hours, the dividing lines are actually not straight. In addition, since no readings were taken between 5 hours and 25 hours, or between 29 hours and 40 hours, the shapes of the deflection and temperature curves in these two intervals are very uncertain. It is very likely that constant temperatures were reached on the heating and cooling cycles before 25 hours and 40 hours respectively. Therefore, this line possibly should drop to a deflection of -0.147 in. before a time of 25 hours. However, the dividing lines are shown merely to illustrate graphically, the approximate deflections due to the two different causes.

In order to calculate exactly the deflection due to difference in expansion coefficients, it is necessary to proportion it in the same ratio as the slab temperature change. This was done on Page 70 for times of 2 hours 50 minutes and 27 hours 35 minutes. The remaining portions of the deflections at these times must have been due to differential temperatures. These deflections were calculated, and when they were both referred to a 32° temperature differential, they agreed within 2.5 percent. However, the theoretical deflection for a 32° temperature differential was less than one third of either of the two values actually obtained.

One probable reason for the large discrepancy between the theoretical and actual values is that the value of "n" for the steel and concrete used was assumed to be 10. If a smaller value had been assumed, the

theoretical deflection value would have been increased. However, an error in the value of "n" would not have caused such a large discrepancy in the deflection.

Probably the largest part of this difference is due to the fact that, as described below, there is no sudden temperature drop at the steel-concrete interface.

Temperature Variation Across a Vertical Section

The theory presented in Mr. David's[3] paper gives a method of calculating the stresses produced, due to a difference in expansion coefficients, when a composite beam is subjected to a temperature change. This theory is derived on the assumption that the concrete slab would expand or contract the same amount right across its section, and that the steel would do likewise, if each were independent of the other. This theory would, therefore, apply equally well to the stresses produced by differential heating and cooling, if the concrete and steel sections each had constant temperatures throughout at any given time.

This was not the case, however, in the tests done. The temperatures were measured at five points across the section at the midspan at the unit. Curves of the temperature variation are shown in Fig. 34 for times of 2 hours 35 minutes and 27 hours 10 minutes. These curves are rather incomplete since no thermocouples were located below the neutral axis of the steel. For the calculations in the test, therefore, it was assumed that the temperature was uniform for the section below the steel neutral axis. Nevertheless, it can be seen that there is no sudden temperature change at the steel-concrete interface. In

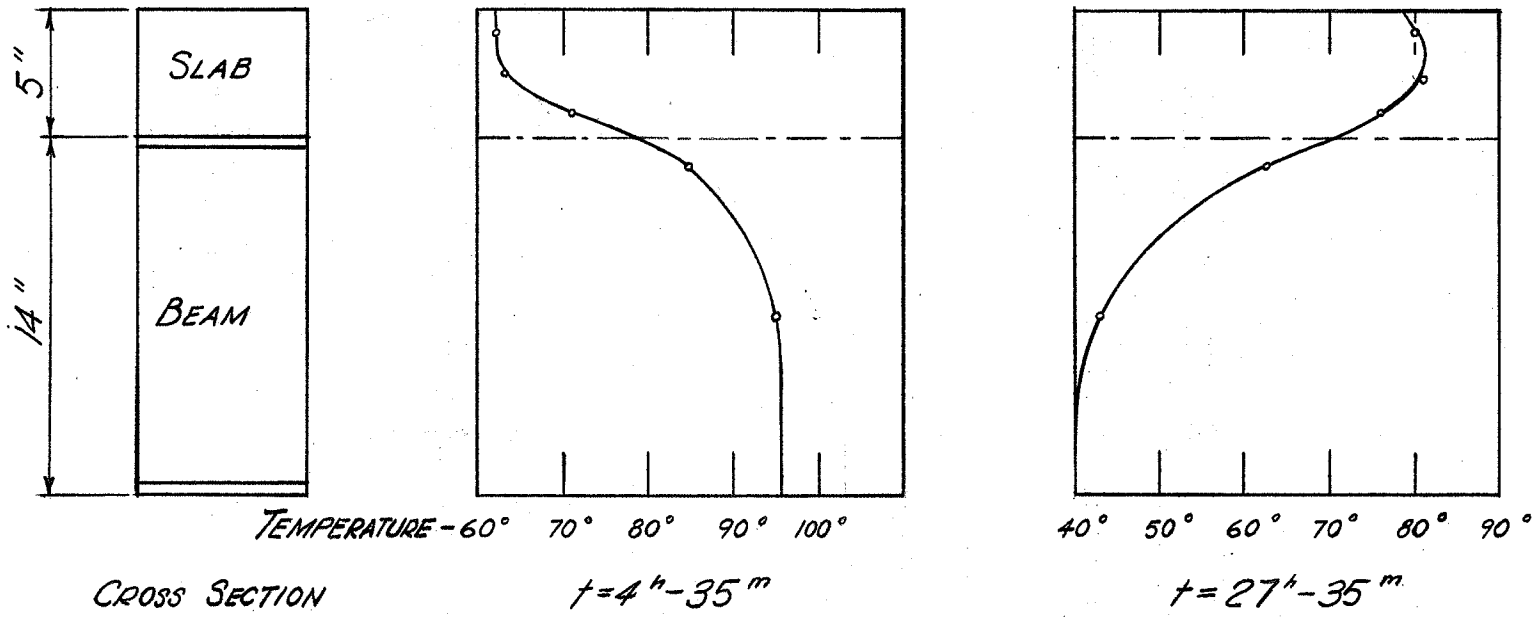

TEMPERATURE VARIATION ACROSS SECTION AT MIDSPAN - TEST 3.

FIG. 34

addition, the curves indicate that the assumption of uniform temperature distribution below the steel neutral axis is not too greatly in error.

As was mentioned in the test procedure, thermocouple 3 was moved from the centre of the slab to the neutral axis of the beam as shown in Fig. 13. This was done to obtain the steel temperature at the end of the beam so that the strain gauge temperatures could be determined by interpolation. Since three thermocouples were located at various depths in the slab at the beam midspan, it was felt that thermocouple 3 was unnecessary in it's original location.

Determination of Difference in Expansion Coefficients

As was stated previously, it has sometimes been assumed in composite beam design that steel and concrete have approximately the same coefficients of expansion. Three tests were done to determine roughly the difference in expansion coefficients for a steel reinforcing bar and for a plain sample of the concrete used in the construction of the slab. These tests indicated a difference in expansion coefficients of 1.93×10^{-6} per degree fahrenheit.

The main difficulty encountered in conducting these tests was the prevention of sudden jarring of the sample. To obtain the necessary temperature variations, the sample was placed on a movable wagon and transported from a warm room to a cold one. Large changes in dial readings could be noticed when the specimen was handled roughly.

To prevent breaking of the concrete specimen,

it was left in it's wood forms during the expansion tests. Although the forms were oiled previous to the pouring of the concrete, it was felt that the concrete may have been partially held due to friction or bond between the wood and the concrete. Since woods have widely varying thermal expansion coefficients, it is not known exactly how great the resulting errors would be.

The theoretical deflection that should have resulted from this difference in expansion coefficients, was calculated for a time of 25 hours for test 3. As for the differential heating and cooling deflections, the theoretical deflection in this case was much less than that measured.

Strain Measurement

As has been mentioned, the strain gauge circuit used in these tests was a Wheatstone bridge circuit in which each active gauge was balanced against an unstressed gauge at approximately the same temperature. Strain measurements are obtained with electrical resistance gauges, by measuring a change in the resistance of the gauge wire. However, the resistance of these wires also changes with a change in temperature, since such a change affects their cross-section and length. Therefore, because the active and dummy gauges used in this test were not always kept at the same temperature, the test described on Page 40 had to be done to relate this temperature difference to the apparent strain it produced.

The main difficulty encountered in this test was that of transferring the dummy gauge, in it's glass box,

from one large container to another. The slightest disturbance of the dummy gauge leads changed their resistance and, therefore, affected the strain readings. This was the largest source of error and it's magnitude is impossible to estimate since the readings varied with the slightest disturbance of the leads.

Nevertheless, the curves in Fig. 23 indicate a fairly close check for the apparent strains at a temperature difference of approximately 10°F. As was stated previously, the relationship between temperature difference and apparent strain is probably not linear. However, an approximate linear relationship was determined to quickly obtain the temperature corrections for the many strain readings, recorded during Tests 1, 2 and 3.

When the apparatus was originally set up, each set of strain gauge leads was made just long enough to connect it's corresponding gauge. Consequently, the leads were of varying lengths. However, it was later realized that a change in the temperatures of the leads would change their resistances. Therefore, to prevent differential resistance changes, which would result in apparent strains, from this cause, the leads were later all made equal in length. In addition, the leads were supported and suspended in the air where possible so that they would not take heat from the slab or the ground, but would all cool uniformly.

Another possible source of error in the strain gauge readings was the presence of the three--way switch in the dummy gauge circuit. The magnitude of this error was found by balancing an active gauge, moving the switch

several times and again reading the potentiometer. Since the gauge always remained balanced, it was assumed that the error from this source was negligible.

The other large source of error in the strain gauge circuits was the possibility of disturbing the strain gauge leads. However, to minimize this possibility, the switch boxes were rigidly fastened down and care was taken not to disturb the leads.

As can be seen in Tables IV, VI and VIII, dummy gauges 21, 22 and 23 were used in the first two tests but number 22 was not used in the final test. At the beginning of test 3, the readings for all gauges balanced against gauge 22, began to increase by extremely large amounts, indicating that the gauge must have come loose from the dummy beam section or become short circuited. Consequently, only dummy gauges 21 and 23 were used in Test 3. However, this failure did not seriously affect the results since gauges 22 and 23 were always at approximately equal temperatures, and since temperature corrections were made.

Strain Readings

The most notable fact observed in connection with the strain gauge readings was that while the readings at the bottom of the beam web varied exactly as expected, those at the top of the web and in the concrete slab did not follow any set pattern.

The curves of strain vs time for the gauges located on the beam are shown in Figs. 31 and 32. The shapes of the curves for gauges 10, 15, 6, 8, 16 and 18, (all of which were located at the bottom of the web) were

very similar. Close examination of these figures indicates that the curves have similar shapes as regards small fluctuations in ordinates from one set of readings to the next. These small fluctuations in the curves are seen to be common to all of the strain-time curves plotted. Therefore, they are probably due to a slight disturbance of the leads causing one set of readings to be higher or lower than it should have been.

Comparison of the strain-time curves for any of these gauges indicates a very similar shape to the mid-span deflection-time curve in Fig. 26, except that the strain curves are inverted with respect to the time axis.

The fact that these strain curves are so similar in shape, and have approximately the same maximum ordinates, indicates that the strain, and therefore the stress, is very nearly constant across the span. This fact is illustrated by the curves of longitudinal bottom flange stresses in Fig. 33(a). These curves indicate that the longitudinal stress distribution is very nearly constant. They, therefore, verify the theoretical assumption that the stresses caused by a differential rate of cooling, or by a difference in expansion coefficients, are uniform over the length of the beam and are accompanied by a uniform moment over the entire span.

The points on the stress curves in Fig. 33(a) do not trace out exactly straight lines. However, since the vertical displacements of each point between the curves representing stresses at the three different times are very nearly equal, the lines are nearly parallel. This

indicates that the discrepancies are probably due to errors in the initial readings and not due to a variation in the magnitudes of the stresses as the beam was heated and cooled.

The strain readings for the two active gauges (14 and 20) located at the steel neutral axis, are shown graphically in Fig. 31 and Fig. 32. Once again they follow generally the pattern they were expected to follow. Their ordinates on the first part of the cycle lie between these for the gauges above and below them on the steel beam. However, their readings are slightly more erratic than those for the gauges at the bottom of the web.

At first glance, the strain curves in Fig. 30, 31, and 32 for the gauges at the top of the beam web and for those in the slab, do not follow any orderly pattern. This fact is probably very largely due to the influence of the shear connectors. Theoretically, the shear between the concrete and the steel is uniformly distributed along the top flange of the beam. However, in the actual beam, this shear is concentrated at the shear connectors. Because of this, when the top flange was in tension, a gauge located right beside a shear lug, between the lug and the support, could be in compression or to a lesser degree in tension. Therefore, the gauges along the top of the web could not be used to give accurate strain readings. However, the fact that their readings were relatively small suggests that the neutral axis for temperature stresses was near the top flange, as theoretically determined. This, in turn, suggests that under the

influence of a sudden temperature change, composite action rather than independent bending of the beam and slab, occurs.

In Fig. 33(b) an attempt was made to draw mid-span stress distribution diagrams. However, the fact that the strain readings at the top flange were inaccurate, also made these diagrams inaccurate, and an impossible stress diagram resulted for a time of 27 hours 35 minutes.

The strain diagrams for gauges 1, 4 and 5 located near the top of the concrete slab are shown in Fig. 30. The strains for all three gauges are almost identical during the first part of the cycle. However, the strain for gauge 5 increases much more than that for the other two gauges in the latter part of the test. This increase would be expected to be due to the effect of the heavy angle used at the expansion end. However, since gauge 5 was located at the fixed end, this variation must have been due to some other cause. Possibly it was due to the fact that the building was usually slightly cooler at the end of the building corresponding to the expansion end of the beam. The fact that the strain for gauge 1 is slightly less than that for gauge 4 seems to indicate that the large angle shear lug did not affect the shear distribution and was, therefore, not necessary.

The fact that most of the gauges located at the top of the beam web, and those in the concrete slab, were constantly in compression can be seen from Figs. 31, 31 and 32.

The author can think of no reason for this, but the fact that the signs of the stresses in the top flange of the beam, and in the slab, were the same, is an indication that the bending in the beam was composite action.

CHAPTER VI

CONCLUSIONS AND RECOMMENDATIONS

Conclusions

On the basis of the reaults obtained in the preliminary tests described in this thesis, the following conclusions are drawn:

(a) The actual stresses and deflections caused, due to a difference in expansion coefficients of concrete and steel, when a composite beam is cooled, are larger than those calculated theoretically. The maximum stress set up in the steel beam tested, due to this cause, was approximately 3,000 p.s.i. This stress corresponded to a temperature change of the unit of approximately 80°F.

(b) The temperature variation across the section of the beam-slab unit, when it was subjected to a rapid temperature change was a gradual change from one extreme at the centre of the slab, to the other extreme below the neutral axis of the steel beam.

(c) Because of the nature of the above temperature variation, the theory does not apply to the situation where stresses are set up due to differential heating or cooling of a unit. The actual measured stresses and deflections due to this cause were more than three times as great as the theoretical values, for the unit tested.

(d) In the tests performed, a change in the air temperature of approximately 80° in 4 hours, caused a temperature

differential of approximately 38° between the steel and the concrete in the test section. This differential would probably be greater in an 8 inch slab commonly used in bridge construction.

(e) The maximum deflection caused in the test section due to a differential of 32°F was 0.176 in. The corresponding stress was 4,320 p.s.i.

(f) The measured stresses at the top of the beam web were much smaller than those at the bottom of the web. The theoretical stresses on the other hand, were larger. This suggests that composite action occurred in the bending of the beam rather than separate bending of the beam and the slab as is theoretically assumed.

(g) The fact that the bottom chord stress was constant over the entire span of the beam indicates that these stresses must have been caused by a moment which was also constant over the entire span. The theoretical assumption of constant moment is, therefore, verified.

(h) The strain at the top of the slab was not influenced by the presence of a heavy angle shear lug at the expansion support. This indicates that an extra large end shear connector is not necessary to resist the shears that occur along the steel-concrete interface.

Recommendations

(a) The fact that electric resistance strain gauges are so susceptible to the influence of temperature is a source of possible error in tests such as these, where their temperatures are constantly varying. If they are available and practical, temperature compensating gauges would probably increase the accuracy obtained.

(b) In the absence of temperature compensating gauges, a series of tests, such as the one herein described, could be done to determine the apparent strain resulting from a temperature difference between the active and dummy gauges.

(c) Another possible alternative for avoiding errors due to differing gauge temperatures, would be to glue dummy gauges to unstrained steel plates located near each active gauge.

(d) To determine more accurately, the temperature variation across a section of the unit, as many as 8 thermocouples could be used in a vertical line. More thermocouples should also be located at various points throughout the beam, to determine the strain gauge temperatures more accurately.

(e) Tests to determine temperature differentials caused by different rates of variation of air temperatures would also be of value. These would necessitate means for measuring air temperatures in the building.

(f) Another type of test is very necessary in connection with the determination of temperature stresses and deflections in a composite beam-slab unit. This test involves the determination of the expansion coefficients for different types of concrete with varying amounts of reinforcing.

BIBLIOGRAPHY

1. University of Illinois Bulletin - Volume 49, No. 45 February, 1952.
2. Viest, I. M. - Shear Connector Design Data - Gregory Industries - Lorain Ohio - August, 1956.
3. David, R. and Meyerhoff, G. C. - Composite Construction of Bridges Using Steel and Concrete. - A paper presented to the E. I. C. Annual Meeting - Banff; Alberta - July, 1957.
4. Porete Manufacturing Co., New Jersey - Alpha Composite Construction Engineering Handbook.
5. Public Roads - Journal of Highway Construction - Volume 28, No. 1.